2. Nondimensional Representation of the Boundary-Value Problem

Given that an experiment can be considered to represent a physically realizable boundary value (bv) problem and given that the derived measurements are to represent aspects of the solution to the bv problem, it is rational to extend this understanding such that a maximum amount of information can be obtained from a given experiment. The first portion Sect. 2.2.1 establishes the bases for obtaining information regarding the flow associated with a prototype (the object/flow of actual interest) from measurements made in a model study. This section focuses on the large class of flows for which a Newtonian fluid and its governing equations establish the model-to-prototype information exchange.

Dimensional analysis Sect. 2.2.2 provides a complement to Section 2.1 with a less structured – and therefore a more flexible – approach to problems that extend beyond those readily addressed by the Sect. 2.2.1 material. The important issue of collecting experimental results in non-dimensional groups is addressed in Sect. 2.2.2.

The discussion of self-similarity Sect. 2.2.3 addresses the immense compaction of experimental data that is made possible for those flows that exhibit this property. The bases for, and utilization of, self-similarity are explored in detail.

2.1 **Similitude, the Nondimensional Prototype and Model Flow Fields** 34
- 2.1.1 Governing Equations – Newtonian and Incompressible 34
- 2.1.2 Boundary Conditions 35
- 2.1.3 Initial Conditions 36
- 2.1.4 Parameters that Influence the Solution to the Boundary-Value and/or the Initial-Value (BV/IV) Problem 36
- 2.1.5 Governing Equations – Newtonian and Compressible 38
- 2.1.6 Flows for Which U and L May Not Be Apparent 39

2.2 **Dimensional Analysis and Data Organization** 42
- 2.2.1 Variables, Function List, and Extra Information 42
- 2.2.2 Dimensions and Scale Ratios 43
- 2.2.3 Natural Scales and Repeating Variables 43
- 2.2.4 Π Theorem 45
- 2.2.5 Example with Rank Less than the Number of Dimensions 45
- 2.2.6 Example with Redundant Dimensions 46
- 2.2.7 Anatomy of a Nondimensional Variable 47
- 2.2.8 Nonuniqueness of Scales 48
- 2.2.9 Reference 48
- 2.2.10 Scales Chosen for Experimental Purposes 48
- 2.2.11 Nondimensional Variables Interpreted as Physical Ratios 50
- 2.2.12 Scales Found from Boundary Conditions and Equations 50
- 2.2.13 Limiting Cases 51
- 2.2.14 Singular Perturbations 52
- 2.2.15 Overlap Behavior and Composite Expansions 52
- 2.2.16 Common Scales and Nondimensional Parameters 55

2.3 **Self-Similarity** 57
- 2.3.1 General Causes of Self-Similar Behavior in Certain Situations in Fluid Mechanics and Heat Transfer 57
- 2.3.2 Implications of Self-Similarity in Experimental Studies 58
- 2.3.3 Particular Examples of Self-Similar Navier–Stokes Flows 59
- 2.3.4 Particular Examples of the Boundary Layer Flows 62
- 2.3.5 Gas Dynamics: Strong Explosion 79
- 2.3.6 Free-Surface Flows 80

References 82

2.1 Similitude, the Nondimensional Prototype and Model Flow Fields

An important class of experiments in fluid mechanics is that in which a model study of a prototype is to provide reliable information on the predicted flow properties of the associated prototype. It is this class of experiments in which the concept and principles of *similitude* are used to ensure a reliable transfer of information from the model study to the prototype. Specifically, dimensional measurements from the model (e.g., quantities such as pressure, velocity, angular speed, aerodynamic drag and lift) are used to predict the numerical values for the same quantities that would be present in the prototype flow field.

The fundamental basis for similitude is firmly grounded in the description of an experiment as a *boundary, and possibly an initial, value problem*. If the model flow can be made to represent exactly the same boundary (initial) value problem, then, of course, the *solution* to the model and prototype problems must be the same. The solution, as noted above, is represented by the experimental data acquired from the well-defined experiment. Since an *exact* solution often cannot be ensured one can substitute an *adequate* solution in order to gain useful predictions of the prototype's flow field.

This section of the Handbook is to provide guidance on how these *in principle* concepts can be transformed to *in practice* guidelines for representative application areas.

2.1.1 Governing Equations – Newtonian and Incompressible

Linearly viscous (Newtonian) fluids (air, water, oils, etc.) are widely present in fluid mechanics applications. Their ubiquity serves as part of the basis for the first restriction (Newtonian fluids in an incompressible flow environment) that is considered in this section.

The governing equations (with this restriction) are known for prototype and model flows. If the boundary and, if appropriate, initial conditions can also be made identical for the two flows, then identical solutions can be expected. This expectation is typically experienced in an experimental environment. Interesting exceptions can, and do, occur. For example, if one is investigating a *steady-state flow*, the observed values may show a strong sensitivity to the starting conditions (the initial transient period) for a given experiment. If this condition occurs, then different steady-state behaviors may exit as a result of differences in the initial transient period. Obviously, if the flow is turbulent, then only the appropriately averaged results can be predicted for the prototype from the measured model values.

The designation of an *incompressible* flow for the prototype and, therefore, for the model is one that includes many applications. The term *incompressible* must, of course, apply to the fluid. The common phrase *incompressible flow* indicates a flow in which $\mathrm{D}\rho/\mathrm{D}t = 0$ is adequately met. For gases, this is often characterized by the Mach number ≤ 0.3, where $\rho/\rho_0 \leq 0.956$ for an isentropic flow at this Mach number. Liquid flows form one segment of this class of flows, although dissolved gases that can lead to *water hammer* and explosions in a submerged liquid environment are two examples in which the incompressible assumption would not be physically appropriate. Low-speed gas flows are a second (and large) segment of this class. There are only two attributes of the flow field to be characterized for an incompressible flow: the velocity $\boldsymbol{V}(x, y, z, t)$ and the pressure $p(x, y, z, t)$ fields, where Cartesian coordinates are used to indicate the spatial and temporal dependencies of the dependent ($\boldsymbol{V}$, p) variables. Cartesian coordinates are used for symbolic convenience. The derived results are applicable to any coordinate system.

It is affirmed that the analyst will be able to identify a *characteristic* length (L) and velocity (U) to *scale* the problem. In some cases the selections for U and L will be apparent. The flow past an airfoil that is not influenced by the conditions at its lateral ends is advanced as an example of the apparent choices for U and L (Fig. 2.1). In other cases (Sect. 2.1.6), L and U may have to be *created* from other characteristic properties of the prototype flow field.

Using U and L, the governing equations can be made nondimensional (for an incompressible flow) as

$$\frac{\mathrm{D}\boldsymbol{V}^*}{\mathrm{D}t^*} = -\nabla^* p_k^* + \frac{1}{\mathrm{Re}}\nabla^{*^2}\boldsymbol{V}^* \,, \tag{2.1}$$

$$\nabla^* \boldsymbol{V}^* = 0 \,, \tag{2.2}$$

$$\mathrm{Re} = \frac{UL}{\nu} \,, \tag{2.3}$$

where $p_k^* = (p + \rho\, gh)/\rho U^2$, $\boldsymbol{V}^* = \boldsymbol{V}/U$ and $x^* = x/L$, $y^* = y/L$, $z^* = z/L$. Note, $\nu = \mu/\rho$ is the kinematic viscosity.

The term p_k clearly combines the (static) pressure and the gravitational body-force term as expressed by the elevation, h, above a datum plane. The ability to express the net force effect caused by ∇p and by $\nabla \rho\, gh$

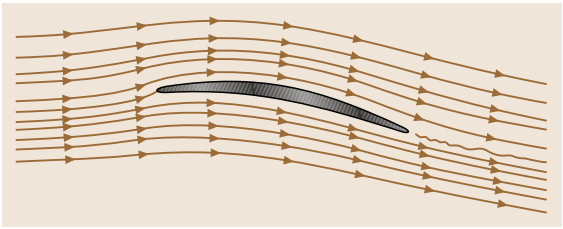

Fig. 2.1 Streamlines from a time averaged LES calculation of the flow past a Valeo CD airfoil as abstracted from the work of Moreau et al. [2.1]. Courtesy of D. R. Neal

permits this useful combination. Two other aspects of this form of the equations are noteworthy.

1. Any other body force (electrical, magnetic, etc.) that *can* be expressed using the gradient operator can be incorporated with (p and $\rho\, gh$), and
2. If the flow of a uniform density fluid exists in a submerged environment, then the portion of the pressure field that balances the body force effect need not be explicitly considered in the problem formulation. Specifically, the hydrostatic variation of pressure ($\partial p/\partial z = -\rho\, g$) does not contribute to the dynamics of the flow in such a submerged environment.

Examples wherein the electrical forces act as surface and not body forces include electrohydrodynamics and *leaky* dielectrics.

Identical governing equations for model and prototype are, therefore, obtained if the Reynolds number (Re) is the same for the two flows. This is a necessary (if viscous effects are present) but not a sufficient condition for similitude. It is also a condition that, in general, is easily satisfied when the similitude experiment is established.

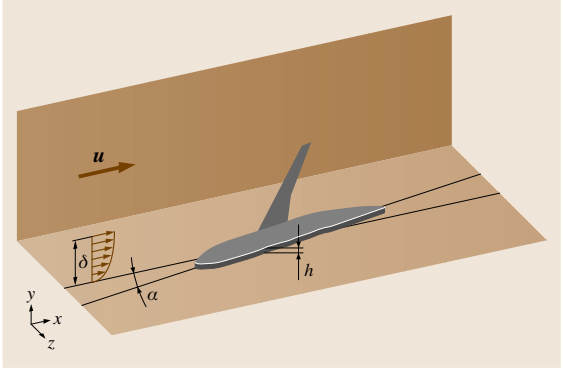

Fig. 2.2 Half-span model of an airplane

2.1.2 Boundary Conditions

Identical – or *adequately identical* – boundary conditions is often the greatest challenge for ensuring the same boundary-value problem between model and prototype. As a simple example, consider that the airfoil shape of Fig. 2.1 is the mid-span shape of a wing that

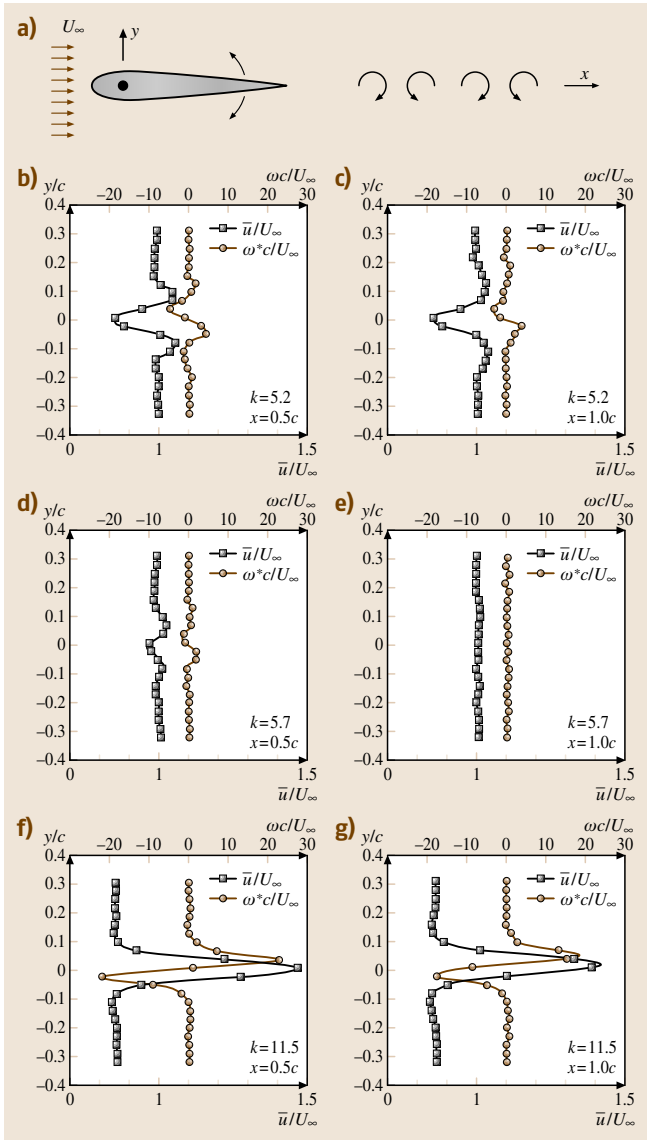

Fig. 2.3a–g A sinusoidally pitching airfoil as an example of an externally imposed reduced frequency. Note: i) the mean streamwise velocity ($\bar{u}$ and the transverse voriticy ($\bar{\omega}_z$) for $A = 2$ degrees oscillation amplitude are shown. ii) $k = \pi C f/U_0$

is attached to an airplane fuselage. If the wing were to be tested at model scale, then not only would the span-to-mid-chord-length ratio need to be represented but the flow at the wing root should also be accurately represented. This would require a full model of the airplane in order to ensure that the flow at the attachment location of the wing to the fuselage is properly represented. In order to make the model as large as possible for a given wind tunnel, a half model (attached to the tunnel wall as shown in Fig. 2.2) is often used in order to allow a larger length ratio: L_m/L_p in the model study. (Note: $[(\,)_m = (\,)_{model}$, $(\,)_p = (\,)_{prototype}]$.) A challenging aspect of such a model study is to ensure that important surface features: material roughness, (vents, hinges, etc.) are represented to proper scale. If the chord length is C (C now replaces the generalized L), then the rivet head diameter (d) and its protrusion (δ) should be the same relative size: (d/C) and (δ/C), for the model and the prototype. These details can be relaxed only if it is shown that such length ratios do not influence the flow parameters of interest. A challenge in wind tunnel studies is also presented by the bounding tunnel walls. If the imposed straight streamlines of the tunnel are different from the free streamlines (same nondimensional distance from the model), then the model-to-prototype common boundary conditions constraint would be violated. Adaptive tunnel walls and open test sections are two approaches to address this inherent *conflict* between using as large a model as possible for a given tunnel cross section.

2.1.3 Initial Conditions

If the flow field is one that temporally evolves from an initial condition, then the characterization of the initial conditions, in a manner that mimics that of the boundary conditions, must be established. The nondimensional representation of the evolving time will be

$$t^* = \frac{tU}{L} \,. \tag{2.4}$$

2.1.4 Parameters that Influence the Solution to the Boundary-Value and/or the Initial-Value (BV/IV) Problem

Nondimensional Time

There are two types of nondimensional times that must be considered in experimental fluid mechanics: the reduced frequency (ω_R) and Strouhal number (St).

Consider a flow field in which an external forcing function provides a *controlling influence* on the flow field. For example, the airfoil of Fig. 2.1 might be operated with a sinusoidal pitching motion where its angle of attack: $\alpha(t)$, is described as

$$\alpha(t) = \alpha_0 \sin \omega t \;;$$

this flow field is shown schematically in Fig. 2.3. A necessary condition for similitude between model and prototype will be that the imposed time variation is similar. Namely, the model and prototype must have equal reduced frequencies

$$\omega_R|_m = \left(\frac{\omega_0 L}{U_\infty}\right)_m = \omega_R|_p = \left(\frac{\omega_0 L}{U_\infty}\right)_p \,. \tag{2.5}$$

The nondimensional α_0 is itself a similarity parameter between the model and prototype. Note that, in this case, the characteristic length L is designated as the chord length C and the characteristic velocity U is designated as U_∞.

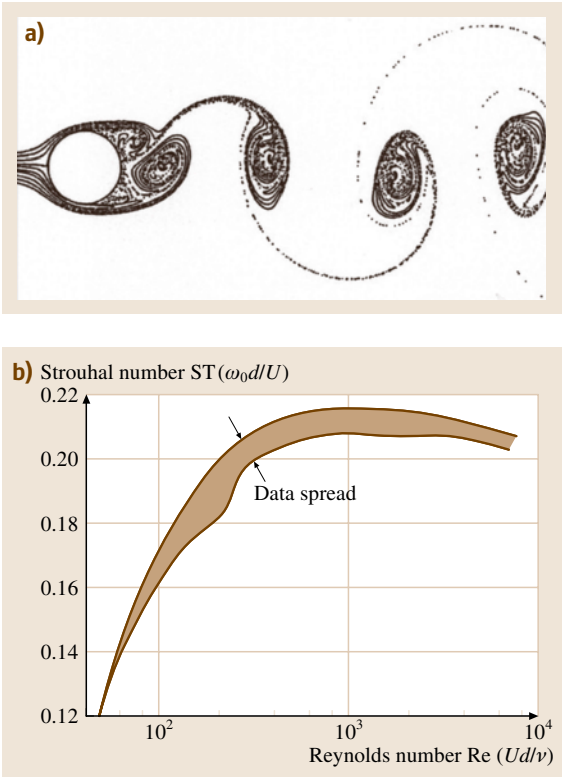

Fig. 2.4a,b Vortex shedding from a cylinder as an example of an intrinsic Strouhal number **(a)** A representation of the vortex shedding behind a cylinder **(b)** Strouhal number versus Reynolds number [2.2]

In contrast to the imposed (ω_0) time scale, which is characterized as a reduced frequency, the Strouhal number (St) represents a derived (or flow-field-dependent) time scale as in the case of *vortex shedding*. Here, the shedding frequency (f) of, for example, the flow past a cylinder (Fig. 2.4) represents a nondimensional quantity that is dependent upon the governing parameter for such a flow. Namely,

$$S_T = \frac{fd}{U_0} = \text{function(Re)}\,,$$

since, as stated above, the Re is the controlling parameter in the equation of motion.

Froude Number

Consider a flow in which the gravitational body force influences the velocity field. Specifically, consider a flow in which the gradient of ($\rho\, gh$) must be considered in the BV problem. Figure 2.5, in which an airfoil serves as a hydrofoil near the free surface, provides a specific example.

Let H represent the immersion depth to the 1/4 chord location of the hydrofoil. It is considered to be apparent that the flow over the hydrofoil will be influenced by this immersion depth if H/C is sufficiently small. H/C then becomes a length scale ratio that defines one of the boundary conditions of the BV problem.

The relative body force effect is, for this BV problem, expressed by the nondimensional parameter:

$$\text{Froude no.} = \text{FR} = \frac{\rho U_0^2}{\rho\, gC} = \frac{U_0^2}{gC} \tag{2.6}$$

for this $\rho =$ constant (below the free surface) BV problem.

For completeness, it is noted that h, the elevation above a datum plane, was made nondimensional with the chord length as (h/C) in order to isolate the Froude number as a *governing parameter* in this BV problem.

The relative influence of the gravitational body force is expressed by two parameters: H/C and (U_0^2/gC). It is instructive to note that a large value of H/C renders U^2/gC irrelevant. Physically, it is observed that a planar free surface above the submerged hydrofoil indicates that the hydrofoil will not experience a dynamically significant influence on its pressure distribution from the body force term.

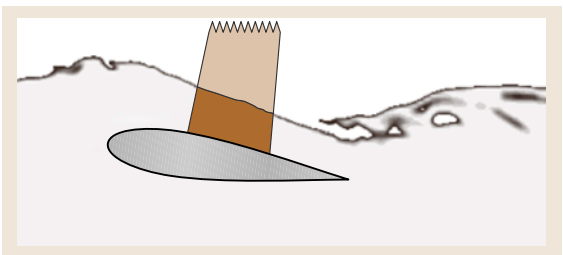

Fig. 2.5 A near-free-surface hydrofoil flow

It is quite difficult to satisfy *both* Re and FR matching in an application where both play important roles. The hydrofoil of Fig. 2.5 provides a relevant example. Specifically, for matched Froude numbers:

$$\left.\frac{U^2}{gC}\right|_m = \left.\frac{U^2}{gC}\right|_p$$

and matched Reynolds number values,

$$\left.\frac{UC}{\nu}\right|_m = \left.\frac{UC}{\nu}\right|_p\,,$$

the combined constraints require that

$$\frac{U_m^2}{U_p^2} = \frac{C_m}{C_p} = \frac{\nu_m}{\nu_p}\frac{U_p}{U_m}$$

or

$$\frac{U_m^3}{U_p^3} = \frac{\nu_m}{\nu_p}\,. \tag{2.7}$$

It is apparent that liquids with the indicated ratio of ν values would be difficult to find (in bulk) if U_m and U_p were very different.

The practical solution, in those cases (e.g., surface ships) where the FR is the dominant parameter, is to match the FR and to make corrections for the Re mismatch.

Densimetric Froude Number

Consider that the approach airflow, for the airfoil of Fig. 2.1, experiences a strong temperature increase as a result of absorbing thermal energy from a heated airfoil. It can clearly be expected that the wake of the airfoil will be influenced by these elevated temperatures. Specifically, the wake fluid would be lifted by the buoyancy provided by the surrounding ambient temperature fluid acting on the heated wake fluid.

The control parameter that ensures similarity between model and prototype would be the densimetric Froude number

$$\text{FR}|_D = \frac{(\Delta\rho)gC}{\rho_0 U_0^2}\,, \tag{2.8}$$

where $\Delta\rho$ would express a characteristic density change in the airflow and ρ_0 would be the density of the approach flow. [Since, for a perfect gas, $p = \rho RT$ and

the absolute pressure can be taken to be a constant, the $\Delta\rho/\rho_0$ value could be obtained from a characteristic temperature change as $-\Delta\rho/\rho_0 = \Delta T/T_0$ if $\Delta T/T_0$ is sufficiently small: $(\Delta T/T_0) \ll 1$.] Again, it is noted that the elevation term, h, is made nondimensional with C in this example.

As noted before, it would not be expected that a condition of complete similarity would be obtained. If density effects are dominant, then Re corrections would have to be made in the model results while the densitometric Froude number was held constant between model and prototype.

Weber Number

Surface tension effects, the presence of mechanical stresses that are present at the gas–liquid or the gas–liquid–solid boundary, can be an important factor in establishing the behavior of a liquid flow bounded by a gaseous medium. The basic property that describes the effect of the surface tension is the parameter σ or the *surface* tension force per unit length.

It is important to understand that σ is introduced in order to *preserve* the continuum mechanics understanding that the pressure is isotropic. That is, that *pressure* is unchanged in the neighborhood of the free surface whereas the normal stresses in the plane of, and those normal to, the gas–liquid interface are not equal. If the physical problem under consideration admits the introduction of a single quantity, σ, to describe the complex physical chemistry (Sect. 3.1.2) at the gas–liquid interface, then the Weber number (We) will be represented in the problem description as

$$\mathrm{We} = \frac{\rho U^2 L}{\sigma} \,. \tag{2.9}$$

If the prototype involves significant surface tension effects as well as viscous effects, then the challenge would be to equate both parameters as:

$$\rho\frac{UL}{\mu}\bigg|_{\mathrm{m}} = \rho\frac{UL}{\mu}\bigg|_{\mathrm{p}}$$

and

$$\rho\frac{U^2 L}{\sigma}\bigg|_{\mathrm{m}} = \rho\frac{U^2 L}{\sigma}\bigg|_{\mathrm{p}}$$

or

$$\frac{\mu U}{\sigma}\bigg|_{\mathrm{m}} = \frac{\mu U}{\sigma}\bigg|_{\mathrm{p}} \,, \tag{2.10}$$

where the indicated ratio is referred to as the capillary number. Hence the liquid materials and the velocities would have to be selected to satisfy the capillary number constraint if a condition of similitude were to be established.

If the σ, μ and U values cannot be so manipulated, the experimentalist can attempt to *bracket* the correct condition or to make analytical adjustments to the data to gain an approximation to the complete similitude condition.

2.1.5 Governing Equations – Newtonian and Compressible

The Lagrangian (or material) derivative of the density of a fluid dynamic particle (fixed mass element) can be used to define a compressible flow succinctly. Namely,

$$\frac{\mathrm{D}\rho}{\mathrm{D}t} \neq 0 \tag{2.11}$$

denotes a compressible flow.

Thompson [2.3] provides an excellent introduction to similitude considerations for compressible flows; this reference is recommended for a more thorough exposition of the compressible flow issues considered in this section.

A fundamental statement of the conservation of mass for an Eulerian cube can be written as

$$0 = \frac{\partial\rho}{\partial t} + \nabla\cdot\rho\boldsymbol{V} \tag{2.12}$$

from which

$$\nabla\cdot\boldsymbol{V} = -\frac{1}{\rho}\frac{\mathrm{D}\rho}{\mathrm{D}t} \tag{2.13}$$

follows.

Thompson makes use of (2.13) to develop a nondimensional representation of $\nabla\cdot\boldsymbol{V}$ as {[2.3] (3.46)}

$$\begin{aligned}\nabla\cdot U = {} & \frac{c_0^2}{c^2}\left(\frac{\mathrm{M}_0^2}{2}U\cdot\nabla U^2 - U\cdot\tilde{G}\right) \\ & + \frac{c_0^2}{c^2}\frac{l_0}{c_0 l_0}\left(\frac{\mathrm{M}_0}{2}\frac{\partial U^2}{\partial\tau} - \frac{\rho_0}{\rho}\frac{\partial\tilde{P}}{\partial\tau}\right) \\ & - \frac{\rho_0 c_0^2}{\rho c^2}\frac{\mathrm{M}_0^2}{\mathrm{Re}_0}\Bigg[U\cdot\nabla^2 U \\ & + \left(\frac{\mu_\nu}{\mu} + \frac{1}{3}\right)U\cdot\nabla(\nabla\cdot U)\Bigg] \\ & + \frac{1}{\mathrm{Re}_0}\frac{T_0}{\nu_0}\left(\frac{\partial\nu}{\partial T}\right)_{\mathrm{p}}\left(\frac{u_0^2}{c_{\mathrm{p}}T_0}\tilde{\gamma} + \frac{1}{\mathrm{Pr}}\nabla^2\tilde{T}\right) \,,\end{aligned} \tag{2.14}$$

where the nondimensional values are defined as {[2.3] (3.45)}

$$U = \frac{u}{u_0}\,, \qquad \tilde{G} = \frac{G l_0}{c_0^2}\,, \qquad X = \frac{x}{l_0}\,,$$
$$\tilde{P} = \frac{P}{\rho_0 c_0 u_0}\,, \qquad \tau = \frac{t}{t_0}\,, \qquad \tilde{\gamma} = \frac{l_0^2}{\mu u_0^2}\gamma\,,$$
$$\tilde{T} = \frac{T}{T_0}\,, \tag{2.15}$$

and the parameters {[2.3] (3.47)}

$$\text{Mach number:} \qquad \mathrm{M}_0 \equiv \frac{u_0}{c_0}\,,$$
$$\text{Reynolds number:} \qquad \mathrm{Re}_0 \equiv \frac{\rho_0 u_0 l_0}{\mu}\,,$$
$$\text{Prandtl number:} \qquad \mathrm{Pr} \equiv \frac{\mu c_\mathrm{p}}{k}\,, \tag{2.16}$$

arise naturally in the subject equation. The nomenclature for this subsection is adapted from Thompson's text. As noted, that presentation is strongly recommended for those interested in compressible flows and the present nomenclature change will facilitate the use of that reference. For completeness, it is noted that $V = u$, $L = l_0$, and $g = G$ when comparing the present nomenclature to that of Thompson. Note that G represents the body force and γ represents the dissipation or degradation of kinetic energy to the thermal form.

It is apparent that the addition of compressibility adds greatly to the complexity of the similitude considerations. It is also apparent that mutually satisfying the Mach number and Reynolds number constraints for a given model study will be essentially impossible as shown by the following.

Substitute the Mach-number-based velocity ratio into the Reynolds number as

$$\frac{u_0|_\mathrm{m}}{u_0|_\mathrm{p}} = \frac{\rho_0 l_0|_\mathrm{p}}{\rho_0 l_0|_\mathrm{m}} \frac{\mu_\mathrm{m}}{\mu_\mathrm{p}} = \frac{c_0|_\mathrm{m}}{c_0|_\mathrm{p}}\,.$$

Isolate the length ratio as

$$\frac{l_0|_\mathrm{m}}{l_0|_\mathrm{p}} = \frac{\rho_0|_\mathrm{p}}{\rho_0|_\mathrm{m}} \left(\frac{\mu_\mathrm{m}}{\mu_\mathrm{p}} \frac{c_0|_\mathrm{p}}{c_0|_\mathrm{m}} \right)\,. \tag{2.17}$$

Consider the representative application of a high-speed aircraft ($\mathrm{M}_0 = 3.5$) that is to be evaluated in a model study. A length ratio of 50:1 would be typically enforced by the available tunnel size. The bracketed term, the right-hand side of (2.17), will be sensitive to the model-to-prototype temperature ratio. To decrease $(\mu_\mathrm{m}/\mu_\mathrm{p})$, the model study temperature would need to be reduced since, for a gas, $\partial\mu/\partial T > 0$. Given the *low* temperature of the prototype environment (at altitude) this is a difficult condition to achieve. To increase $c_0|_\mathrm{m}/c_0|_\mathrm{p}$ would require the opposite condition: an elevated temperature of the model flow.

A pressurized tunnel would address the $(\rho_0|_\mathrm{p}/\rho_0|_\mathrm{m})$ ratio but this is at the price of mechanical complexity and limited capability to match the required length ratio.

The practical solution is to match the Mach number values (independent of the length ratio) and attempt to address Reynolds number issues via computational corrections.

2.1.6 Flows for Which *U* and *L* May Not Be Apparent

Some flows, unlike the airfoil example discussed above, do not offer an apparent length or velocity scale. This section provides examples that suggest strategies to extract fabricated length and/or velocity scales in such circumstances. The fabricated scales then allow the experimentalist to directly utilize the parameters as described above.

A *U*-Tube Flow

Figure 2.6 shows a U-shaped tube with, at time $t \le 0$, an elevated liquid column on one side. The fluid viscosity and density are ν and ρ and the tube diameter is D. The initial elevation difference is $h(0)$. If a model study

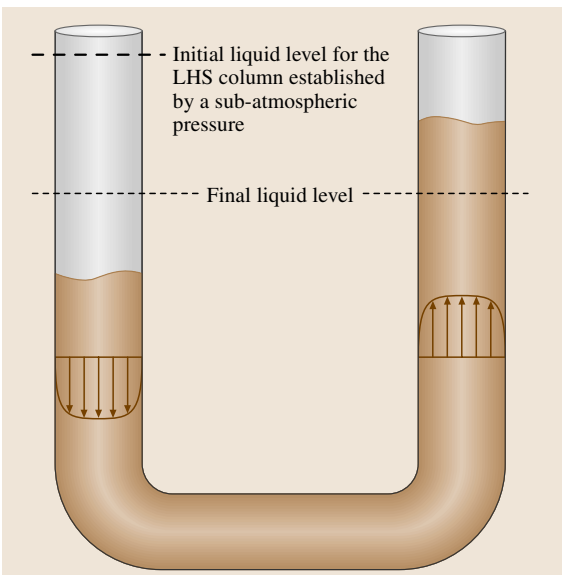

Fig. 2.6 A U-tube flow

were to be made of the prototype, it is apparent that the Reynolds number should be used as the similarity parameter with D as the length scale.

Since the flow will start with the release of the *holding pressure* (either negative on the high side or positive on the low side) there is no velocity for $t \leq 0$. The elevation difference can, however, be used to express a characteristic velocity as

$$U = \sqrt{gh} \tag{2.18}$$

from which

$$\mathrm{Re} = \frac{UD}{\nu} = \frac{\sqrt{gh(0)}D}{\nu}$$

would provide a necessary condition for model-to-prototype similarity.

If surface tension were important in the prototype, then the Weber number would also have to be matched as

$$\mathrm{We} = \frac{\rho U^2 L}{\sigma} = \frac{\rho g h(0) D}{\sigma} \, .$$

It is interesting to observe that, if We is important for the prototype, then

$$\frac{\sigma_\mathrm{m}}{\sigma_\mathrm{p}} = \frac{\left\{\mu\,[gh(0)]^{1/2}\right\}_\mathrm{m}}{\left\{\mu\,[gh(0)]^{1/2}\right\}_\mathrm{p}} \, . \tag{2.19}$$

That is, σ_m and σ_p must satisfy this additional constraint. If We is not important for the prototype, the experimentalist would need to ensure that it is also not important in the model study.

A Single Stream Shear Layer

One of the many possible examples of a flow without a defined length scale is that of a single stream shear layer. Figure 2.7 presents a schematic representation of such a flow which, in its idealized form, draws fluid from $y = -\infty$ by the entrainment action of the *infinitely wide* primary flow whose velocity scale is U_0.

Morris and *Foss* [2.4] provide a detailed examination of the developing region in which the separating turbulent boundary layer gradually loses its identity and a self-preserving single stream shear layer is established. As emphasized in that reference, and in the numerous prior studies cited by these authors, this is a flow without a defined length scale.

By convention and because it provides a well-defined experimental length scale, the momentum thickness at

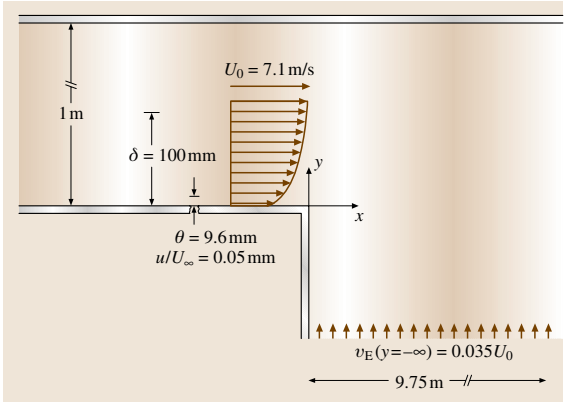

Fig. 2.7 The momentum thickness at $x = 0$ for a single stream shear layer: the flow's *length scale*

$x = 0$ is utilized as the reference condition for both the separating boundary layer and the evolving shear layer. Specifically, in the cited study, $R_{\theta(0)} = U_0\theta(0)/\nu$ was 4860 at $x = 0$ and the self-preservation condition for the shear layer was established by $x/\theta(0) = 200$. The required length to establish self-preservation is a function of R_θ, as discussed in detail in that reference.

For completeness, it is worth noting that a planar jet (width w) is a flow *with* a defined length scale. In that flow, the role of $\theta(0)$ becomes one of a characterizing length scale ratio, $\theta(0)/w$, but the Reynolds number would be characterized as

$$\mathrm{Re} = \frac{wU_0}{\nu} \, ,$$

if the jet, and not the separating shear layer at the sides of the jet, was the focus of the investigation. It can be readily appreciated that the jet flow, especially the region near the jet exit, will be influenced by the momentum thickness at the jet exit and, if turbulent, the relevant characteristics of the turbulent motion at the jet exit. These features constitute the influence of the boundary conditions on the solution.

However, as discussed by *Yarin* in Sect. 2.3, at sufficiently large streamwise locations the idealization that the jet nozzle width is effectively zero and the exit velocity is effectively infinite (in such a manner that the *line-source momentum flux*, $\dot{M}$, describes each downstream plane's momentum flux) leads to a condition of self-similarity. An extension to this modeling idealization is that all flows with the same $\dot{M}$ value and sufficient streamwise distance will have the same flow fields given the same distance from the apparent origin.

A Spinning Disc

Consider a flat and spinning disc whose diameter extends far beyond the central region of experimental interest. A flow from the central region outward will be established by the spinning motion. There is no apparent length scale in this problem albeit the viscous effects (i.e. Re) obviously play an important role in the resulting velocity field.

The angular speed, ω, combined with the fluid kinematic viscosity, ν, can be combined to form a velocity scale

$$U \sim \sqrt{\omega\nu}\,, \tag{2.20}$$

as well as a length scale

$$L \sim \sqrt{\frac{\nu}{\omega}}\,. \tag{2.21}$$

Not surprisingly, with these definitions, the Re value becomes unity:

$$\mathrm{Re} = \frac{\sqrt{\omega\nu}\sqrt{\nu/\omega}}{\nu} = 1 \tag{2.22}$$

and, as a result, all nondimensional and nonturbulent velocity fields are identical. That is, $\boldsymbol{V}^*(r^*, z^*)$ will be the same for any ν and ω, where

$$\boldsymbol{V}^* = \frac{\boldsymbol{V}(r, z)}{U} \tag{2.23}$$

and

$$r^* = \frac{r}{L}\,, \quad z^* = \frac{z}{L}\,. \tag{2.24}$$

A turbulent flow established by the rotating discs will have the same scaling parameters and its time-averaged quantities will, similarly, be identical at the same (r^*, z^*) positions.

This example problem is also a celebrated example of a clever analytical solution. It was carried out by *von Kármán* [2.5] and is presented in detail by *White* [2.6]. The latter reference does not make explicit use of the above result that $\mathrm{Re} = 1$; however, this result is fully compatible with White's presentation. Specifically, from (3-183) of [2.6]

$$\begin{aligned} v_r &= r\omega F(z^*)\,, & v_\theta &= r\omega G(z^*)\,, \\ v_Z &= \sqrt{\omega\nu}H(z^*)\,, & p &= \rho\omega\nu P(z^*)\,. \end{aligned} \tag{2.25}$$

It is evident, using the symbols of (2.20–2.24) above, that White's equations (3-183) are compatible with the message of this section. Specifically, with the normalization provided by (2.20)

$$v_z^* = H(z^*) \quad \text{and} \quad p^* = P(z^*)\,,$$

and with the added normalization provided by (2.21),

$$v_r^* = r^*(Fz^*) \quad \text{and} \quad v_\theta^* = r^*(Gz^*)\,. \tag{2.26}$$

It is useful to note that the von Kármán solution (2.25, 26) is a good example of the self-similarity solutions that are considered in Sect. 2.3.

The viewpoint expressed in this presentation does differ with White in a substantive manner with regard to the cited experimental result (from the work of *Kobayashi* et al. [2.7]) that instabilities occur for

$$\mathrm{Re} = \frac{\omega r^2}{\nu} = 8.8\times10^4$$

with the added result that turbulence is observed at $\mathrm{Re} = 3.2\times10^5$.

The disagreement can be stated as follows: *It is not* correct *to state these values as a Reynolds number since* $\mathrm{Re} \equiv 1$ *in the understanding of this section. Rather, the quoted values are simply nondimensional* (radii)^2 and *their universal values attest to the present statement that all such flows are in a condition of similitude with unit Re.*

To carry the argument further for its instructive value, consider that two experimentalists were to make measurements using *large* but different disc diameters. Large, in this context, would be an r_0 value whose r_0^* is much larger than 3.2×10^5. If the experimentalists used the same ω value and their large, but finite, disc sizes (r_0) to specify a Reynolds number as they examined the issue of *when does turbulence occur*, they would conclude that the transition value for r/r_0 would be different in the two experiments.

It is instructive, in this example, that the similarity parameters for an idealized ($r_0 \to \infty$) experiment yield a more useful result than the similarity parameters ($U_0 = r_0\omega$, $L = r_0$) that would be suggested by the physical experiment.

Finally, for this example, it is considered to be evident that the von Kármán solution will be invalid as the observation location approaches the coordinates $r \to r_0$ for $z \ll r_0$ and for smaller r as z increases (where r_0 is the radius of the experimental plate).

2.2 Dimensional Analysis and Data Organization

The organization and interpretation of experimental data is an essential activity that requires careful thought. There is not a specific recipe for organizing data. Ingenuity, insight, analysis, and creative ideas are needed. However, there are some concepts and methods that will provide guidance. One basic principle is that the simplest relationship will have the fewest number of variables. Another basic principle is that the simplest relationship will use nondimensional variables. *Dimensional analysis* is the basic procedure to produce nondimensional variables, but it needs to be refined and supplemented. Section 2.2 will present the elements of dimensional analysis followed by several examples that illustrate exceptional cases and supplemental techniques. The examples demonstrate the general features of dimensional analysis. They provide results that could in some cases be obtained from familiar analyses of fluid mechanics. The agreement between the dimensional analysis results and those from general fluid mechanics will give confidence in the ability of dimensional analysis to give valuable results in complex new problems.

The presentation of numerical results should have the most extensive validity. This is not always done. Consider the following formula to predict the flow rate of natural gas through a pipeline. Based on experimental data the following is an algebraic curve fit used in industry.

$$Q_0 = 737 \frac{T_0}{p_0} d^{2.53} \left(\frac{p_1^2 - p_2^2}{L_\mathrm{m} G T_\mathrm{f}} \right)^{0.510} \tag{2.27}$$

where Q_0 is the standard cubic feet per day, T_0 is the reference temperature in °R, p_0 is the reference pressure in psia, d is the pipe dimeter in inches, T_f is the fluid temperature in °R, L_m is the pipe length in miles, p_1 is the initial pressure in psia, p_2 is the final pressure in psia, G specific gravity referenced to air at 60 °F and 14.696 psia.

The constants in (2.27) implicitly have units raised to irrational powers. For example, $d^{2.53}$ must be compensated for by a length dimension with power of -2.53. It would be inappropriate to use this formula for a CO_2 pipeline. Such dimensional formulas exist in most applied fields and are quite useful. However, from a scientific viewpoint a simpler and universally valid formula could be developed, one that in principle could be applied to CO_2. The data used to produce (2.27) could have been organized into a more universal form.

2.2.1 Variables, Function List, and Extra Information

A physical experiment, event, or situation is in principle described quantitatively by a mathematical function. It is a mathematical necessity to have one dependent variable. The remaining variables are independent variables or parameters as we choose to regard them. Whether a variable is independent or a parameter is a physical choice. A correct list of variables requires knowledge of physics and is sometimes not an easy task. After a variable list is established, one should employ known physical equations and extra assumptions that reduce the number of variables.

As an example consider the question of the pressure drop between two stations, denoted as 1 and 2, in a straight pipe when the flow is incompressible. The variables are p pressure, z elevation, ρ density, ν kinematic viscosity, Q volume flow rate, g acceleration of gravity, D pipe diameter, ε relative roughness of pipe wall, L length of pipe between 1 and 2. Consider the second pressure as the dependent variable.

$$p_2 = f(p_1, \rho, Q, D, L, \varepsilon, \nu, g, z_1, z_2) \,. \tag{2.28}$$

We have already used some knowledge of the physics in making this list. Velocity is not included because it is given by the flow rate divided by the cross-section area. The temperature of the fluid is not included because heat transfer effects are separated from flow effects in incompressible flow.

The problem can be simplified if we observe the kinetic energy equation (1.71) for incompressible flow. It is written in average values as

$$\left(p_2 + \rho \frac{1}{2} V_2^2 + \rho g z_2 \right) - \left(p_1 + \rho \frac{1}{2} V_1^2 + \rho g z_1 \right) = - \int \Phi \, \mathrm{d}A \, \mathrm{d}x = h_\mathrm{L} \,. \tag{2.29}$$

To be more precise one sometimes uses a coefficient in front of V_1^2 to account for the shape of the velocity profile. Here Φ is the viscous dissipation. The integral over the cross section $\mathrm{d}A$ and pipe length $\mathrm{d}x$ represents the head loss h_L between stations 1 and 2. We assume the flow in the straight pipe is fully developed so that the velocities at 1 and 2 are the same. Moreover, the dissipation depends on the velocity profile, which is unchanged along the length and does not depend on

z or p. Comparing (2.28) and (2.29) we write

$$(p_2+\rho g z_2)-(p_1+\rho g z_1)=f_1(\rho, Q, D, L, \varepsilon, \nu)\,. \tag{2.30}$$

Furthermore, we propose that the dissipation should increase directly with the length of the pipe. To be precise $\int \Phi\,\mathrm{d}A\,\mathrm{d}x = L\int \Phi\,\mathrm{d}A$.

$$\begin{aligned}(p_2+\rho g z_2)-(p_1+\rho g z_1) &= L f_2(\rho Q D \varepsilon \nu)\,,\\ \frac{\mathcal{P}_2-\mathcal{P}_1}{L} \equiv \frac{(p_2+\rho g z_2)-(p_1+\rho g z_1)}{L} &= f_2(\rho, Q, D, \varepsilon, \nu)\,.\end{aligned} \tag{2.31}$$

Thus, based on physics and guesswork the number of variables has been reduced from 11 to six. Moreover it will not be necessary to test at different values of p_1 or different changes in elevation, or even different lengths of pipes.

2.2.2 Dimensions and Scale Ratios

The basis of simplifying mathematical relationships that contain physical variables is dimensional analysis. We may define two categories of variables. Things that are counted are dimensionless. For instance, the number of molecules or the number of people in a room is dimensionless. Things that are measured require that we essentially compare the item to a scale that has a defined unit. An example here is the length of a room or its floor area. The size of a scale unit is arbitrary. There are no universal natural size units that are relevant to all physical processes. Dimensional analysis employs the fact that a physical event is independent of the scale units used to measure the variables.

Consider a length variable that has a size l when measured with a certain length unit. If a new length unit is used the value becomes $\hat{l}$. The *dimension symbol* L is the ratio of the new unit to the old unit

$$\hat{l} = lL\,. \tag{2.32}$$

In a similar way a time unit could be changed with scale unit ratio T or a mass unit could be changed with a scale unit ratio M

$$\hat{t} = tT\,, \tag{2.33}$$

$$\hat{m} = mM\,. \tag{2.34}$$

We could also imagine a force unit with a scale change ratio F.

$$\hat{f} = fF\,. \tag{2.35}$$

The symbols F, M, L, and T stand for scale change ratios for an imaginary process of changing units.

It is a fact of experience that three dimensions are sufficient to measure any physical quantity. These are called primary dimensions and may be taken as M, L, and T. Equivalently we could take F, L, and T as *primary dimensions*. However, the choice of four primary dimensions is redundant and requires, in general, that we expand the list of variables to include a *unifying dimensional constant*. The choice F, M, L, and T requires the unifying constant g_c with dimensions ML/FT^2. In principle, equations such as Newton's second law should be written with the constant included.

$$\mathcal{F} = \frac{ma}{g_c} \tag{2.36}$$

Here $\mathcal{F}$ is force and a is the acceleration. Current custom is to write equations as if a consistent system of units is employed. The dimensional constant is required in the English Engineering system, but not in the international SI system.

All other physical variables have dimensions that are combinations of the primary dimensions raised to some power. For example a velocity is

$$\hat{v} = \frac{\mathrm{d}\hat{l}}{\mathrm{d}\hat{t}} = \frac{\mathrm{d}(lL)}{\mathrm{d}(tT)} = \frac{L}{T}\frac{\mathrm{d}l}{\mathrm{d}t} = L^1 T^{-1} v\,. \tag{2.37}$$

To be precise, the value of a variable in new units $\hat{x}$ is related to the size in old units x by

$$\hat{x} = x M^a L^b T^c\,. \tag{2.38}$$

Bridgman [2.8] first derived this equation. Not all scale units will change in this manner. A pressure measured in decibels does not fit this relation. The Richter scale for earthquake intensity or the Rockwell hardness scale for metals are other examples of units that do not obey Bridgman's equation. However, all physical concepts can be measured with primary units so that they obey the Bridgman equation.

2.2.3 Natural Scales and Repeating Variables

As an introduction to the essential elements of dimensional analysis consider the problem of the incompressible flow at speed V over a cylinder of diameter D. The fluid density is ρ and its viscosity is μ. The question is what is the frequency ω of the *von Kármán vortex street*? The proposed mathematical function is

$$\omega = f(V, D, \rho, \mu)\,. \tag{2.39}$$

It is useful to form a *dimensional matrix* that contains the coefficients a, b, c of Bridgman's (2.38) for each variable. For instance the frequency equation is

$$\hat{\omega} = \omega T^{-1} \,. \tag{2.40}$$

The powers 0, 0, −1 are placed in the matrix.

	ω	V	D	ρ	μ
M	0	0	0	1	1
L	0	1	1	−3	−1
T	−1	−1	0	0	−1

Here we have chosen M, L, and T as the primary dimensions.

Consider the variables V, D, and ρ. What combination of these variables will produce a variable with the dimension of length? The obvious answer is D. What combination of these variables will produce a variable with the dimension of time? The answer is D/V. What combination of these variables will produce a variable with the dimension of mass? The answer is ρD^3. Instead of measuring mass quantities in units of kilograms, we will use the value of ρD^3 as the unit. This is a natural unit for this physical phenomenon. Length, time, and mass units that are associated with the physical event are

$$\begin{aligned} L_{\text{event}} &= D \,, \\ T_{\text{event}} &= \frac{D}{V} \,, \\ M_{\text{event}} &= \rho D^3 \,. \end{aligned} \tag{2.41}$$

The frequency variable has the dimension of $1/T$ and the viscosity variable has the dimensions of mass/(length-time).

$$\omega \left[\frac{1}{T}\right] \,, \quad \mu \left[\frac{M}{\mathrm{LT}}\right] \,. \tag{2.42}$$

Multiplying frequency and viscosity to eliminate the appropriate units produces nondimensional variables:

$$\Pi_1 = \omega\left(\frac{D}{V}\right) = \frac{\omega V}{D} \,, \quad \Pi_2 = \frac{\mu D(D/V)}{\rho D^3} = \frac{\mu}{\rho D V} \,. \tag{2.43}$$

One can observe that Π_1 is the reduced frequency and Π_2 is the reciprocal of the Reynolds number that was introduced in Sect. 2.1. This method of producing nondimensional variables is known as the method of scales. The mass, length and time units that society has defined in order to quantify physical variables are arbitrary and are not inherent to the physical event under study. We can form mass, length, and time units from variables associated with the event. Using these as units essentially produces nondimensional variables of a universal magnitude.

Let us look at the method of scales in a more general context. Consider a physical experiment that has n dimensional variables. There is one dependent variable that we write on the left-hand side

$$x_n = f(x_1, x_2, x_3, \ldots, x_{n-1}) \,. \tag{2.44}$$

A given experiment might have several dependent variables of interest, but we should deal with them and their functions one at a time. A physical process is independent of the units used to make the measurements. Thus, in the rescaled units the same function holds

$$\hat{x}_n = f(\hat{x}_1, \hat{x}_2, \hat{x}_3, \ldots, \hat{x}_{n-1}) \,. \tag{2.45}$$

Let us use three primary dimensions. If the scale units were changed, the first three variables would change according to

$$\begin{aligned} \hat{x}_1 &= x_1 M^{a_1} L^{b_1} T^{c_1} \,, \\ \hat{x}_2 &= x_2 M^{a_2} L^{b_2} T^{c_2} \,, \\ \hat{x}_3 &= x_3 M^{a_3} L^{b_3} T^{c_3} \,. \end{aligned} \tag{2.46}$$

All other x variables would change by similar relations. a, b, c are known coefficients of the Bridgman equations.

Consider the following question, is there a combination of x_1, x_2, x_3 in (2.46) that, when raised to some powers, α, β, γ, has the dimension of mass? The choice of the first three variables in the list is arbitrary. The variables can be renumbered or relisted as we see fit. The variables chosen as x_1, x_2, x_3 are called repeating variables. Let the combination that produces a mass scale y_{M} be

$$y_{\mathrm{M}} = x_1^{\alpha_{\mathrm{M}}} x_2^{\beta_{\mathrm{M}}} x_3^{\gamma_{\mathrm{M}}} \,. \tag{2.47}$$

After a change in scale units the value would be

$$\hat{y}_{\mathrm{M}} = (\hat{x}_1)^{\alpha_{\mathrm{M}}} (\hat{x}_2)^{\beta_{\mathrm{M}}} (\hat{x}_3)^{\gamma_{\mathrm{M}}} \,. \tag{2.48}$$

Inserting the relations (2.47) and (2.48) into (2.41) yields

$$\begin{aligned} \hat{y}_{\mathrm{M}} &= (\hat{x}_1)^{\alpha_{\mathrm{M}}} (\hat{x}_2)^{\beta_{\mathrm{M}}} (\hat{x}_3)^{\gamma_{\mathrm{M}}} \\ &= x_1^{\alpha_{\mathrm{M}}} x_2^{\beta_{\mathrm{M}}} x_3^{\gamma_{\mathrm{M}}} M^{\alpha_{\mathrm{M}} a_1 + \beta_{\mathrm{M}} a_2 + \gamma_{\mathrm{M}} a_3} \\ &\quad \times L^{\alpha_{\mathrm{M}} b_1 + \beta_{\mathrm{M}} b_2 + \gamma_{\mathrm{M}} b_3} T^{\alpha_{\mathrm{M}} c_1 + \beta_{\mathrm{M}} c_2 + \gamma_{\mathrm{M}} c_3} \,. \end{aligned} \tag{2.49}$$

However, by design we want y_{M} to have the dimension of mass. Thus, we require that

$$\hat{y}_{\mathrm{M}} = y_{\mathrm{M}} M^1 L^0 T^0 \,. \tag{2.50}$$

Comparing (2.50) and (2.49) shows that that the powers of M, L, and T obey the relations

$$\begin{aligned}\alpha_M a_1 + \beta_M a_2 + \gamma_M a_3 &= 1\,,\\ \alpha_M b_1 + \beta_M b_2 + \gamma_M b_3 &= 0\,,\\ \alpha_M c_1 + \beta_M c_2 + \gamma_M c_3 &= 0\,.\end{aligned} \tag{2.51}$$

For given choices of x_1, x_2, and x_3 the coefficients a, b and c are known, and values α_M, β_M and γ_M are to be found. Cramer's rule says that a unique solution of the nonhomogeneous equation set is possible if the determinate of the coefficient matrix is not zero.

$$\det \begin{vmatrix} a_1 & a_2 & a_3 \\ b_1 & b_2 & b_3 \\ c_1 & c_2 & c_3 \end{vmatrix} \neq 0 \tag{2.52}$$

In other words the *rank of the coefficient matrix* must be three. The rank is the size of the largest square submatrix that has a nonzero determinate. If the variables x_1, x_2, x_3 are chosen so that the rank of the dimensional matrix is three we will be able to form a mass scale from them.

We can continue to form a combination variable with the dimension of length using the same x_1, x_2, x_3. The algebra problem to find another set of coefficients α_L, β_L, γ_L is the same problem as (2.50) except that the inhomogeneous right hand side is now 0, 1, 0. A solution is still guaranteed because the coefficient matrix (2.51) is unchanged and it rank is still three. Moreover, the same process can be repeated to produce a time variable. Bridgman's equations for the length and time units are

$$\hat{y}_L = y_L M^0 L^1 T^0\,, \tag{2.53}$$

$$\hat{y}_T = y_T M^0 L^0 T^1\,. \tag{2.54}$$

The critical issue is that the choice of *repeating variables* x_1, x_2, x_3 is valid for all three problems if the rank of their dimensional matrix is three. If so, x_1, x_2, x_3 are said to be dimensionally linearly independent, and they may be organized into combinations that have dimensions of mass, length, and time.

2.2.4 Π Theorem

Consider any variable in the function (2.44) except x_1, x_2, and x_3. For convenience call it x_4. The Bridgman equation for x_4 is

$$\hat{x}_4 = x_4 M^{a_4} L^{b_4} T^{c_4}\,. \tag{2.55}$$

Dividing (2.55) by (2.49, 53) and (2.54) yields the nondimensional Π variable

$$\begin{aligned}\hat{\Pi}_4 &\equiv \frac{\hat{x}_4}{(\hat{y}_M)^{a_4}(\hat{y}_L)^{b_4}(\hat{y}_T)^{c_4}}\\ &= \frac{x_4 M^{a_4} L^{b_4} T^{c_4}}{(y_M M)^{a_4}(y_L L)^{b_4}(y_T T)^{c_4}}\,,\end{aligned} \tag{2.56}$$

$$\frac{\hat{x}_4}{(\hat{y}_M)^{a_4}(\hat{y}_L)^{b_4}(\hat{y}_T)^{c_4}} = \frac{x_4}{(y_M)^{a_4}(y_L)^{b_4}(y_T)^{c_4}}\,,$$

$$\hat{\Pi}_4 = \Pi_4\,. \tag{2.57}$$

The variable Π_4 is nondimensional and its size is universal in the sense that it is independent of the measuring units.

The Π theorem tells us how many nondimensional variables are needed for a given problem with dimensional variables. The Π theorem can be stated as follows.

Theorem 2.1

If the physical problem is described by a function of n dimensional variables

$$x_n = f(x_1, x_2, x_3, \ldots, x_{n-1})$$

and the rank of the dimensional matrix is r, then the function may be reorganized into nondimensional variables that are $n-r$ in number

$$\Pi_{n-r} = f(\Pi_1, \Pi_2, \ldots, \Pi_{n-r-1})\,.$$

Obviously r cannot be greater that the number of dimensions, but it can be less. It is not a unique solution because a multiplication of two variables say $\Pi_1\Pi_2 = \Pi_3$ is a nondimensional variable while any power $\Pi^\alpha = \Pi_4$ is also a valid nondimensional variable. Any answer that uses all the dimensional variables and has $n-r$ nondimensional variables is valid. A rigorous proof of the Π theorem can be found in [2.9].

2.2.5 Example with Rank Less than the Number of Dimensions

As an example where the rank of the dimensional matrix is smaller than the number of dimensions, consider a shock wave in a perfect gas. Let the thermodynamic state in front of the *shock wave* be specified by p_1, ρ_1 and the type of gas denoted by the specific heat ratio γ. The state of motion is fixed by the initial velocity V_1 that is measured from a coordinate system fixed to the wave. Our interest is in the pressure after the shock p_2. With some experience in fluid mechanics we know that

the function describing this problem has the form

$$p_2 = f_1(p_1, \rho_1, V_1, \gamma)\,, \tag{2.58}$$

The dimensional matrix has three dimensions.

	p_2	p_1	ρ_x	V_1	γ
M	1	1	1	0	0
L	−1	−1	−3	1	0
T	−2	−2	0	−1	0

Try p_1, ρ_1 and V_1 as repeating variables. They will not work because the determinate of the coefficients of p_1, ρ_1 and V_1 is zero. Using p_2 or γ as a repeating variable will not correct the situation. The determinate of any 3×3 square submatrix is zero, so the rank is not three. However, the determinate of any 2×2 square submatrix is nonzero, hence the rank is two. The Π theorem predicts that the relation (2.58) can be reorganized with $5-2=3$ nondimensional variables.

Since the problem does not have three linearly independent variables, the method of scales or the other standard textbook methods does not work and we must reorganize. The purpose of the reorganization is to place zeros in one of the rows or columns of the dimensional matrix. To do this we will consider p_2/p_1 as a variable instead of p_2. This is equivalent to dividing (2.57) by p_1.

$$\frac{p_2}{p_1} = \frac{1}{p_1} f_1(p_1, \rho_1, V_1, \gamma) = f_2(p_1, \rho_1, V_1, \gamma)\,. \tag{2.59}$$

The dimensional matrix for f_2 is

	p_2/p_1	p_1	ρ_x	V_1	γ
M	0	1	1	0	0
L	0	−1	−3	1	0
T	0	−2	0	−1	0

One can check that the rank is still two. The Π theorem still guarantees that we can form three nondimensional variables for f_2. We note from the dimensional matrix that p_1 and ρ_1 can only occur in the combination p_1/ρ_1 and the function must have a simpler form.

$$\frac{p_2}{p_1} = f_3\left(\frac{p_1}{\rho_1}, V_1, \gamma\right)\,. \tag{2.60}$$

The dimensional matrix for the f_3 problem is

	p_2/p_1	p_1/ρ_1	V_1	γ
M	0	0	0	0
L	0	2	1	0
T	0	−2	−1	0

The rank is now one, so there are $4-1=3$ nondimensional variables for the f_3 problem. By inspection of the dimensional matrix, a solution will contain the combination $V_1/\sqrt{(p_1/\rho 1)}$. An answer is

$$\frac{p_2}{p_1} = f_4\left(\frac{V_1}{\sqrt{p_1/\rho_1}}, \gamma\right)\,. \tag{2.61}$$

The dimensional matrix for f_4 is all zeros and (2.61) contains only nondimensional variables. We have used all the dimensional variables of (2.58) and produced three nondimensional variables. Equation (2.61) is a simpler relation as predicted by the Π theorem. Those familiar with compressible flow of a perfect gas will recognize that $\sqrt{p_1/\rho_1} = \sqrt{\gamma RT/\gamma} = a/\sqrt{\gamma}$, where a is the speed of sound. Thus, the nondimensional variable $V_1/\sqrt{(p_1/\rho_1)}$ is the Mach number Ma divided by $\sqrt{\gamma}$.

2.2.6 Example with Redundant Dimensions

Previously we noted that the choice F, M, L, and T requires the *unifying dimensional constant* g_c with dimensions ML/FT^2. In principle, equations like Newton's second law should include the constant:

$$\mathcal{F} = \frac{ma}{g_c}\,. \tag{2.62}$$

A change in the scale units would change the value of g_c. For example

$$g_c = 32.2\,\frac{\mathrm{lb_m ft}}{\mathrm{lb_f s^2}} = 980\,\frac{\mathrm{Kg_m m}}{\mathrm{Kg_f s^2}}\,.$$

Consider a problem

$$x_n = f(x_1, x_2, x_3, \ldots, x_{n-1})\,. \tag{2.63}$$

In the $FMLT$ system the function is

$$x_n = f(x_1, x_2, x_3, \ldots, x_{n-1}, g_c)\,. \tag{2.64}$$

The dimensional matrix includes the dimensional constant g_c.

	x_1	x_2	...	x_n	g_c
F					−1
M					1
L					1
T					−2

The additional dimension increases the rank by one and the unifying constant increases the number of variables by one. There is no effect on the Π theorem's prediction of the number of nondimensional variables. There are other examples of dimensional unifiers. If we have angles and use the degree as a unit there would be a dimensional unifier $2\pi/360$ with units of $1/\text{degree}$. Next, we will illustrate the use of extra dimensions where temperature denoted by Θ is used. The unifying constant is R with dimensions $L^2/(\Theta T^{-2})$. Again consider a *shock wave* in a perfect gas. This time the initial thermodynamic state will be specified by initial pressure p_1, and temperature T_1. The pressure after the shock is again the dependent variable. The physical function includes R (i. e., the constant $R = p/(\rho T)$ for a perfect gas) as a variable. This compensates for the use of Θ as a dimension

$$p_2 = f(p_1, V_1, T_1, \gamma, R)\,. \tag{2.65}$$

One finds the dimensional matrix as

	p_2	p_1	T_1	V_1	R	γ
M	1	1	0	0	0	0
L	−1	−1	0	1	2	0
T	−2	−2	0	−1	−2	0
Θ	0	0	1	0	−1	0

The rank of this matrix is three (the determinant of any four variables is zero). Thus, there are not four variables that are dimensionally independent. From the Π theorem we must have $6-3=3$ nondimensional variables. If we produce three nondimensional variables and use all variables in the function list, we have a solution to the problem. Inspection of the dimensional matrix shows that p_2/p_1 can be one variable because pressures are the only variables with mass dimensions. Another combination that must occur must is RT_1 because they are the only variables with temperature dimensions. Hence, the functional form must be

$$\frac{p_2}{p_1} = f(RT_1, V_1, \gamma)\,. \tag{2.66}$$

The dimensional matrix is now

	p_2/p_1	RT_1	V_1	γ
M	0	0	0	0
L	0	2	1	0
T	0	−2	−1	0
Θ	0	0	0	0

Checking the Π theorem shows that the rank is one and there should be $4-1=3$ nondimensional variables. Thus, we have not altered the problem by leaving out p_1 by itself. The final list of nondimensional variables is

$$\Pi_1 = \frac{P_2}{P_1}\,, \quad \Pi_2 = \gamma\,, \quad \Pi_3 = \frac{V_1}{\sqrt{RT_1}}\,. \tag{2.67}$$

We have satisfied the Π theorem because all dimensional variables have been used in producing three nondimensional variables. This is the same result arrived at in (2.61) since $RT_1 = p_1/\rho_1$.

2.2.7 Anatomy of a Nondimensional Variable

The formulation of nondimensional variables based on the Π theorem leads to non-unique answers. Mathematically the various forms are equally valid. However, some forms are more useful than others. Let us consider the anatomy of a nondimensional variable. Specifically, we consider a nondimensional variable (other than a parameter). The general form is

$$\Pi = \frac{x - x_{\text{Ref}}}{x_{\text{Scale}}}\,. \tag{2.68}$$

In physical events a variable has a natural *reference*, which may be zero, and often a preferred *scale* unit. It is desirable that the nondimensional variable be a reasonable numerical size, say 0.01–100. In addition to variables, another physical interpretation of some nondimensional numbers is that of a parameter. In the case of a parameter the nondimensional variable is often interpreted as a ratio of physical quantities or scales.

$$\Pi = \frac{x_{\text{Scale A}}}{x_{\text{Scale B}}}\,. \tag{2.69}$$

For example, the Reynolds number is often interpreted as a ratio of inertia effects to viscous effects. A fuller discussion of physical interpretation of parameters is given later.

The origin of a coordinate system is arbitrary, so position variables always have a natural reference. Sometimes we implicitly include the reference in stating the problem. For example, in flow over a flat plate we take the distance variable from the leading edge. This sets the distance coordinate reference implicitly. In compressible flow the absolute pressure is important and the reference pressure must be zero. In incompressible flows the pressure in the flow field increases in the same amount that the pressure at a reference location p_∞ increases. Thus, the correct nondimensional pressure is of

the form

$$\Pi_p = \frac{p - p_\infty}{p_{\text{Scale}}} \,. \tag{2.70}$$

Whenever a quantity is governed by only gradient ∇x terms, a reference is arbitrary since $\nabla(x + x_{\text{Ref}}) = \nabla x$.

2.2.8 Nonuniqueness of Scales

Scale units in a nondimensional variable depend on the choice of *repeating variables*. Consider the following problem discussed by *White* [2.10] (attributed to Professor Jacques Lewalle) and by *Çengel* and *Cimbala* [2.11]. A body falls under gravity g from a height position S_0 above the ground with an initial vertical velocity V_0. The height of the body S at any time t is under study. The initial vertical velocity V_0 will be considered as a positive quantity so there will be two problems, one problem for V_0 upward and another for V_0 downward. The dimensional function is

$$S = f(t, V_0, g, S_0) \,. \tag{2.71}$$

There are five variables and the rank of the dimensional matrix is two so there must be three nondimensional variables. The form of these depends on the choice of repeating variables. White gives the following options for nondimensional functions (the exact answer is of course known; $S = S_0 + V_0 t - (1/2) g t^2$). These variables are related as power products of the original Π variables; $S^{**} = S^* \alpha$, $t^{**} = t^* \alpha$, and $t^{***} = t^* / \sqrt{\alpha}$. As remarked earlier if Π_1 and Π_2 are nondimensional, then Π_3 formed by and product of powers, $\Pi_3 = \Pi_1^n \Pi_2^m$, is also nondimensional. It is not necessary that a problem have a single set of repeating variables. For example, another relation $S^* = f_4(t^{**}, \alpha)$ is possible if we would substitute $t^* = t^{**}/\alpha$ into $S^* = f_1(t^*, \alpha)$. The physical meaning of the scales is:

S_0 Initial distance above the ground;

V_0^2/g Distance measure of the trajectory. If V_0 is upward, S maximum is $V_0^2/2g$ above S_0;

S_0/V_0 Time to travel S_0 at speed V_0;

V_0/g Time measure of the trajectory. If V_0 is upward, V_0/g is the time to reach S maximum;

$\sqrt{S_0/g}$ Time to fall distance S_0 if V_0 is zero is $\sqrt{2S_0/g}$.

The parameter α or $\sqrt{\alpha}$ can be interpreted as ratios of these times or distances.

2.2.9 Reference

If a variable has a natural *reference* it reduces the number of variables by one. Essentially we add a little physical knowledge to the problem and simplify the result. In the falling body problem of Sect. 2.2.8 the origin of the coordinate can be placed at the initial particle position without affecting the physics. Equivalently we can consider $S - S_0$ as the dependent variable. This will give an even simpler answer than those of Sect. 2.2.8

$$S - S_0 = f(t, V_0, g) \,. \tag{2.72}$$

The dimensional matrix is now

	$S - S_o$	t	V_o	g
M	0	0	0	0
L	1	0	1	1
T	0	−1	−1	−2

With a rank of two there will be $4 - 2 = 2$ nondimensional variables (Table 2.2).Recognizing that nondimensional variables have natural references produces a sharper result.

The exact answer is

$$\hat{S} = \pm\hat{t} - \frac{1}{2}\hat{t}^2 \begin{cases} + & \text{if } V_0 \text{ is upward} \,, \\ - & \text{if } V_0 \text{ is downward} \,. \end{cases} \tag{2.73}$$

Table 2.1

Repeating variables	Distance variable	Time variable	Parameter	Function form
S_0, V_0	$S^* = \frac{S}{S_0}$	$t^* = \frac{t}{S_0/V_0}$	$\alpha = \frac{gS_0}{V_0^2}$	$S^* = f_1(t^*, \alpha)$
g, V_0	$S^{**} = \frac{S}{V_0^2/g}$	$t^{**} = \frac{t}{V_0/g}$	$\alpha = \frac{gS_0}{V_0^2}$	$S^{**} = f_2(t^{**}, \alpha)$
S_0, g	$S^{***} = S^* = \frac{S}{S_0}$	$t^{***} = \frac{t}{\sqrt{S_0/g}}$	$\alpha = \frac{gS_0}{V_0^2}$	$S^{***} = f_3(t^{***}, \alpha)$

Table 2.2

Repeating variables	Distance variable	Time variable	Parameter	Function form
g, V_0	$\hat{S} = \frac{S - S_0}{V_0^2/g}$	$\hat{t} = \frac{t}{V_0/g}$	None	$\hat{S} = \hat{f}(\hat{t})$

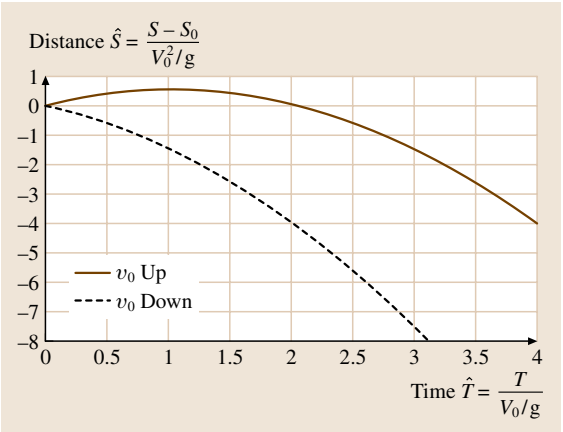

Fig. 2.8 Simplest nondimensional representation of the falling body solution

Now we have a function of only two variables. The solution is displayed in Fig. 2.8. In this figure the position of the ground is $\hat{S}_{\text{ground}} = -\alpha = -gS_0/V_0^2$.

2.2.10 Scales Chosen for Experimental Purposes

It is often desirable to choose the dependent and independent variables to match the variables being changed in the experiment. Then the repeating variables are chosen from the remaining variables. As an example consider the problem of determining the volume of an earth crater produced by an explosive charge. The explosion is at the surface of a soil that lacks cohesion; a soil like sand. A related problem is the crater formed by impact of a projectile or meteor. The dependent variable of interest is the crater volume V. Characteristics of the explosive charge are the energy per unit mass of the charge e_c, the mass of the charge m_c, and the density of the charge ρ_c. The acceleration of gravity is g, soil density ρ, and the angle of repose Φ. It requires some knowledge of the process to produce the proper list of variables. Sometimes extra variables are included only to be shown by experiments to be extraneous. Functionally, the problem is

$$V = f(e_c, m_c, \rho_c, g, \rho, \Phi)\,. \tag{2.74}$$

The dimensional matrix is

	V	e_c	m_c	ρ_c	g	ρ	Φ
M	0	0	1	1	0	1	0
L	3	2	0	−3	1	−3	0
T	3	−2	0	0	−2	0	0

In choosing the repeating variables, note that a repeating variable may appear in several of the final nondimensional variables. Thus, we avoid V because we want it to appear in only one Π variable. It is the dependent variable. In the tests a centrifuge is used to effectively change the acceleration of gravity. Hence, we would like to use g as a major test independent variable and have it occur in only one Π group. Thus it should not be a repeating variable. Also the soil density ρ will not be varied and we would like to isolate its effect into one Π variable. Since Φ is already nondimensional, the repeating variables should be chosen from e_c, m_c, and one of the densities, say ρ_c. The determinant of these three variables (e_c, m_c, ρ_c) is nonzero so the rank is three. Hence, e_c, m_c, and ρ_c are dimensionally independent and may be formed into scales for the MLT units as follows:

$$M \sim m_c\,, \quad L \sim \left(\frac{m_c}{\rho_c}\right)^{1/3}\,,$$
$$T \sim e_c^{-1/2}\left(\frac{m_c}{\rho_c}\right)^{1/3}\,. \tag{2.75}$$

The remaining variables that were not used in scales, V, ρ, g, and Φ are $m-r$ in number. This is just the number of nondimensional variables predicted by the Π theorem. They are taken one at a time and made non dimensional by eliminating MLT as required. We have used all the variables in the original list and produced $n-r$ nondimensional variables. Hence, the Π theorem is satisfied. In nondimensional form the final function is

$$\frac{V}{m_c/\rho_c} = f\left[\frac{g}{e_c}\left(\frac{m_c}{\rho_c}\right)^{1/3}, \frac{\rho}{\rho_c}, \Phi\right]\,. \tag{2.76}$$

As intended, variations in g can be used to simulate variations in the explosion strength e_c. If it is arranged so that variable occurs in only one Π group, the effect can be assessed by changing not the variable itself, but by changing another variable in that Π group.

From a series of experiments with Φ constant, *Schmidt* and *Housen* [2.12] found that for explosions (2.75) may be represented by the power relation

$$\frac{V}{m_c/\rho_c} = 0.218\left(\frac{\rho}{\rho_c}\right)^{0.002}\left[\frac{g}{e_c}\left(\frac{m_c}{\rho_c}\right)^{1/3}\right]^{-0.464}\,. \tag{2.77}$$

The dependence on ρ/ρ_c is negligible according to the experiments. This is another useful aspect of dimen-

sional analysis. The effect of soil density has been shown to be unimportant with experiments where only g and ρ_c are varied.

2.2.11 Nondimensional Variables Interpreted as Physical Ratios

Next, we try and reorganize the results of the explosion problem of Sect. 2.2.10 into a form that has a physical interpretation. We can consider a nondimensional variable as the ratio of two, dimensional, physical quantities. Let us divide the quantities in the explosion problem into two groups; those that characterize the soil and crater, ρ. V, and g, and those that characterize the charge, m_c, ρ_c and e_c. Listed below are physical concepts that are characterized by parameter groups for the charge and the crater. The mass of material from the crater is ρV, the size of the crater is characterized by $V^{1/3}$ the time to move the soil in a gravity field g is scaled by $V^{1/6}g^{-1/2}$ and so on.

Quantity	Dimensions	Crater	Charge
Mass	M	ρV	m_c
Length	L	$V^{1/3}$	$(m_c/\rho_c)^{1/3}$
Time	T	$(V/g^3)^{1/6}$	$(m_c/\rho_c)^{1/3}e_c^{-1/2}$
Volume	L^3	V	m_c/ρ_c
Density	ML^{-3}	ρ	ρ_c
Velocity	LT^{-1}	$g^{1/2}V^{1/6}$	$e_c^{1/2}$
Acceleration	LT^{-2}	g	$e_c(\rho_c/m_c)^{1/3}$
Force–weight	MLT^{-3}	$\rho g V$	$e_c(\rho_c/m_c^2)^{1/3}$
Momentum	MLT^{-1}	$\rho g^{1/2}V^{7/6}$	$e_c^{1/2}m_c$
Energy	ML^2T^{-2}	$\rho g V^{4/3}$	$e_c m_c$

We ignore the ρ/ρ_c dependence as it is negligible in (2.77). Let us replace the power 0.464 by a rational fraction. After some trial and error choose 3/7 (which is equal to 0.428). This will leave the variable m_c with a power of one. A little algebra shows that (2.74) is roughly equivalent to

$$\frac{\rho_c V^{7/6} g^{1/2}}{m_c e_c^{1/2}} = \frac{\text{Characteristic momentum of crater}}{\text{Characteristic momentum of charge}} = 0.218^{7/6} = 0.169 \,. \tag{2.78}$$

So the results indicate that the momentum ratio is almost, but not quite, constant for the explosion crater formation process.

2.2.12 Scales Found from Boundary Conditions and Equations

In many cases we know at least some of the equations and boundary conditions that govern a situation. They can be used as a guide in forming nondimensional variables. The object is to define variables so that the boundary conditions and equations contain pure numbers or, if that is not possible, a minimum number of nondimensional parameters. As an illustration we consider the flow in a slot with a moving upper wall, the Couette–Poiseuille problem. The lower wall will be $y = 0$ and the upper wall $y = h$. Two effects drive the flow. The upper wall is sliding with velocity V_0 and there is a constant pressure gradient $\mathrm{d}p/\mathrm{d}x$. The dependent variable is the velocity profile $v(y)$.

$$v = v(y, h, V_0, \mu, \mathrm{d}p/\mathrm{d}x) \tag{2.79}$$

The differential equation and boundary conditions that govern the flow are

$$0 = -\frac{\mathrm{d}p}{\mathrm{d}x} + \mu\frac{\mathrm{d}^2 v}{\mathrm{d}y^2} \,, \quad v(y=0) = 0 \,, \quad v(y=h) = V_0 \,. \tag{2.80}$$

The Π theorem applied to (2.79) predicts that the problem is governed by three nondimensional variables. We have already assumed a reference value for y by setting the lower wall to zero. From the boundary conditions it is obvious that variables of reasonable size will be

$$y^* = \frac{y}{h} \,, \quad v^* = \frac{v}{V_0} \,. \tag{2.81}$$

Substituting for the dependent variable and transforming the independent variable gives

$$0 = -\frac{\mathrm{d}p}{\mathrm{d}x} + \mu\frac{\mathrm{d}^2(v^* V_0)}{\mathrm{d}y^{*2}}\left(\frac{\mathrm{d}y^*}{\mathrm{d}y}\right)^2 \,,$$
$$0 = -\frac{h^2}{\mu V_0}\frac{\mathrm{d}p}{\mathrm{d}x} + \mu\frac{\mathrm{d}^2 v^*}{\mathrm{d}y^{*2}} \,. \tag{2.82}$$

The problem now contains a nondimensional parameter

$$\mathcal{P} = -\frac{h^2}{\mu V_0}\frac{\mathrm{d}p}{\mathrm{d}x} \,. \tag{2.83}$$

In nondimensional variables the problem is

$$0 = \mathcal{P} + \frac{\mathrm{d}^2 v^*}{\mathrm{d}y^{*2}} \,, \quad v^*(y^*=0) = 0 \,, \quad v^*(y^*=1) = 1 \,. \tag{2.84}$$

We expect a nondimensional answer $v^*(y^*, \mathcal{P})$ with three nondimensional variables as the Π theorem predicts. Sometimes, nondimensionalizing the equations results in fewer nondimensional variables, however, in this case it does not.

2.2.13 Limiting Cases

If a parameter is very large, or very small, the other nondimensional variables must have the proper scales. Consider a nondimensional relationship that contains a parameter and we are interested in the behavior as the parameter takes on an extreme value. Say the relation is

$$\Pi_1 = f(\Pi_2, \Pi_3) \tag{2.85}$$

and $\Pi_3 \to \infty$ is of interest. It makes no difference whether the extreme value is 0 or ∞ as we could redefine the parameter as $\hat{\Pi}_3 = 1/\Pi_3$. It is important that the nondimensionalized dependent variable remain bounded and nonzero in this limit; $0 < \Pi_1 < \infty$. Often the nondimensional variable needs to be redefined in order to remain bounded. We will consider three examples.

In the Couette–Poiseuille flow problem of (2.38) we nondimensionalized the velocity by the wall velocity V_0. What if the cases we are interested in have a very small V_0. This corresponds to very large value of the parameter $\mathcal{P}$. Thus small V_0 actually means small compared to the quantity $-(h^2/\mu)\,\mathrm{d}p/\mathrm{d}x$. This latter quantity is a measure of the maximum velocity caused by the pressure gradient. The parameter $\mathcal{P}$ has the physical interpretation as the ratio of the velocity caused by the pressure gradient to the velocity caused by the wall motion. In the limit $\mathcal{P} \to \infty$ the variable $v^*(y^*, \mathcal{P})$ becomes unbounded. The velocity v^* has been nondimensionalized by the wall velocity which is improper when the pressure gradient dominates the flow. A hint of the difficulty is that the differential equation in (2.84) has an infinite term as $\mathcal{P} \to \infty$. The correct dependent variable for small wall velocities is

$$\hat{v} = \frac{v}{-\frac{h^2}{\mu}\,\mathrm{d}p/\mathrm{d}x} = \frac{v^*}{\mathcal{P}} \,. \tag{2.86}$$

In terms of this variable the problem is

$$0 = 1 + \frac{\mathrm{d}^2\hat{v}}{\mathrm{d}y^{*2}} \,, \quad \hat{v}(y^* = 0) = 0 \,, \quad \hat{v}(y^* = 1) = \frac{1}{\mathcal{P}} \to 0 \,. \tag{2.87}$$

A properly nondimensionalized variable is bounded in the limit.

The next example is a little more complex. Consider the falling body problem of Sect. 2.2.8. What if the initial velocity V_0 is zero? This does not fundamentally change the problem, but the previously used nondimensional variables of (2.70) are not appropriate as they all involve V_0.

$$\hat{S} = \hat{f}(\hat{t}) \,, \quad \hat{S} = \frac{S - S_0}{V_0^2/g} \,, \quad \hat{t} = \frac{t}{V_0/g} \,. \tag{2.88}$$

Another way to look at this problem is to ask what is the behavior of $\hat{S} = \hat{f}(\hat{t})$ as $\hat{t} \to \infty$? Applying the Π theorem to (2.72) without V_0

$$S - S_0 = f(t, g) \tag{2.89}$$

shows that only one nondimensional variable is needed. We could find this in the usual way or we can ask ourselves what combination of $\hat{S}$ and $\hat{t}$ will eliminate V_0. If the initial velocity V_0 is zero the nondimensional variable is

$$\tilde{S} = \frac{\hat{S}}{\hat{t}^2} = \frac{S - S_0}{gt^2} = \text{const} \,. \tag{2.90}$$

In fact, we see from the exact answer (2.73) that as $\hat{t} \to \infty$, $\hat{S}/\hat{t}^2 = -1/2$.

For a final example we consider the pressure. In compressible flow the pressure has a thermodynamic role, as well as a mechanical role, and the absolute pressure occurs in the equation of state. The nondimensional pressure has a zero reference and the scale is some reference pressure. In incompressible flow the scale unit depends on the flow situation. Consider an incompressible flow with a reference velocity U_0 and a reference length L. What is the proper pressure scale p_S for a nondimensional pressure

$$p^* = \frac{p - p_{\mathrm{Ref}}}{p_S} \,. \tag{2.91}$$

Let us write the x-direction momentum equation and nondimensionalize the velocities with U_0 and the lengths with L.

$$\begin{aligned} \rho\left(u\frac{\partial u}{\partial x} + v\frac{\partial u}{\partial y}\right) &= -\frac{\partial p}{\partial x} \\ &\quad + \mu\left(\frac{\partial^2 u}{\partial x^2} + \frac{\partial^2 u}{\partial y^2}\right) \,, \\ \rho U_0^2\left(u^*\frac{\partial u^*}{\partial x^*} + v^*\frac{\partial u^*}{\partial y^*}\right) &= -p_S\frac{\partial p^*}{\partial x^*} + \frac{\mu U}{L} \\ &\quad \times\left(\frac{\partial^2 u^*}{\partial x^{*2}} + \frac{\partial^2 u^*}{\partial y^{*2}}\right) \,. \end{aligned} \tag{2.92}$$

There are three possibilities. If the inertia and pressure terms are dominant, the pressure scale is $p_S = \rho U_0^2$ and the viscous term will be small if the Reynolds number $\rho UL/\mu = \mathrm{Re}$ is large. If the viscous and pressure terms are dominant, the pressure scale is $p_S = \mu U_0/L$ and the inertia term will be small if the Reynolds number Re is small. If all terms are important then either scale is useful and the Reynolds number is moderate.

2.2.14 Singular Perturbations

In Sect. 2.2.13 the dependent variable Π_1 as required to be well behaved as the parameter Π_3 approached a limit.

$$\Pi_1 = f(\Pi_2, \Pi_3) \quad \text{as} \quad \Pi_3 \to 0 \quad \text{or} \quad \infty \,. \tag{2.93}$$

The situation for this section is more complex in that the dependent variable Π_1 is well-behaved for a range of the Π_2 variable, but is ill behaved for another range of Π_2. Mathematically this type of behavior is called a *singular perturbation*. One set of nondimensional variables is not appropriate for the whole space region. Wall boundary layers are the common example.

Here we consider the *fluctuations of pressure on the wall* under a turbulent boundary layer. The wavenumber k of a fluctuation of wavelength λ is

$$k = \frac{1}{2\pi} \cdot \lambda \,. \tag{2.94}$$

The spectral density $\phi(k)$ is a function such that its integral gives the mean square pressure.

$$\left\langle p'^2 \right\rangle = \int \phi(k)\,\mathrm{d}k \,. \tag{2.95}$$

The fluid is characterized by a density ρ and kinematic viscosity ν while the turbulent boundary layer has a thickness δ and a characteristic velocity u_* (this is the friction velocity). The spectrum is the dimensional function

$$\phi = \phi(k, \rho, \nu, \delta, u_*) \,. \tag{2.96}$$

The boundary layer has two length scales: the thickness of the turbulent region is δ and the viscous scale is ν/u_*. The largest fluctuations scale with δ while ν/u_* measures the smallest possible fluctuations. The physics of the turbulent fluctuations at these two different scales is different. Low-wavenumber fluctuations are inviscid and high-wavenumber fluctuations are viscous. Straightforward dimensional analysis with inviscid parameters ρ, u_*, δ as repeating variables produces the nondimensional form

$$\frac{\phi}{\rho^2 u_*^4 \delta} = \phi\left(k_1\delta, \frac{u_*\delta}{\nu}\right) \,. \tag{2.97}$$

For convenience we define the nondimensional variables as

$$\Phi = \frac{\phi}{\rho^2 u_*^4 \delta} \,, \quad K = k_1\delta \,, \quad \mathrm{Re} = \frac{u_*\delta}{\nu} \,. \tag{2.98}$$

The Reynolds number Re is the ratio of the boundary layer thickness to the viscous length scale. In terms of these variables the result is

$$\Phi = \Phi(K, \mathrm{Re}) \,. \tag{2.99}$$

For high Reynolds numbers

$$\Phi_0 = \Phi_0(K) \equiv \Phi(K, \mathrm{Re} \to \infty) \,. \tag{2.100}$$

In the limit $\mathrm{Re} \to \infty$ the spectrum is finite for low wavenumbers (frequencies), however, it approaches zero for high wavenumbers.

To obtain the spectrum function valid for the high wavenumbers we must rescale both the dependent and independent variables

$$\Phi^* = \frac{\phi}{\rho^2 u_*^3 \nu} = \Phi\,\mathrm{Re} \,, \quad k^* = \frac{k_1}{u_*/\nu} = \frac{K}{\mathrm{Re}} \,. \tag{2.101}$$

The proper wavenumber rescaling, say for instance K/Re, $K/\mathrm{Re}^{1/2}$, or $K/\mathrm{Re}^{2/3}$, depends on the physics of the process. This must be determined by analysis or experiment.

For high wavenumbers the correct nondimensional form is

$$\Phi^* = \Phi^*(k^*, \mathrm{Re}) \,, \tag{2.102}$$

$$\Phi_0^* = \Phi_0^*(k^*) \equiv \Phi^*(k^*, \mathrm{Re} \to \infty) \,. \tag{2.103}$$

This nondimensional form scales the wavenumber by the viscous length and is valid only for high wavenumbers. Thus, depending on the range of the independent wavenumber variable, there are two different nondimensional forms that are of order one.

2.2.15 Overlap Behavior and Composite Expansions

Singular perturbation problems have one set of nondimensional variables for small values of the independent variable, and another set for high values of the independent variable. These independent variables are related by the parameter that is taking on a limit. One might expect, and it is indeed true, that there is a range of moderate values of the independent variable where either set of variables is valid. This is called the overlap region. The behavior of the func-

tions in the *overlap region* is called the common part. The common part depends only on the amount of rescaling needed to make the dependent variable well behaved.

If no rescaling of the dependent variable is needed then the common part is a constant. Ordinary boundary layers fall into this category. If the rescaling of the dependent variable is a power law of the parameter, then the common part is also a power law in the independent variable. In the *pressure spectrum* problem of Sect. 2.2.14 the rescaling was Re^{-1}. The corresponding overlap behavior is

$$\Phi_0 \sim \frac{1}{K} \quad \text{as} \quad K \to \infty \,, \tag{2.104}$$

$$\Phi_0^* \sim \frac{1}{k^*} \quad \text{as} \quad k^* \to 0 \,. \tag{2.105}$$

These are really the same equation because of the relations (2.98)

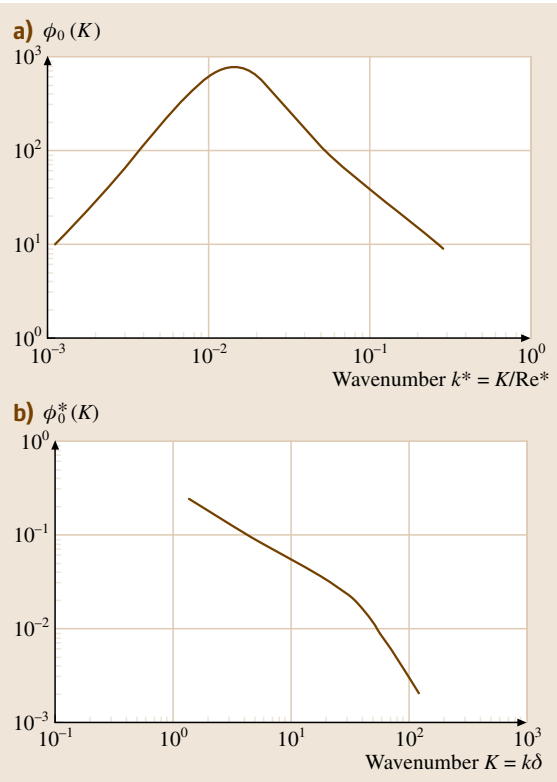

Fig. 2.10 **(a)** The pressure spectrum function $\Phi_0(K)$ valid for low wavenumbers. **(b)** The pressure spectrum function $\phi_0^*(k^*)$ valid for high wavenumbers

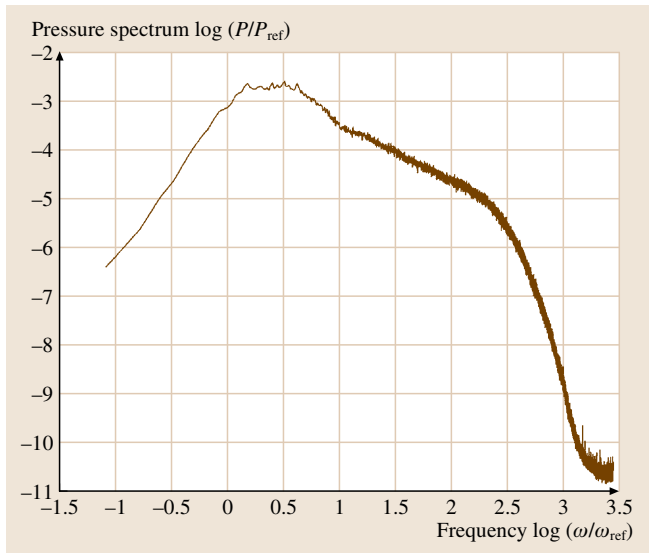

Fig. 2.9 Experimental measurement of the pressure spectrum of the turbulent atmosphere (after [2.13])

$$\begin{aligned} \Phi_0 &\sim \frac{1}{K} \,, \\ \Phi_0\,\mathrm{Re} &\sim \frac{\mathrm{Re}}{K} \,, \\ \Phi_0^* &\sim \frac{1}{k^*} \,. \end{aligned} \tag{2.106}$$

Figure 2.9 shows experimental data taken on the atmospheric boundary layer at a very high Reynolds number. The frequency axis is equivalent to the wavenumber axis since they are connected by a convective velocity $\omega = kU_c$. The overlap region where the spectrum falls as a minus one power is obvious. This spectrum is a combination of an inviscid spectrum $\Phi_0(K)$ and a viscous spectrum $\Phi_0^*(k^*)$. Sketches of the $\Phi_0(K)$ and $\Phi_0^*(k^*)$ functions are given in Fig. 2.10. At a lower Reynolds number the drop off of the viscous part of Fig. 2.9 would occur at a lower frequency. If the Reynolds number is low enough, the overlap region disappears.

Another subtle type of overlap is where a defect law matches to a single function law. In this instance the behavior is logarithmic. A more complete description of overlap behavior is found in *Panton* [2.9, 14].

Experiments cannot be conducted at infinite values of a parameter, say the Reynolds number. Singular perturbations have a different mixture of the two different functions as the parameter changes. The importance of this mixing depends on the exact nature of the functions.

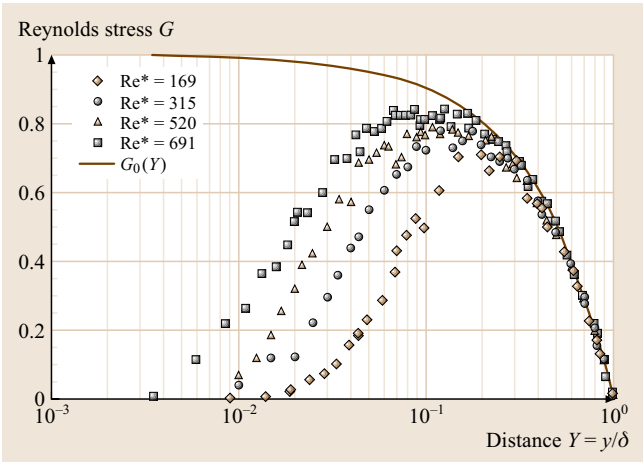

Fig. 2.11 Experimental measurement of the Reynolds stress across a pipe for several Reynolds numbers in the outer distance variable Y (after [2.15])

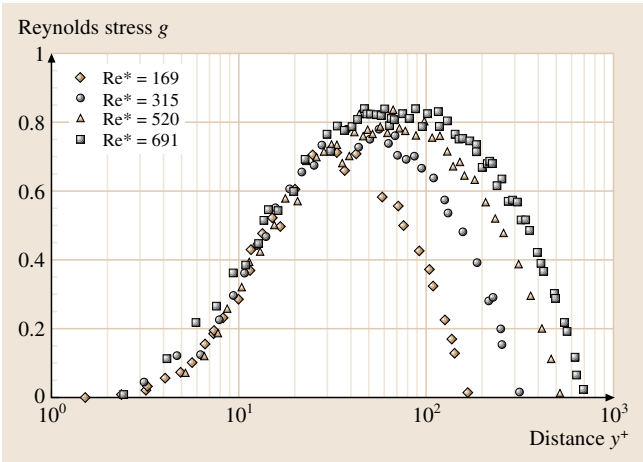

Fig. 2.12 Experimental measurement of the Reynolds stress across a pipe for several Reynolds numbers in the inner distance variable y^+ (after [2.15])

For laminar boundary layers it is not very important. For turbulent wall layers is not too important for the velocity profile. A situation where explicit variation of the parameter needs to be accounted for in the data analysis is the *Reynolds stress in pipe flow*. For pipe (or channel) flow the nondimensional Reynolds stress $\langle uv\rangle$ is a function of the distance from the wall $Y = y/R$ and the Reynolds number $\mathrm{Re} = u_* R/\nu$.

$$-\frac{\langle uv\rangle}{u_*^2} = G(Y, \mathrm{Re})\,. \tag{2.107}$$

Figure 2.11 shows experimental data for the Reynolds stress in turbulent pipe flow. For high Reynolds numbers theb *outer* form of this relation is

$$G_0(Y) = G(Y, \mathrm{Re}\to\infty)\,. \tag{2.108}$$

Analysis shows that the exact equation for G_0 is

$$G_0 = 1 - Y\,. \tag{2.109}$$

Away from the wall, $Y > 0.2$, the data in Fig. 2.11 follow (2.109), but near the wall, $Y < 0.2$, the data do not follow $G_0 = 1 - Y$. At the wall $G_0(0) = 1$ is invalid and a rescaled independent variable is required. The proper independent variable scaling near the wall is

$$y^+ = \frac{yu_*}{\nu} = Y\,\mathrm{Re}\,. \tag{2.110}$$

Near the wall the proper *inner* representation of the Reynolds stress is a different relation.

$$-\frac{\langle uv\rangle}{u_*^2} = g(y^+, \mathrm{Re})\,. \tag{2.111}$$

Figure 2.13 shows the experimental data in the *inner* representation. For high Reynolds numbers the *inner* form of this relation is

$$g_0(y^+) = g(y^+, \mathrm{Re}\to\infty)\,. \tag{2.112}$$

Table 2.3 Length scales

Lengths	Formula	Interpretation
Flow region size	L	Characteristic length scale of flow pattern
Viscous diffusion distance	$\sqrt{\nu t}$	Distance viscous shear stress or vorticity diffuses in time t
Mean free path length	λ	Typical distance a gas molecule travels between collisions
Thermal conduction distance	$\sqrt{\alpha t}$	Distance thermal energy is conducted in time t
Capillary length	$\sqrt{\frac{\sigma}{\rho g}}$	Length scale for interface shape in gravity field
Kolmogorov	$\left(\frac{\nu^3}{\varepsilon}\right)^{1/4}$	Size of smallest turbulent eddy

Table 2.4 Velocity scales

Velocity	Formula	Interpretation
Flow	U	Velocity imposed in a boundary specification
Sound	a	Speed of an acoustic wave in a still medium
Viscous diffusion	$\sqrt{\frac{\nu}{t}}$	Velocity of the diffusion of viscous region at time t
Friction velocity	$u_* \equiv \sqrt{\frac{\tau_0}{\rho}}$	Convenient scale in wall turbulence
Thermocapillary	$\frac{1}{\mu}\partial\sigma/\partial x$	Velocity from surface tension gradient opposed by viscosity
Kolmogorov	$(\nu\varepsilon)^{1/4}$	Characteristic velocity fluctuation of smallest turbulent eddy

Near the wall, $y^+ < 20$, the data collapse to a single curve and follow (2.112), but away from the wall, $y^+ > 20$, the data do not follow $g_0 = g_0(y^+)$.

The overlap region between the inner and outer functions has a constant common part $G_{CP} = G_0(Y \to 0) = 1 = g_0(y^+ \to \infty)$.

At finite Reynolds numbers the Reynolds stress does not fit either representations for all distances. For this reason G_0 and g_0 are not experimentally observed. A composite expansion is a combination of the two functions into a single uniformly valid representation. A composite expansion contains the first effects of Reynolds number. An additive *composite expansion* is

$$-\frac{\langle uv\rangle}{u_*^2} = g_0(y^+) + G_0\left(Y \to \frac{y^+}{\mathrm{Re}}\right) - G_{CP}$$
$$= g_0(y^+) + (1-Y) - 1 = g_0(y^+) - \frac{y^+}{\mathrm{Re}}\,. \tag{2.113}$$

Since we know $G_0(Y) = 1 - Y$ and $G_{CP} = 1$, there is only one unknown function $g_0(y^+)$ in (2.113). Solving this equation allows the data to be *corrected* for Reynolds number effects

$$g_0(y^+) = -\left.\frac{\langle uv\rangle}{u_*^2}\right|_{\text{data}} + \frac{y^+}{\mathrm{Re}}\,. \tag{2.114}$$

Figure 2.12 shows data processed according to (2.114). Experimental data at a variety of Reynolds numbers is plotted in Fig. 2.13, where, within the experimental uncertainty, it falls onto a single curve. The line on Fig. 2.13 is drawn also considering channel flow experiments and direct numerical simulations.

The composite expansion (2.113) is plotted in Fig. 2.13, which shows that the Reynolds number effect is well represented by a composite expansion.

2.2.16 Common Scales and Nondimensional Parameters

Nondimensional parameters can be interpreted as a ratio of dimensional properties. The dimensional properties of the ratio can be length scales, time scales, velocity scales, forces, fluxes, energies, or other physical concepts. The

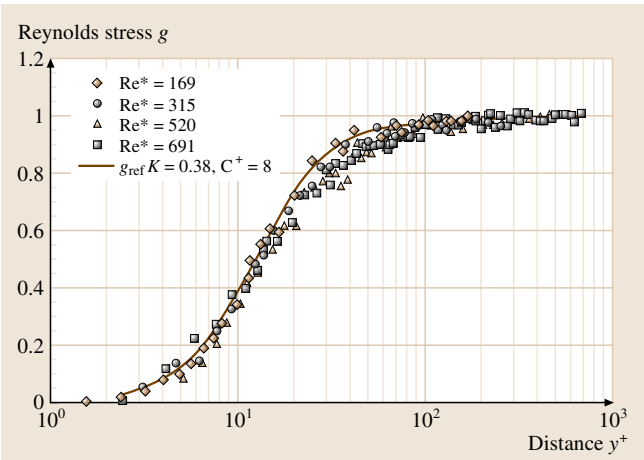

Fig. 2.13 Experimental measurement of Reynolds stress represented as the inner function $g(y^+)$ (after [2.15])

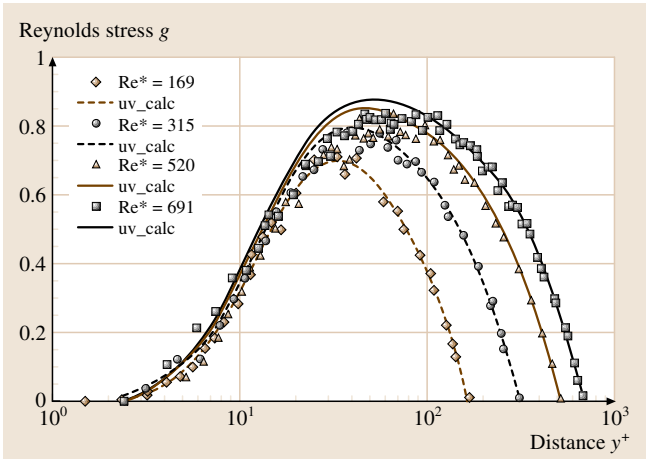

Fig. 2.14 Experimental measurement of Reynolds stress compared with the composite expansion (2.113) where g_0 is a curve fit of Fig. 2.12 (after [2.15])

Table 2.5 Nondimensional parameters

Name	Symbol	Definition	Comparison ratio
Biot number	Bi	$\frac{h}{\kappa/L}$	Convection heat transfer/conduction heat transfer
Bond number	Bo	$\frac{g(\rho-\rho_f)L^2}{\sigma}$	Buoyancy force/surface tension force (geometric length/capillary length)^2
Capillary number	Ca	$\frac{\mu V}{\sigma}$	Viscous effect/surface tension effect
Cavitation number	Cav	$\frac{p-p_v}{\rho V^2}$	Pressure difference from vapor pressure/dynamic pressure
Drag coefficient	C_D	$\frac{F_D}{1/2\rho V^2 A_x}$	Drag force/dynamic pressure times cross section area (for aircraft planform area)
Eckert number	Ec	$\frac{V^2}{c_p \Delta T}$	Kinetic energy/enthalpy change
Ekman number	E	$\frac{\nu}{f_R L^2}$	Viscous force/Coriolis force (Coriolis frequency $f_R = 2\sin\theta\Omega$ for earth rotation)
Fourier number	F	$\frac{\alpha t}{L^2}$	Heat conduction rate/energy storage rate
Friction coefficient	C_f	$\frac{\tau}{1/2\rho V^2}$	Shear stress/dynamic pressure
Friction factor	f	$\frac{h_L D/L}{1/2V^2}$	Head loss (viscous dissipation) in pipe of length D/incoming kinetic energy
Froude number	Fr	$\frac{V^2}{gL}$	Kinetic energy/gravity potential Inertia force/gravity force
Grashof number	Gr	$\frac{g\alpha\Delta TL^3}{\nu^2}$	Bouyancy force/viscous force
Head loss coefficient	K	$\frac{h_L}{1/2V^2}$	Head loss (viscous dissipation)/incoming kinetic energy
Knudsen number	Kn	$\frac{\lambda}{L}$	Mean free path/flow length
Lift coefficient	C_L	$\frac{F_L}{1/2\rho V^2 A_x}$	Lift force/dynamic pressure times cross section area (for aircraft planform area)
Mach number	M	$\frac{V}{a}$	Velocity/speed of sound
Marangoni number	Ma	$\frac{L}{\mu\alpha}\partial\sigma/\partial x$	Thermocapillary flow/thermal conduction
Nusselt number	Nu	$\frac{hL}{k}$	Nondimensional heat convection coefficient
Peclet number	Pe	$\frac{VL}{\alpha}$	= Re Pr bulk heat transfer/conduction heat transfer
Prandtl number	Pr	$\frac{\mu c_p}{k}$	Viscous diffusion effect/thermal diffusion effect
Pressure coefficient (Euler number)	C_p	$\frac{p-p_{Ref}}{1/2\rho V^2}$	Pressure change/dynamic pressure
Rayleigh number	Ra	$\frac{g\alpha\Delta TL^3}{\nu k}$	Modified Grashof number Gr Pr
Reynolds number	Re	$\frac{VL}{\nu}$	Inertia effects/viscous effects
Richardson number	Ri	$\frac{g\alpha\Delta TL}{V^2}$	Bouyancy force/inertia force
Rossby number	Ro	$\frac{V}{f_R L}$	Rotation time/flow time (Coriolis frequency $f_R = 2\sin\theta\Omega$ for earth rotation)
Stanton number	St	$\frac{h}{\rho c_p V}$	Heat transfer/thermal capacity of fluid
Strouhal number	St	$\frac{fL}{V}$	Frequency/(flow time)$^{-1}$
Weber number	We	$\frac{\rho V^2 L}{\sigma}$	Dynamic pressure/surface tension

exact problem under consideration and the definition of the nondimensional parameter determine the specific interpretation. For example, the *Reynolds number* is a ratio of an inertia *force* to a viscous force. The inertia effect is proportional to ρU^2 (twice the kinetic energy per unit volume) and the shear stress proportional to $\mu U/L$

$$\mathrm{Re} = \frac{\rho UL}{\mu} = \frac{\rho U^2}{\mu U/L} \,. \tag{2.115}$$

However, in boundary layers and entrance length problems the shear stress is proportional to $\mu U/\delta$. Here δ is the thickness of the viscous region and is $\delta \sim \sqrt{\nu L/U}$. Hence

$$\mathrm{Re} = \frac{UL}{\nu} = \frac{L^2}{\nu L/U} = \left(\frac{L}{\delta}\right)^2 \,. \tag{2.116}$$

A high Reynolds number indicates that the layer is thin compared to the length L. In the boundary layer the shear stress and inertia force are of equal importance. Nevertheless, the Reynolds number is some measure of viscous effects and inertia effects. Table 2.3 gives some length scales and Table 2.4 velocity scales that are typically defined. In Table 2.5 the reader will find common nondimensional parameters and a typical interpretation.

2.3 Self-Similarity

Certain flows lend themselves to some idealization which consists of excluding a length, time or velocity scale. This is the first sign that self-similar behavior is expected. In many important cases self-similar asymptotics *attract* real flow patterns even though the latter are *polluted* by some minor *non-ideal* details. Then, self-similar asymptotics are realizable experimentally and *attract* the initially non-self-similar flow fields. Being recognized, self-similarity can relatively readily be found analytically or numerically. Moreover, the very recognition of flow self-similarity, even without finding the corresponding solution, enables one to detect important general features in the pile of raw experimental (or numerical) data, dramatically reduces the volume of the experimental work needed for flow characterization, and makes data processing highly effective. In the present chapter the self-similarity approach is elaborated through particular examples of viscous Navier–Stokes flows, the boundary layer and gas dynamics flows, as well as a flow with the free surface. In most cases both hydrodynamic and thermal flow fields are considered and the general procedure that establishes self-similarity is demonstrated.

2.3.1 General Causes of Self-Similar Behavior in Certain Situations in Fluid Mechanics and Heat Transfer

Hydrodynamic and heat transfer problems are generally described by partial differential equations (PDEs), which implies that their solutions depend on several variables (say, spatial coordinates and/or time). The equations of motion responsible for the hydrodynamic part are nonlinear (for example, the Navier–Stokes equations), or reduce to linear equations in certain simple cases. The thermal balance equation is typically linear, but even in the simplest cases it can be solved only after the fluid mechanical part of the problem has been disposed of and the flow field established. As a rule, solution of linear and nonlinear PDEs is a much more complicated task than that of ordinary differential equations (ODEs) where functions of a single variable are sought. Fortunately, in certain cases of practical importance PDEs with the corresponding initial and boundary conditions can be reduced to ODEs subject to related conditions.

Such a reduction is possible if the problem at hand lends itself to some idealization. For example, one can consider:

- a semi-infinite depth of a fluid (instead of a finite depth) in contact with a horizontally moving infinite plate,
- a pointwise vortex core (instead of a finite one) in viscous fluids,
- fluid suction from a wedge into an infinitesimally thin (instead of a finite) slit at the wedge tip,
- viscous fluid flow, forced or due to natural convection, along a semi-infinite (instead of a finite) plate,
- jets issuing from a pointwise nozzle or buoyant plumes generated by a pointwise heat source (instead of finite ones),
- gas flows due to pointwise explosions in air (instead of finite-size ones),
- capillary waves generated by impact of a pointwise droplet or a stick (instead of finite ones) onto a thin layer of fluid.

In all these cases the idealization consists of excluding a length scale (or possibly a time or velocity scale) from the problem [2.16]. The latter is the first sign that self-similarity can exist in the given problem and its description can be reduced to ODEs. There are, however, certain restrictions. For example, there is no guarantee that the physical parameters of interest tend to finite nonzero values anywhere in the flow domain at the limit corresponding to the length scale (in fact, one of the given parameters) tending to zero. Where such finite nonzero limits exist, we are dealing with complete self-similarity (also called self-similarity of the first kind), which can be fully established by means of dimensional analysis [2.17]. Only such cases are considered in the present chapter. The situation, however, can be more complicated when the above mentioned limit tends to zero or infinity, or tends to no limit and demonstrates power-law asymptotics. In such cases, we are dealing with incomplete self-similarity (or self-similarity of the second kind). Then the exponents of the power-law asymptotics (scaling) cannot generally be found by applying dimensional analysis, but rather as the eigenvalues of the relevant eigenvalue problems. Nevertheless, the asymptotics could be fully determined only via matching the power-law *tails* to the fully non-self-similar part of the solution (which is not always possible) [2.17].

As mentioned above, self-similarity is easily recognizable and relatively readily found analytically or numerically. It also enables one to detect the instruc-

tive invariant features sometimes buried under the pile of raw experimental or numerical data. Moreover, the very recognition of intrinsic self-similarity in a certain case, even without finding the corresponding solution, dramatically reduces the volume of experimental data needed for characterizing the flow, as is shown in brief in the next subsection.

2.3.2 Implications of Self-Similarity in Experimental Studies

The idea of disregarding the detailed flow structure at certain points (for example, at the exit of a *small* nozzle releasing a jet) inevitably leads to localized singularities. At the origin of a jet flow the velocity becomes infinite, while for example the momentum flux remains finite. In spite of the singularity, such a self-similar solution is useful if the actual flow tends to the self-similar one far from the nozzle. If such is the case, we can conclude that in the far field the memory of the initial details at the nozzle exit has already faded and only such an integral characteristic as the momentum flux is important. One could actually argue that the self-similar solution should not necessarily *attract* any jet flow originating from a near-field zone, since this has not been rigorously proven so far. In other words, it is not proven that the flow field in a real non-self-similar jet will tend to the flow field corresponding to the idealized self-similar situation. However, in most fluid-mechanical cases involving boundary layers near a solid wall or free flows (as in jets and plumes), self-similar asymptotics *attract* the flow pattern even though the latter is *initially polluted* by some minor details, and as soon as the memory of the latter has faded (as in the far field of the jet) self-similar behavior is expected. The very fact that self-similar behavior is realizable experimentally shows that it *attracts* the initially non-self-similar flow fields.

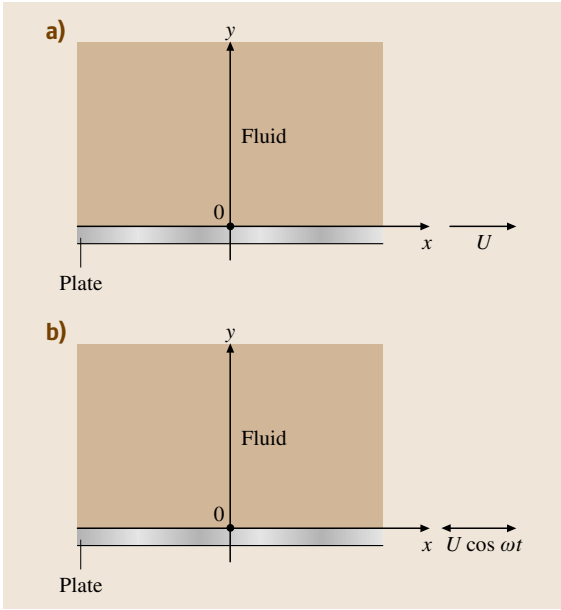

Fig. 2.15 **(a)** Suddenly accelerated plate **(b)** Vibrating plate

Self-similar behavior can also be disrupted by the presence of unaccounted-for distant walls. A jet, for example, is never fully free, since certain confinements are present. Nevertheless, actual flow structures at sufficient distances from such walls agree fairly well in many cases with the idealized self-similar ones. This makes them valuable intermediate asymptotics of a real flow field. The self-similar solutions can be described as a tiny *island* in the *ocean* of non-self-similar flows but, their influence extends far into the latter.

The fact that the flows in the far field of, say, a steady turbulent submerged axisymmetric jet are expected to be self-similar has major implications regarding the measurement strategy in experimental study of the jet. Self-similarity implies that the longitudinal velocity in the jet is given by $u = u_{\mathrm{ax}}(x)\Phi(\eta)$, where $u_{\mathrm{ax}}(x)$ is the axial velocity, and the self-similar variable $\eta = \mathrm{const} \cdot y \cdot x^{\beta}$, β being a known exponent. An experimenter has to measure only $u_{\mathrm{ax}}(x)$ and the velocity profile in a single jet cross section $x = x_*$ and the values of the self-similar variable η_* in this cross section are derived from y using x_*. The measured velocity values u are also normalized by $u_{\mathrm{ax}}(x_*)$, and the function $\Phi(\eta_*) = u/u_{ax}(x_*)$ is then established in the cross section $x = x_*$. However, self-similarity also implies that the same function describes the normalized velocity profile in all other cross sections of the jet in the far field, hence, no additional measurements are needed there. The fact that the flow is expected to be self-similar (which can be established a priori even without solving the equations of motion) permits drastic reduction of the volume of measurements.

In the following subsections the self-similarity approach will be elaborated through particular examples, beginning with the simplest ones. In Sect. 2.3.3 several examples of viscous Navier–Stokes flows are considered. Section 2.3.4 deals with flows in boundary layers, including forced and natural convection as well as laminar and turbulent flows. In Sect. 2.3.5 a self-similar flow in gas dynamics is shown, while in Sect. 2.3.6 self-similarity in a free surface flow is discussed. In all cases,

the general procedure which establishes self-similarity is demonstrated. Where possible, reference is made only to the monographs in which the original works can be found.

2.3.3 Particular Examples of Self-Similar Navier–Stokes Flows

Suddenly Accelerated Flat Plates (Stokes's First Problem) and the Corresponding Thermal Problem on a Suddenly Cooled Slab

Consider an infinite plate at $y = 0$, in contact with a viscous fluid at $y \geq 0$ (Fig. 2.14a). Both plate and fluid were at rest at $t < 0$, while at the initial time $t = 0$ the plate begins to move in the x-direction with a velocity $U = \text{const}$. The kinematic viscosity of the fluid is ν. Pressure is uniform in the fluid domain, and fluid entrainment by the plate is described by the reduced Navier–Stokes equations with the appropriate initial and boundary conditions: the no-slip condition at $y = 0$ and the condition that the fluid is always at rest at infinity [2.18]. Namely,

$$\frac{\partial u}{\partial t} = \nu \frac{\partial^2 u}{\partial y^2} \tag{2.117}$$

with the initial conditions

$$t = 0\,; \quad u = 0 \tag{2.118}$$

and boundary conditions

$$t > 0 : \begin{cases} y = 0\,, & u = U\,, \\ y = \infty\,, & u = 0\,. \end{cases} \tag{2.119}$$

The assumption that the fluid domain is semi-infinite, $0 \leq y \leq \infty$, is an idealization of real situations where the domain is sufficiently large but finite in the y-direction. Due to the idealization the problem does not contain any given length scale. To normalize the problem (2.117–2.119) any *arbitrary* length scale L can be used, whereas the time scale becomes L^2/ν, where the dimensionality of ν is $[\nu] = \mathrm{m}^2/\mathrm{s}$. The velocity scale can certainly be taken as U. The dimensionless problem reads

$$\frac{\partial \overline{u}}{\partial \overline{t}} = \frac{\partial^2 \overline{u}}{\partial \overline{y}^2} \tag{2.120}$$

with the initial and boundary conditions

$$\begin{aligned} &\overline{t} = 0\,, \quad \overline{u} = 0\,, \\ &\overline{t} > 0 : \begin{cases} \overline{y} = 0 & \overline{u} = 1 \\ \overline{y} = \infty & \overline{u} = 0\,, \end{cases} \end{aligned} \tag{2.121}$$

where t, y and u are rendered dimensionless by L^2/ν, L and U, respectively. Any solution of (2.120, 121) should have the form $\overline{u} = f(\overline{t}, \overline{y})$, such that the arbitrary length scale L is automatically absent in the final result. This is the case with the function

$$f(\overline{t}, \overline{y}) = F(\eta)\,, \quad \eta = \frac{\overline{y}}{\overline{t}^{1/2}}\,, \tag{2.122}$$

since for any L, $\eta = y/(\nu t)^{1/2}$. Any dependence of f on $\overline{t}$ and $\overline{y}$, other than that of (2.122), does not exclude an arbitrary L which should not appear in the solution. The solution (2.122) is called self-similar and depends on the self-similar variable η. The fact of self-similarity, as established above, obviates the need to solve an equation. Once it has been established, a particular function F can be found experimentally using a time series for the velocity u at a certain location y. On the other hand, in the present case the self-similar solution can easily be found after (2.122) has been substituted in (2.120) and the resulting ordinary differential equation solved with the boundary conditions as per (2.121). The corresponding self-similar solution reads

$$\frac{u}{U} = 1 - \mathrm{erf}\left(\frac{y}{2(\nu t)^{1/2}}\right)\,, \tag{2.123}$$

where

$$\mathrm{erf}(z) = \frac{2}{\sqrt{\pi}} \int_0^z \mathrm{e}^{-\zeta^2}\,\mathrm{d}\zeta \tag{2.124}$$

is the error function.

It is emphasized that, if a gap of a finite width W filled with fluid ($0 \leq y \leq W$) is considered, a length scale $L = W$ should be taken. No self-similarity would arise in that case. The self-similar solution serves, however, as a reasonable approximation of such a case at times when the presence of the wall at $y = W$ is still not strongly felt by the flow, i. e., at t significantly shorter than $W^2/(4\nu)$. During this time interval the self-similar solution represents itself as an intermediate asymptotics of the non-self-similar situation [2.17].

A kindred thermal problem arises in the case where material occupying a semi-infinite space $0 \leq y \leq \infty$ and having an initial temperature T_i is brought at $t = 0$ at $y = 0$ into contact with a *refrigerator* of temperature $T_0 < T_\mathrm{i}$. The self-similar solution for the temperature field T reads

$$\frac{T - T_0}{T_\mathrm{i} - T_0} = \mathrm{erf}\left(\frac{y}{2(\alpha t)^{1/2}}\right)\,, \tag{2.125}$$

where α is the thermal diffusivity of the material in question, $[\alpha] = \mathrm{m}^2/\mathrm{s}$.

Lack of Self-Similarity in the Case of a Vibrating Flat Plate (Stokes's Second Problem)

The reason for lack of self-similarity can be more subtle than in the case discussed in the preceding subsection. Consider, for example, a vibrating plate in contact with a viscous fluid (Fig. 2.14b). The problem is given by (2.117–2.119) with the no-slip condition replaced by

$$y = 0\,, \quad u = U\cos\omega t\,, \tag{2.126}$$

where U and ω are the amplitude and frequency of the vibration. In spite of the fact that the fluid domain is semi-infinite, a given length scale arises from the given parameters as $L = \sqrt{\nu/\omega}$. Then, self-similarity is not expected. In such cases, typically a numerical solution should be sought, but in the present case an analytical non-self-similar solution is available [2.16, 18]

$$\frac{u}{U} = \mathrm{e}^{-ky}\cos(\omega t - ky)\,, \tag{2.127}$$

where $k = [\omega/(2\nu)]^{1/2} = 2^{-1/2}L^{-1}$. This shows how the flow field depends on t and y separately, rather than on a self-similar variable.

Vorticity Diffusion

The vorticity transport equation is obtained by applying the curl operator to the Navier–Stokes equation. In the case of planar motion shown in Fig. 2.15, the vorticity transport equation takes the form [2.19]

$$\frac{\partial w}{\partial t} = \frac{\nu}{r}\frac{\partial}{\partial r}\left(r\frac{\partial w}{\partial r}\right)\,. \tag{2.128}$$

It is assumed here that the flow depends only on the radial coordinate r, while being circularly symmetric. The vorticity $\boldsymbol{w} = \mathrm{curl}\boldsymbol{v}$, $\boldsymbol{v}$ being the velocity vector, has a single nonzero component, which is the one normal to the flow plane in Fig. 2.15. Its magnitude is denoted by w. Consider the evolution of an initially pointwise vorticity line normal to the flow plane and located at $r = 0$ (Fig. 2.15). Its strength is characterized by the initial circulation Γ_0, which implies that the velocity distribution at $t = 0$ is given by

$$t = 0\,, \quad v_\theta = \frac{\Gamma_0}{2\pi r} \tag{2.129}$$

with the subscript θ denoting the azimuthal direction.

The initial velocity distribution is related to the initial vorticity distribution about the vortex

$$t = 0\,, \quad r > 0 \qquad w = 0\,. \tag{2.130}$$

The boundary condition for the vorticity reads

$$r \to \infty \qquad w \to 0\,. \tag{2.131}$$

As a spatial length scale an arbitrary L should be taken, since in the present idealization of a pointwise vortex no cross-sectional radius is given. The time scale becomes L^2/ν. The corresponding vorticity scale is Γ_0/L^2, since $[\Gamma_0] = \mathrm{m}^2/\mathrm{s}$. Any solution of (2.128) should have the dimensionless form

$$\overline{w} = f(\overline{t}, \overline{r}) \tag{2.132}$$

with $\overline{w} = w/(\Gamma_0/L^2)$, $\overline{t} = t/(L^2/\nu)$, $\overline{r} = r/L$, which yields the dimensional vorticity

$$w = \frac{\Gamma_0}{L^2} f(\overline{t}, \overline{r})\,. \tag{2.133}$$

The only particular form of the dimensionless function f that permits automatic absence of an arbitrary length scale L in the final result is

$$f(\overline{t}, \overline{r}) = \frac{1}{\overline{t}}F(\eta)\,, \quad \eta = \frac{\overline{r}}{\overline{t}^{1/2}}\,. \tag{2.134}$$

Then (2.133) and (2.134) yield

$$w = \frac{\Gamma_0}{\nu t}F(\eta)\,, \quad \eta = \frac{r}{(\nu t)^{1/2}}\,. \tag{2.135}$$

The function F can be found if (2.134) is substituted into (2.128) and the resulting ordinary differential equation solved. It has the form

$$F = \frac{1}{4\pi}\exp\left(-\frac{r^2}{4\nu t}\right)\,. \tag{2.136}$$

The corresponding velocity field becomes

$$v_\theta = \frac{\Gamma_0}{2\pi r}\left[1 - \exp\left(-\frac{r^2}{4\nu t}\right)\right]\,. \tag{2.137}$$

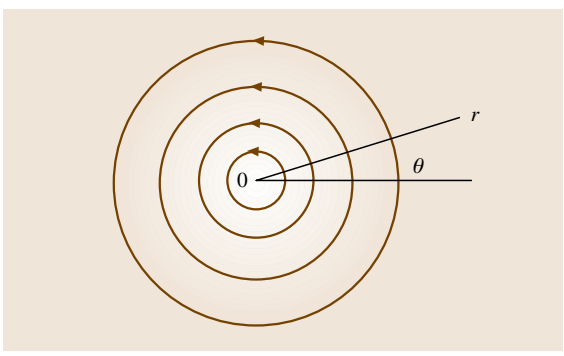

Fig. 2.16 Vorticity diffusion. The initially pointwise vortex is located at $r = 0$

The vorticity field is obviously self-similar, since

$$\frac{w}{\Gamma_0/(\nu t)} = F(\eta)\,, \tag{2.138}$$

which permits expression of the vorticity magnitude at a distance r_2 and time t_2 via its magnitude at any other location r_1 at time t_1.

In reality, a vortex would have a finite core of radius r_0, the flow inside of which can be visualized as solid-state rotation with an angular rate w_0. At the core boundary the angular velocity is continuous, thus $w_0 r_0 = \Gamma_0/(2\pi r_0)$. This yields $2\pi r_0^2 w_0 = \Gamma_0$. The self-similarity found holds in a real situation in the far field, where $r \gg r_0$. On the other hand, as $r_0 \to 0$ while $\Gamma_0 = \mathcal{O}(1)$, the angular rate in the core is $w_0 \to \infty$.

As usual, the fact that the vorticity field of an initially pointwise vortex in a viscous fluid should be self-similar can be (and has been) established without recourse to the solution of the governing equation (2.128) itself, merely by consideration of the problem as posed. The equation should be solved, or the experimental measurements should be undertaken, only when a particular form of the vorticity distribution is needed. The experiments, however, are simplified dramatically by the fact that due to the self-similarity expected beforehand, the measurements can be confined to a single location r. It would be instructive to do an experiment with a small-diameter rod mounted in a lathe.

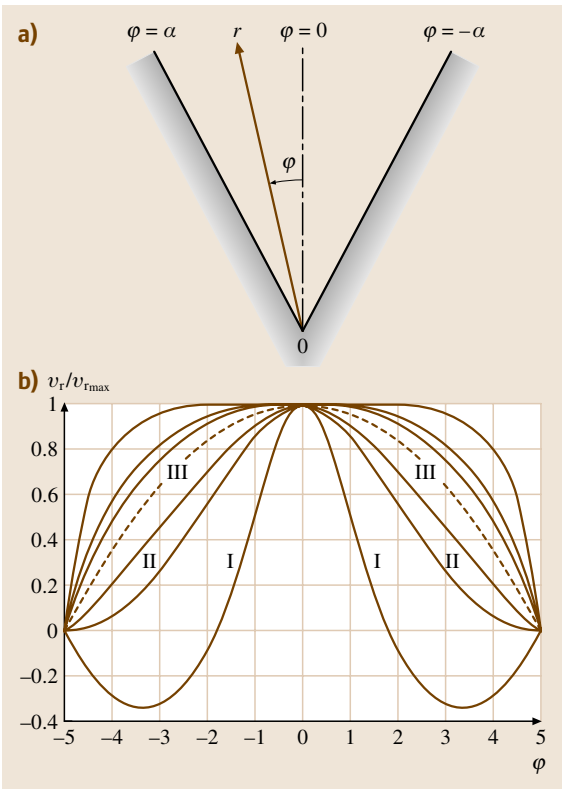

Fig. 2.17a,b Viscous flow in a wedge. **(a)** Sketch, **(b)** the velocity profiles

Flow in a Wedge

Planar flow in a wedge is shown in Fig. 2.16a. In the approximation we accept, the slit width at the wall intersection is negligibly small, and a pointwise sink or source is located at point O. In fact, this approximation corresponds to the far field where coordinates r are much larger than the slit width. The no-slip boundary conditions at the wedge walls also do not introduce any length scale. The viscous fluid involved is characterized by its kinematic viscosity ν, the sink/source strength per unit depth is given by Q, and the wedge semi-angle is α. The stream function of the flow ψ in the general case should depend on r and on the polar angle φ. Since in the present case ν, Q and ψ have the same dimensionality m^2/s, and no length scale is given due to the assumption of a pointwise sink/source, the stream function can be taken as [2.16, 20]

$$\psi = \nu f\left(\frac{r}{L}, \varphi, \frac{Q}{\nu}\right)\,. \tag{2.139}$$

In the solution any arbitrary length scale L used for nondimensionalization should disappear. This can be achieved only in the case where $f(r/L, \varphi, Q/\nu) = f_1(\varphi, Q/\nu)$, i. e.,

$$\psi = \nu f_1\left(\varphi, \frac{Q}{\nu}\right)\,. \tag{2.140}$$

The velocity components are

$$v_r = \frac{1}{r}\frac{\partial \psi}{\partial \varphi}\,, \quad v_\theta = -\frac{\partial \psi}{\partial r}\,. \tag{2.141}$$

Therefore

$$v_r = \frac{\nu}{r} F\left(\varphi, \frac{Q}{\nu}\right)\,, \quad v_\theta = 0\,, \tag{2.142}$$

where $F = f_1'$, the prime denoting differentiation with respect to φ. A solution of the Navier–Stokes equations yields F, when (2.142) are substituted therein. From the solutions, a function F satisfying the no-slip conditions at the wedge walls can be found. This yields F as a solution for the flow in the wedge. It can be expressed with the aid of the elliptic functions sn and cn. The velocity profiles for $\alpha = 5°$ are shown

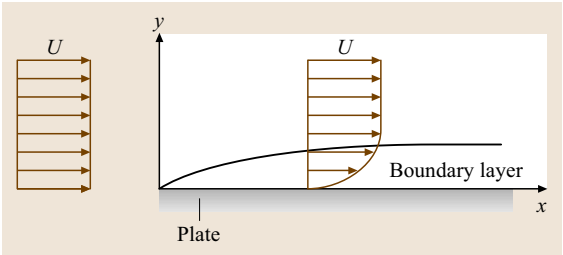

Fig. 2.18 Boundary layer near a flat plate

in Fig. 2.16b in the self-similar form $v_r/(v_r)_{\max}$, where the maximal velocity value (corresponding to $\varphi = 0$) is $(v_r)_{\max} = (\nu/r)F(0, Q/\nu)$. It is emphasized that the fact of self-similarity was established in (2.142) without any recourse to the solution of the Navier–Stokes equations, just by considering the governing physical parameters.

The velocity profiles in Fig. 2.16b are quite peculiar. Those corresponding to flows in a diverging channel (with $Q > 0$) can contain regions of reverse flow toward the source (where $v_r < 0$, as for example for profile I). The borderline diffuser profile where reverse flows disappear is denoted II. The velocity profile III is $v_r/(v_r)_{\max} = 1 - (\tan\varphi/\tan\alpha)^2$, which is the Poiseuille profile inserted in the wedge. It is located as a border line between the flows in diverging ($Q > 0$) and converging ($Q < 0$) channels. Above profile III, only confuser-like flows exist (for them v_r is, in fact, the velocity magnitude).

2.3.4 Particular Examples of the Boundary Layer Flows

Flow and Heat Transfer in Laminar Boundary Layers Near a Flat Wall

A uniform laminar flow which encounters a semi-infinite plate parallel to it adjusts itself to the no-slip condition at the plate surface and develops the boundary layer as shown in Fig. 2.17. The dynamic and thermal problems are described in the framework of the boundary layer equations [2.18]

$$\begin{aligned} \frac{\partial u}{\partial x} + \frac{\partial v}{\partial y} &= 0\,, \\ u\frac{\partial u}{\partial x} + v\frac{\partial u}{\partial y} &= \nu\frac{\partial^2 u}{\partial y^2}\,, \\ u\frac{\partial T}{\partial x} + v\frac{\partial T}{\partial y} &= \alpha\frac{\partial^2 T}{\partial y^2}\,, \end{aligned} \qquad (2.143)$$

with u and v being the longitudinal and transverse velocity components, and α the thermal diffusivity. If we assume a uniform temperature T_w, at the plate surface and a uniform temperature of the flow at infinity T_∞, the complete set of boundary conditions reads

$$\begin{aligned} y = 0 \qquad & u = v = 0\,, \qquad T = T_w \\ y = \infty \qquad & y = U\,, \qquad T = T_\infty\,. \end{aligned} \qquad (2.144)$$

The dynamic part of problem (2.143) (Blasius flow) reduces to a single equation for the stream function ψ ($u = \partial\psi/\partial y$, $v = -\partial\psi/\partial x$)

$$\frac{\partial\psi}{\partial y}\frac{\partial^2\psi}{\partial x\partial y} - \frac{\partial\psi}{\partial x}\frac{\partial^2\psi}{\partial y^2} = \nu\frac{\partial^3\psi}{\partial y^3}\,. \qquad (2.145)$$

The viscous length scale ν/U is typically so small (of the order of 10^{-5}–10^{-4} m) that it cannot be considered natural for a plate. No length scale is given, since the plate is idealized as being semi-infinite. Therefore, an arbitrary scale L is used to render the longitudinal coordinate x dimensionless. As usual in a boundary layer, the transverse coordinate y is rendered dimensionless by $L/\mathrm{Re}^{1/2}$, $\mathrm{Re} = UL/\nu$ being the Reynolds number. Then the corresponding scale of the stream function $\Psi = (UL\nu)^{1/2}$ follows from its definition, while (2.145) becomes

$$\frac{\partial\overline{\psi}}{\partial\overline{y}}\frac{\partial^2\overline{\psi}}{\partial\overline{x}\partial\overline{y}} - \frac{\partial\overline{\psi}}{\partial\overline{x}}\frac{\partial^2\overline{\psi}}{\partial\overline{y}^2} = \frac{\partial^3\overline{\psi}}{\partial\overline{y}^3}\,, \qquad (2.146)$$

where the dimensionless parameters are denoted by bars. A solution has to be of the form $\overline{\psi} = f(\overline{x}, \overline{y})$, i. e.

$$\psi = (UL\nu)^{1/2} f\left[\frac{x}{L}, y\left(\frac{U}{L\nu}\right)^{1/2}\right]\,, \qquad (2.147)$$

where f is a dimensionless function.

In the absence of a given length scale, only functions of a special, self-similar type, $f(\overline{x}, \overline{y}) = \overline{x}^{1/2} F(\overline{y}/\overline{x}^{1/2})$ can be admitted. This automatically reduces (2.147) to the form

$$\psi = (U\nu x)^{1/2} F(\eta)\,, \quad \eta = y\left(\frac{U}{\nu x}\right)^{1/2}\,, \qquad (2.148)$$

where L is absent. Substitution of the self-similar solution (2.148) in the dynamic part of the problem (2.143) and (2.144) yields the following boundary value problem for determining F

$$\begin{aligned} F''' + \frac{1}{2}FF'' &= 0\,, \\ F(0) = F'(0) &= 0\,, \\ F'(\infty) &= 1\,, \end{aligned} \qquad (2.149)$$

where the primes denote differentiation with respect to η. The solution of (2.149) was found numerically

Table 2.6 The function $F(\eta)$ for the boundary layer along a semi-infinite flat plate

$\eta = y\sqrt{\frac{U}{\nu x}}$	F	$F' = \frac{u}{U}$	F''
0	0	0	0.33206
0.2	0.00664	0.06641	0.33199
0.4	0.02656	0.13277	0.33147
0.6	0.05974	0.19894	0.33008
0.8	0.10611	0.26471	0.32739
1.0	0.16557	0.32979	0.32301
1.2	0.23795	0.39378	0.31659
1.4	0.32298	0.45627	0.30787
1.6	0.42032	0.51676	0.29667
1.8	0.52952	0.57477	0.28293
2.0	0.65003	0.62977	0.26675
2.2	0.78120	0.68132	0.24835
2.4	0.92230	0.72899	0.22809
2.6	1.07252	0.77246	0.20646
2.8	1.23099	0.81152	0.18401
3.0	1.39682	0.84605	0.16136
3.2	1.56911	0.87609	0.13913
3.4	1.74696	0.90177	0.11788
3.6	1.92954	0.92333	0.09809
3.8	2.11605	0.94112	0.08013
4.0	2.30576	0.95552	0.06424
4.2	2.49806	0.96696	0.05052
4.4	2.69238	0.97587	0.03897
4.6	2.88826	0.98269	0.02948
4.8	3.08534	0.98779	0.02187
5.0	3.28329	0.99155	0.01591
5.2	3.48189	0.99425	0.01134
5.4	3.68094	0.99616	0.00793
5.6	3.88031	0.99748	0.00543
5.8	4.07990	0.99838	0.00365
6.0	4.27964	0.99898	0.00240
6.2	4.47948	0.99937	0.00155
6.4	4.67938	0.99961	0.00098
6.6	4.87931	0.99977	0.00061
6.8	5.07928	0.99987	0.00037
7.0	5.27926	0.99992	0.00022
7.2	5.47925	0.99996	0.00013
7.4	5.67924	0.99998	0.00007
7.6	5.87924	0.99999	0.00004
7.8	6.07923	1.00000	0.00002
8.0	6.27923	1.00000	0.00001
8.2	6.47923	1.00000	0.00001
8.4	6.67923	1.00000	0.00000
8.6	6.87923	1.00000	0.00000
8.8	7.07923	1.00000	0.00000

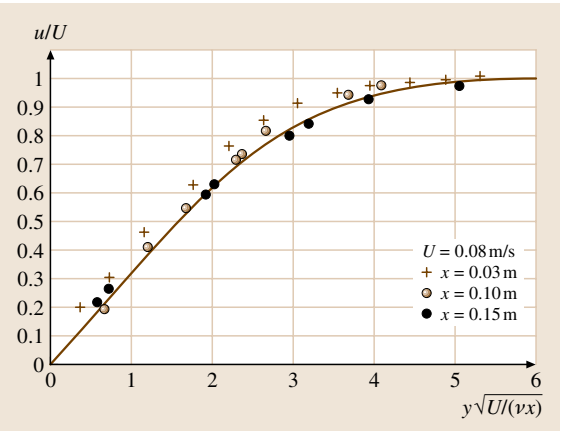

Fig. 2.19 The Blasius velocity profile: *solid line*; the experimental data – *symbols*

(Table 2.6). The corresponding self-similar velocity profile $u = UF'$ is given in Fig. 2.18 versus experimental data. It is clearly seen that in the self-similar coordinates measurements in three different cross sections $x = 0.03$, 0.1 and 0.15 m collapse onto the theoretical Blasius profile represented by the solid line. Since $F''(0) = 0.332$, the friction coefficient $c_f = \mu \partial u/\partial y|_{y=0} / \left(1/2\rho U^2\right)$, μ being the fluid viscosity, is given by

$$c_f = \frac{0.664}{\mathrm{Re}_x^{1/2}}, \quad \mathrm{Re}_x = \frac{Ux}{\nu}. \tag{2.150}$$

The thickness of the boundary layer is $\delta \approx 5(\nu x/U)^{1/2}$.

The flow considered in the present section is incompressible. Generalization to the compressible case could be achieved using the well-known Dorodnitsyn–Howarth transformation [2.21].

In the incompressible case the solution of the corresponding thermal problem should be sought in the form

$$\theta(\eta) = \frac{T(\eta) - T_w}{T_\infty - T_w}. \tag{2.151}$$

It yields

$$\theta(\eta) = \frac{\int_0^\eta \exp\left[-\frac{\mathrm{Pr}}{2}\int_0^\zeta F(\xi)\,\mathrm{d}\xi\right]\mathrm{d}\zeta}{\int_0^\infty \exp\left[-\frac{\mathrm{Pr}}{2}\int_0^\zeta F(\xi)\,\mathrm{d}\xi\right]\mathrm{d}\zeta}, \tag{2.152}$$

where $\mathrm{Pr} = \nu/\alpha$ is the Prandtl number.

The dimensionless heat transfer coefficient h is nothing but the local Nusselt number Nu_x

$$\mathrm{Nu}_x = \frac{hx}{k} = \theta'(0)\mathrm{Re}_x^{1/2}, \tag{2.153}$$

where k is the thermal conductivity of the fluid. The analytical expressions approximating the results following from (2.152) read

$$\theta'(0) = \begin{cases} 0.564\mathrm{Pr}^{1/2}\,, & \mathrm{Pr} < 0.05\,, \\ 0.332\mathrm{Pr}^{1/3}\,, & 0.6 \le \mathrm{Pr} \le 10\,, \\ 0.339\mathrm{Pr}^{1/3}\,, & \mathrm{Pr} > 10\,. \end{cases} \tag{2.154}$$

It is emphasized that the fact that the velocity and temperature fields in the laminar boundary layer near a semi-infinite plate are self-similar could be (and has been) established without solution of the governing equations, merely by consideration of the problem as posed.

Flow and Heat Transfer in Jets

First consider a laminar axisymmetric submerged jet [2.18, 22, 23] issuing from a pointwise nozzle (Fig. 2.19). The assumption that the nozzle is pointwise excludes a length scale (the nozzle radius) from the set of given parameters and should result in self-similarity. It is a legitimate assumption dealing only with the far-field zone of the jet, where it has already spread significantly compared to the nozzle size. In the near-field zone close to the nozzle, such simplification is impossible and a fully non-self-similar velocity field should be tackled experimentally or numerically. The dynamic and thermal problems in question involve the boundary-layer equations

$$\begin{aligned} &\frac{\partial uy}{\partial x} + \frac{\partial vy}{\partial y} = 0\,, \\ &u\frac{\partial u}{\partial x} + v\frac{\partial u}{\partial y} = \frac{\nu}{y}\frac{\partial}{\partial y}\left(y\frac{\partial u}{\partial y}\right)\,, \\ &u\frac{\partial T}{\partial x} + v\frac{\partial T}{\partial y} = \frac{\alpha}{y}\frac{\partial}{\partial y}\left(y\frac{\partial T}{\partial y}\right)\,, \end{aligned} \tag{2.155}$$

with x and y being the axial and radial coordinates, and u and v the longitudinal and radial velocity components, respectively.

The flow is axisymmetric, the fluid at infinity is at rest with a given temperature T_∞, namely

$$\begin{aligned} &y = 0\,, && v = \frac{\partial u}{\partial y} = \frac{\partial T}{\partial y} = 0\,, \\ &y = \infty\,, && u = 0\,,\ T = T_\infty\,. \end{aligned} \tag{2.156}$$

The first two equations (2.155) with the boundary conditions (2.156) show that the momentum flux is constant along the jet

$$2\pi \int_0^\infty \rho u^2 y\,\mathrm{d}y = J_x = \mathrm{const}\,, \tag{2.157}$$

where ρ is the fluid density, and J_x is a given momentum flux.

If we assume that the nozzle exit of the jet had a uniform velocity profile $u = u_0 = \mathrm{const}$, the momentum flux is $J_x = \pi y_0^2 \rho u_0^2$, where y_0 is the nozzle radius. Since in the present case $y_0 \to 0$, we conclude that $u_0 \to \infty$, whence $J_x = \mathcal{O}(1)$.

The dynamic equations (2.155) yield a single equation for the stream function ψ ($uy = \partial\psi/\partial y$, $vy = -\partial\psi/\partial x$), which reads

$$\begin{aligned} &\frac{1}{y}\frac{\partial\psi}{\partial y}\frac{\partial^2\psi}{\partial x\partial y} - \frac{\partial\psi}{\partial x}\left(-\frac{1}{y^2}\frac{\partial\psi}{\partial y} + \frac{1}{y}\frac{\partial^2\psi}{\partial y^2}\right) \\ &= \nu\left(\frac{1}{y^2}\frac{\partial\psi}{\partial y} - \frac{1}{y}\frac{\partial^2\psi}{\partial y^2} + \frac{\partial^3\psi}{\partial y^3}\right)\,. \end{aligned} \tag{2.158}$$

No length scale is given, since the jet is idealized as issuing from a pointwise nozzle. Therefore, an arbitrary length scale L is again used to render x dimensionless. As the velocity scale we take some U. Then the radial coordinate y is rendered dimensionless by $L/\mathrm{Re}^{1/2}$ with $\mathrm{Re} = UL/\nu$. The integral condition (2.157) in the dimensionless form becomes

$$\int_0^\infty \overline{u}^2\overline{y}\,\mathrm{d}\overline{y} = 1 \tag{2.159}$$

the chosen velocity scale being

$$U = \frac{J_x}{2\pi\rho L\nu} \tag{2.160}$$

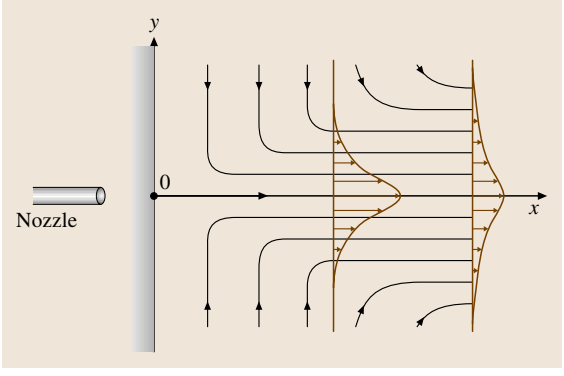

Fig. 2.20 Sketch of the streamlines and velocity profiles in the axisymmetric submerged jet

with the dimensionless parameters denoted by bars. Equation (2.160) shows that, in fact, U is not arbitrary any more, and the only arbitrary scale involved is L.

The corresponding scale of the stream function $\Psi = \nu L$ follows from its definition, while (2.158) becomes

$$\frac{1}{\overline{y}}\frac{\partial\overline{\psi}}{\partial\overline{y}}\frac{\partial^2\overline{\psi}}{\partial\overline{x}\partial\overline{y}} + \frac{1}{\overline{y}^2}\frac{\partial\overline{\psi}}{\partial\overline{x}}\frac{\partial\overline{\psi}}{\partial\overline{y}} - \frac{1}{\overline{y}}\frac{\partial\overline{\psi}}{\partial\overline{x}}\frac{\partial^2\overline{\psi}}{\partial\overline{y}^2} = \frac{1}{\overline{y}^2}\frac{\partial\overline{\psi}}{\partial\overline{y}} - \frac{1}{\overline{y}}\frac{\partial^2\overline{\psi}}{\partial\overline{y}^2} + \frac{\partial^3\overline{\psi}}{\partial\overline{y}^3} \,. \tag{2.161}$$

The solution has to be of the form $\overline{\psi} = f(\overline{x}, \overline{y})$, i. e., due to (2.160)

$$\psi = \nu L f\left[\frac{x}{L}, \frac{y}{L\nu}\left(\frac{J_x}{2\pi\rho}\right)^{1/2}\right] \,. \tag{2.162}$$

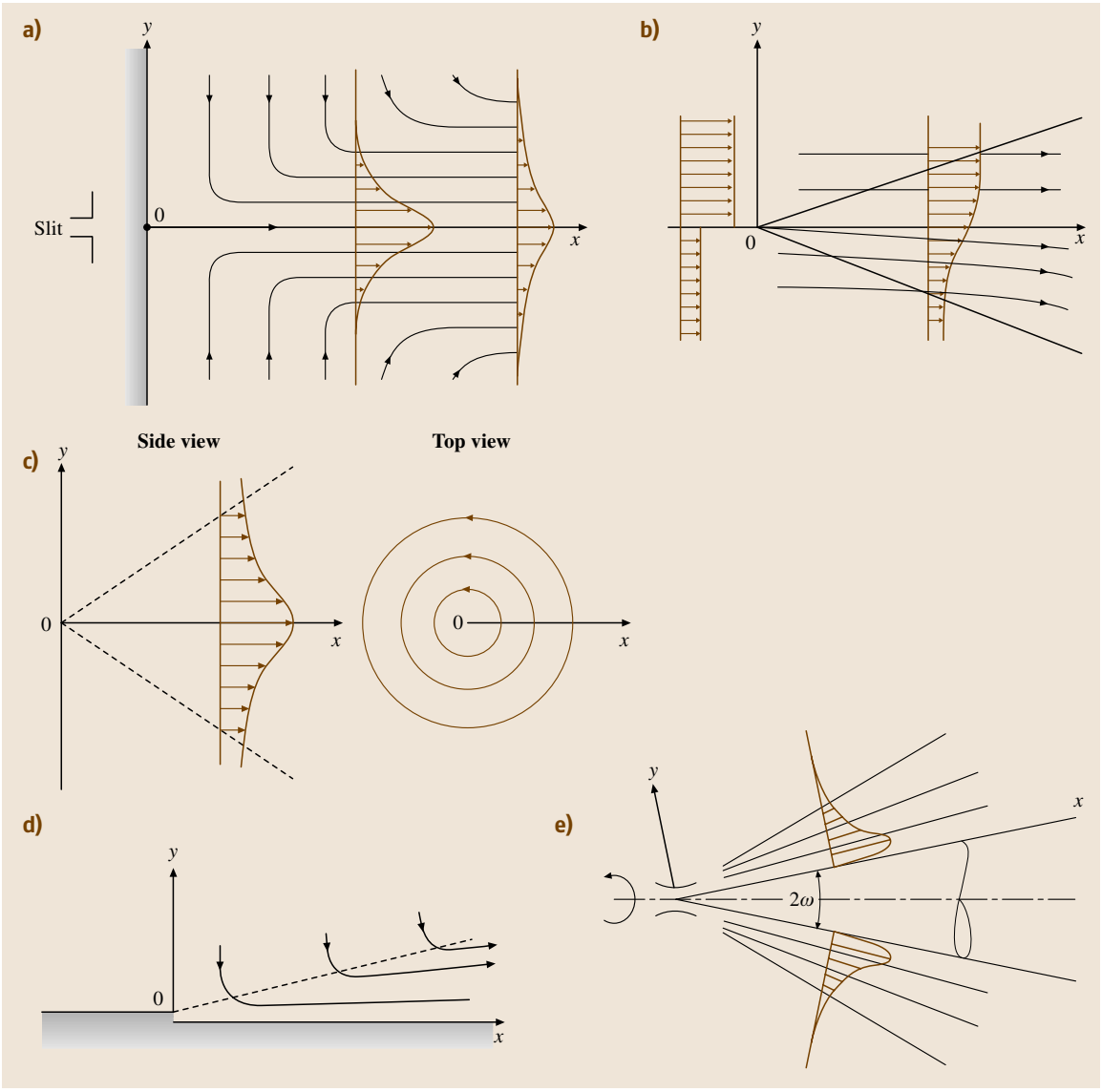

Fig. 2.21a–e Different types of jets. **(a)** Planar submerged jet; **(b)** free mixing layers; **(c)** submerged radial swirling jet; **(d)** planar wall jet; **(e)** slightly swirling jet propagating along a cone

Table 2.7 Self-similar laminar jets

Notation:
$G = \int_s \rho u \, \mathrm{d}s$: mass flow rate; $J_x = \int_s \rho u^2 \, \mathrm{d}s$: momentum flux; $M = \int_s \rho r u w \, \mathrm{d}s$: moment-of-momentum flux;
$E = \frac{1}{2} \int_s \rho u^3 \, \mathrm{d}s$: kinetic energy flux; $Q = \int_s \rho c_\mathrm{p} u \Delta T \, \mathrm{d}s$: excess heat flux;
$K = \int_s \rho u^2 \left(\int_s \rho u \, \mathrm{d}s \right) \mathrm{d}s$: first integral invariant of the wall jets; $N = \int_s \rho r u w \left(\int_s \rho u \, \mathrm{d}s \right) \mathrm{d}s$: second integral invariant of the wall jets;
$K_\mathrm{T} = \int_s \Delta T^{3/2} \, \mathrm{d}s$ – third (thermal) integral invariant of the wall jets; $K_\mathrm{T}^1 = \int_s \rho c_\mathrm{p} u \Delta T \left(\int_s \rho u \, \mathrm{d}s \right) \mathrm{d}s$: same for $\mathrm{Pr} = 1$.
Also, $\mathrm{d}s = (2\pi r)^k \, \mathrm{d}y$ denotes an area element of the jet cross section, where the distance from the symmetry axis is $r \equiv y$ in the jets symmetric about the Ox axis, and $r \equiv x$ in those symmetric about the Oy axis; in the case of jets about a cone $r \equiv x \sin\omega$, 2ω being the angle at the cone apex. In the planar problems $k = 0$, in the axisymmetric ones $k = 1$.

Remarks:
In items *Differential equations*, *Boundary conditions*, etc.: I represents the dynamic problem; II the thermal one.
In items *Boundary conditions*, *General structure of the self-similar solutions*, etc.: IIa represents the thermal problem with symmetric boundary conditions for temperature; IIb that with asymmetric ones.
For wall jets: IIa represents the thermal problem for the case $T_\mathrm{w} = T_\infty$ with T_w being a constant wall temperature; IIb that with an insulating wall; IIc that with an isothermal wall with $T_\mathrm{w} = \mathrm{const} \neq T_\infty$.

Flow type: Planar submerged jet		
Differential equations	I	$u\partial u/\partial x + v\partial u/\partial y = \nu\partial^2 u/\partial y^2 \,; \quad \partial u/\partial x + \partial v/\partial y = 0$
	II	$u\partial T/\partial x + v\partial T/\partial y = \alpha\partial^2 T/\partial y^2$
Boundary conditions	I	$v(x,0) = \partial u/\partial y|_{y=0} = 0 \,; \quad u(x,\pm\infty) = 0$
	IIa	$\partial T/\partial y|_{y=0} = 0 \,, \quad T(x,\pm\infty) = T_\infty$
	IIb	$T(x,+\infty) = T_1 \,, \quad T(x,-\infty) = T_2$
General structure of the self-similar solutions	I	$\frac{u}{u_\mathrm{m}} = F'(\eta) \,, \quad u_\mathrm{m} = Ax^\alpha \,, \quad \eta = Byx^\beta$
	IIa	$\frac{T-T_\infty}{T_\mathrm{m}-T_\infty} = \theta(\eta) \,, \quad T_\mathrm{m} - T_\infty = \Gamma x^\gamma$
	IIb	$\frac{T-T_2}{T_1-T_2} = \theta(\eta)$
Exponents in the self-similar solutions	I	$\alpha = -\frac{1}{3} \,, \quad \beta = -\frac{2}{3}$
	IIa	$\gamma = -\frac{1}{3}$
	IIb	$(\gamma = 0)$
Constants in the self-similar solutions	I	$A = \frac{1}{2}\sqrt[3]{\frac{3J_x^2}{4\rho^2\nu}} \,, \quad B = \frac{1}{2}\sqrt[3]{\frac{J_x}{6\rho\nu^2}}$
	IIa	$\Gamma = \frac{Q}{c_\mathrm{p}}\sqrt[3]{\frac{2}{9\rho^2\nu J_x}}\left[\int_{-\infty}^{+\infty}(F')^{\mathrm{Pr}+1}\,\mathrm{d}\eta\right]^{-1}$
	IIb	$(\Gamma = T_1 - T_2)$
Integral invariants	I	$J_x = \int_{-\infty}^{+\infty} \rho u^2 \, \mathrm{d}y = \mathrm{const}$
	IIa	$Q = \int_{-\infty}^{+\infty} \rho c_\mathrm{p} u (T - T_\infty) \mathrm{d}y = \mathrm{const}$
	IIb	–
Self-similar equations	I	$F''' + 2(FF'' + F'^2) = 0$
	IIa	$\theta'' + 2\,\mathrm{Pr}(F\theta' + F'\theta) = 0$
	IIb	$\theta'' + 2\,\mathrm{Pr}\,F\theta' = 0$
Self-similar boundary conditions	I	$F(0) = 0 \,, \quad F'(0) = 1 \,, \quad F'(\pm\infty) = 0$
	IIa	$\theta'(0) = 0 \,, \quad \theta(\pm\infty) = 0$
	IIb	$\theta(+\infty) = 1 \,, \quad \theta(-\infty) = 0$

Table 2.7 (continued)

Self-similar solutions	I	$F = \tanh\eta\,, \quad F' = 1/\cosh^2\eta$
	IIa	$\theta(\eta) = (F')^{\mathrm{Pr}} = 1/\cosh^{2\,\mathrm{Pr}}\eta$
	IIb	$\theta(\eta) = \left[\int\limits_{-\infty}^{\eta} (\cosh\eta)^{-2\,\mathrm{Pr}}\,\mathrm{d}\eta\right]\left[\int\limits_{-\infty}^{+\infty} (\cosh\eta)^{-2\,\mathrm{Pr}}\,\mathrm{d}\eta\right]^{-1}$
Integral characteristics	I	$G = \sqrt[3]{36\rho^2\nu J_x x}\,, \quad E = \frac{J_x}{30\mu}\sqrt[3]{6\rho\nu^2 J_x^2\frac{1}{x}}$
	IIa	–
	IIb	$Q = \frac{1}{2}c_{\mathrm{p}}(T_1 - T_2)\left(\int\limits_{-\infty}^{+\infty} F'\theta\,\mathrm{d}\eta\right)\sqrt[3]{36\rho^2\nu J_x x}$
Flow type: free mixing layers		
Differential equations	I	$u\partial u/\partial x + v\partial u/\partial y = \nu\partial^2 u/\partial y^2\,; \quad \partial u/\partial x + \partial v/\partial y = 0$
	II	$u\partial T/\partial x + v\partial T/\partial y = \alpha\partial^2 T/\partial y^2$
Boundary conditions	I	$u(x,+\infty) = u_1\,; \quad \partial u/\partial y|_{y=\pm\infty} = 0\,; \quad u(x,-\infty) = u_2$
	IIa	–
	IIb	$T(x,+\infty) = T_1\,, \quad T(x,-\infty) = T_2$
General structure of the self-similar solutions	I	$\frac{u}{u_{\mathrm{m}}} = F'(\eta)\,, \quad u_{\mathrm{m}} = u_1 = \mathrm{const}\,, \quad \eta = Byx^{\beta}$
	IIa	–
	IIb	$\frac{T-T_2}{T_{\mathrm{m}}-T_2} = \theta(\eta)\,, \quad T_{\mathrm{m}} = T_1 = \mathrm{const}\,, \quad T_2 = \mathrm{const}$
Exponents in the self-similar solutions	I	$\alpha = 0\,, \quad \beta = -\frac{1}{2}$
	IIa	–
	IIb	$(\gamma = 0)$
Constants in the self-similar solutions	I	$(A = u_1)\,, \quad B = \frac{1}{2}\sqrt{\frac{u_1}{\nu}}$
	IIa	–
	IIb	$(\Gamma = T_1 - T_2)$
Integral invariants	I	–
	IIa	–
	IIb	–
Self-similar equations	I	$F''' + 2FF'' = 0$
	IIa	–
	IIb	$\theta'' + 2\,\mathrm{Pr}\,F\theta' = 0$
Self-similar boundary conditions	I	$F'(+\infty) = 1\,, \quad F''(+\infty) = 0\,; \quad F'(-\infty) = m = \frac{u_2}{u_1}\,, \quad F''(-\infty) = 0$
	IIa	–
	IIb	$\theta(+\infty) = 1\,, \quad \theta(-\infty) = 0$
Self-similar solutions	I	$\frac{u}{u_1} = F'(\eta) = 1 + \frac{1}{2}(m-1)(1-\mathrm{erf}\,\eta)\,, \quad \left(\mathrm{erf}\,\eta = \frac{2}{\sqrt{\pi}}\int\limits_0^{\eta} \mathrm{e}^{-\xi^2}\,\mathrm{d}\xi\right)$
	IIa	–
	IIb	$\theta = \frac{T-T_2}{T_1-T_2} = \frac{1}{2}[1 + \mathrm{erf}(\eta\sqrt{\mathrm{Pr}})]$
Integral characteristics	I	–
	IIa	–
	IIb	–

Table 2.7 (continued)

Flow type: axisymmetric submerged jet: swirling if $w \neq 0$; no swirling if $w = 0$		
Differential equations	I	$u\partial u/\partial x + v\partial u/\partial y = \nu\frac{1}{y}\partial/\partial y\,(y\partial u/\partial y)$; $\frac{\rho w^2}{y} = \partial p/\partial y$; $u\partial w/\partial x + v\partial w/\partial y + \frac{vw}{y} = \nu\left[\frac{1}{y}\partial/\partial y\,(y\partial w/\partial y) - \frac{w}{y^2}\right]$; $\partial/\partial x(yu) + \partial/\partial y(yv) = 0$
	II	$u\partial T/\partial x + v\partial T/\partial y = \alpha\frac{1}{y}\partial/\partial y\,(y\partial T/\partial y)$
Boundary conditions	I	$v(x,0) = w(x,0) = \partial u/\partial y|_{y=0} = \partial w/\partial y|_{y=0} = 0$, $u(x,\infty) = w(x,\infty) = 0$, $p(x,\infty) = p_\infty$
	IIa	$\partial T/\partial y|_{y=0} = 0$, $T(x,\infty) = T_\infty$
	IIb	–
General structure of the self-similar solutions	I	$\frac{u}{u_\mathrm{m}} = \frac{F'(\eta)}{\eta}$, $\frac{w}{w_\mathrm{m}} = \Phi(\eta)$, $\frac{p-p_\infty}{p_\mathrm{m}-p_\infty} = P(\eta)$; $u_\mathrm{m} = Ax^\alpha$, $w_\mathrm{m} = Cx^\varepsilon$, $p_\mathrm{m} - p_\infty = \rho D x^\delta$, $\eta = Byx^\beta$
	IIa	$\frac{T-T_\infty}{T_\mathrm{m}-T_\infty} = \theta(\eta)$, $T_\mathrm{m} - T_\infty = \Gamma x^\gamma$
	IIb	–
Exponents in the self-similar solutions	I	$\alpha = -1$, $\beta = -1$, $\varepsilon = -2$, $\delta = -4$
	IIa	$\gamma = -1$
	IIb	–
Constants in the self-similar solutions	I	$A = \frac{3J_x}{8\pi\rho\nu}$, $B = \sqrt{\frac{3J_x}{8\pi\rho\nu^2}}$, $C = \frac{3M_x}{32\pi\rho\nu^2}\sqrt{\frac{3J_x}{8\pi\rho}}$, $D = \frac{9}{2048}\frac{M_x^2 J_x}{\pi^3\rho^3\nu^4}$
	IIa	$\Gamma = \frac{(2\,\mathrm{Pr}+1)Q}{8\pi\rho\nu c_\mathrm{p}}$
	IIb	–
Integral invariants	I	$J_x = 2\pi\int_0^\infty \rho u^2 y\,\mathrm{d}y = \mathrm{const}$, $M_x = 2\pi\int_0^\infty \rho u w y^2\,\mathrm{d}y = \mathrm{const}$
	IIa	$Q = 2\pi\int_0^\infty \rho c_\mathrm{p} u(T-T_\infty)y\,\mathrm{d}y = \mathrm{const}$
	IIb	–
Self-similar equations	I	$\left(F'' - \frac{F'}{\eta}\right)' + \left(\frac{FF'}{\eta}\right)' = 0$; $P' = \frac{\Phi^2}{\eta}$; $\Phi'' + \frac{1+F}{\eta}\Phi' + \frac{\eta F' + F - 1}{\eta^2}\Phi = 0$
	IIa	$(\eta\theta')' + \mathrm{Pr}(F\theta)' = 0$
	IIb	–
Self-similar boundary conditions	I	$\frac{F'}{\eta}\Big|_{\eta=0} = 1$, $\frac{F}{\eta}\Big|_{\eta=0} = 0$, $\Phi(0) = 0$; $\frac{F'}{\eta}\Big|_{\eta=\infty} = 0$, $\Phi(\infty) = 0$; $P(\infty) = 0$
	IIa	$\theta'(0) = 0$, $\theta(\infty) = 0$
	IIb	–
Self-similar solutions	I	$F(\eta) = \frac{\frac{1}{2}\eta^2}{1+\frac{1}{8}\eta^2}$, $\frac{F'}{\eta} = \frac{1}{\left(1+\frac{1}{8}\eta^2\right)^2}$, $\Phi = \frac{\eta}{\left(1+\frac{1}{8}\eta^2\right)^2}$, $P(\eta) = \frac{1}{\left(1+\frac{1}{8}\eta^2\right)^3}$
	IIa	$\theta(\eta) = \left(\frac{F'}{\eta}\right)^{\mathrm{Pr}} = \frac{1}{\left(1+\frac{1}{8}\eta^2\right)^{2\,\mathrm{Pr}}}$
	IIb	–
Integral characteristics	I	$G = \int_0^\infty 2\pi\rho u y\,\mathrm{d}y = 8\pi\mu x$; $E = \pi\int_0^\infty \rho u^3 y\,\mathrm{d}y = \frac{\pi}{\mu}\left(\frac{3J_x}{8\pi}\right)^2\left(\int_0^\infty \frac{F'^3}{\eta^2}\,\mathrm{d}\eta\right)\frac{1}{x}$
	IIa	–
	IIb	–
Flow type: submerged radial swirling jet		
Differential equations	I	$u\partial u/\partial x + v\partial u/\partial y = \nu\partial^2 u/\partial y^2$; $u\partial w/\partial x + v\partial w/\partial y + \frac{uw}{x} = \nu\partial^2 w/\partial y^2$; $\partial/\partial x(xu) + \partial/\partial y(xv) = 0$
	II	$u\partial T/\partial x + v\partial T/\partial y = \alpha\partial^2 T/\partial y^2$

Table 2.7 (continued)

Boundary conditions	I	$v(x,0)=0,\ \partial u/\partial y\|_{y=0}=\partial w/\partial y\|_{y=0}=0\,,\quad u(x,\pm\infty)=w(x,\pm\infty)=0$
	IIa	$\partial T/\partial y\|_{y=0}=0\,,\quad T(x,\pm\infty)=T_\infty$
	IIb	$T(x,+\infty)=T_1\,,\quad T(x,-\infty)=T_2$
General structure of the self-similar solutions	I	$\frac{u}{u_\mathrm{m}}=F'(\eta)\,,\quad \frac{w}{w_\mathrm{m}}=\Phi(\eta)\,;\quad u_\mathrm{m}=Ax^\alpha\,,\quad w_\mathrm{m}=Cx^\varepsilon\,,\quad \eta=Byx^\beta$
	IIa	$\frac{T-T_\infty}{T_\mathrm{m}-T_\infty}=\theta(\eta)\,,\quad T_\mathrm{m}-T_\infty=\Gamma x^\gamma$
	IIb	$\frac{T-T_2}{T_1-T_2}=\theta(\eta)$
Exponents in the self-similar solutions	I	$\alpha=-1\,,\quad \beta=-1\,,\quad \varepsilon=-2$
	IIa	$\gamma=-1$
	IIb	$(\gamma=0)$
Constants in the self-similar solutions	I	$A=\frac{1}{4}\sqrt[3]{\frac{9J_x^2}{2\pi^2\rho^2\nu}}\,,\quad B=\frac{1}{2}\sqrt[3]{\frac{3J_x}{4\pi\rho\nu^2}}\,,\quad C=\frac{3M_y}{8\pi\rho}\sqrt[3]{\frac{4\pi\rho}{3\nu J_x}}$
	IIa	$\Gamma=\frac{Q}{2\pi\rho c_\mathrm{p}J_3}\sqrt[3]{\frac{4\pi\rho}{3\nu J_x}}\,,\quad \left(J_3=\int\limits_{-\infty}^{+\infty}F'\theta\,\mathrm{d}\eta\right)$
	IIb	$(\Gamma=T_1-T_2)$
Integral invariants	I	$J_x=2\pi x\int\limits_{-\infty}^{+\infty}\rho u^2\,\mathrm{d}y=\mathrm{const}\,,\quad M_y=2\pi x^2\int\limits_{-\infty}^{+\infty}\rho uw\,\mathrm{d}y=\mathrm{const}$
	IIa	$Q=2\pi x\int\limits_{-\infty}^{+\infty}\rho c_\mathrm{p}u(T-T_\infty)\,\mathrm{d}y=\mathrm{const}$
	IIb	–
Self-similar equations	I	$F'''+2(FF')'=0\,,\quad \Phi''+2(F\Phi)''=0$
	IIa	$\theta''+2\,\mathrm{Pr}(F\theta)'=0$
	IIb	$\theta''+2\,\mathrm{Pr}\,F\theta'=0$
Self-similar boundary conditions	I	$F(0)=0\,,\quad F'(0)=1\,,\quad F'(\pm\infty)=\Phi(\pm\infty)=0\,;\quad \Phi'(0)=0$
	IIa	$\theta'(0)=0\,,\quad \theta(\pm\infty)=0$
	IIb	$\theta(+\infty)=1\,,\quad \theta(-\infty)=0$
Self-similar solutions	I	$F=\tanh\eta\,,\quad F'=1/\cosh^2\eta\,;\quad \Phi=F'=1/\cosh^2\eta$
	IIa	$\theta(\eta)=(F')^{\mathrm{Pr}}=(\cosh\eta)^{-2\,\mathrm{Pr}}$
	IIb	$\theta(\eta)=\left[\int\limits_{-\infty}^{\eta}(\cosh\eta)^{-2\,\mathrm{Pr}}\,\mathrm{d}\eta\right]\left[\int\limits_{-\infty}^{+\infty}(\cosh\eta)^{-2\,\mathrm{Pr}}\,\mathrm{d}\eta\right]^{-1}$
Integral characteristics	I	$G=2\pi x\int\limits_{-\infty}^{+\infty}\rho u\,\mathrm{d}y=2\sqrt[3]{6\pi^2\rho^2\nu J_x}x\,,\quad E=\pi x\int\limits_{-\infty}^{+\infty}\rho u^3\,\mathrm{d}y=\frac{3}{20}\frac{J_x}{\pi\mu}\sqrt[3]{\frac{4}{3}\pi\rho\nu^2J_x^2}\frac{1}{x}$
	IIa	–
	IIb	$Q=c_\mathrm{p}(T_1-T_2)\sqrt[3]{6\pi^2\rho^2\nu J_x}x\int\limits_{-\infty}^{+\infty}F'\theta\,\mathrm{d}\eta$
Flow type: planar wall jet		
Differential equations	I	$u\partial u/\partial x+v\partial u/\partial y=\nu\partial^2u/\partial y^2\,;\quad \partial u/\partial x+\partial v/\partial y=0$
	II	$u\partial T/\partial x+v\partial T/\partial y=\alpha\partial^2T/\partial y^2$
Boundary conditions	I	$u(x,0)=v(x,0)=0\,;\quad u(x,\infty)=0$
	IIa	$T(x,0)=T_\infty\,,\ T(x,\infty)=T_\infty$
	IIb	$\partial T/\partial y\|_{y=0}=0\,,\ T(x,\infty)=T_\infty$
	IIc	$T(x,0)=T_\mathrm{w}\,,\quad T(x,\infty)=T_\infty$

Table 2.7 (continued)

General structure of the self-similar solutions	I	$\frac{u}{u_\mathrm{m}} = F'(\eta)\,, \quad u_\mathrm{m} = Ax^\alpha\,, \quad \eta = Byx^\beta$
	IIa	$\frac{T-T_\infty}{T_\mathrm{m}-T_\infty} = \theta(\eta)\,, T_\mathrm{m} - T_\infty = \Gamma x^\gamma$
	IIb	$\frac{T-T_\infty}{T_\mathrm{m}-T_\infty} = \theta(\eta)\,, T_\mathrm{m} - T_\infty = \Gamma x^\gamma$
	IIc	$\frac{T-T_\infty}{T_\mathrm{w}-T_\infty} = \theta(\eta) \quad (\Gamma = T_\mathrm{w} - T_\infty)$
Exponents in the self-similar solutions	I	$\alpha = -\frac{1}{2}\,, \quad \beta = -\frac{3}{4}$
	IIa	$\gamma = -\frac{1}{2}$
	IIb	$\gamma = -\frac{1}{4}$
	IIc	$(\gamma = 0)$
Constants in the self-similar solutions	I	$A = \sqrt{\frac{K}{4\rho^2\nu J_1}}\,, \quad B = \frac{1}{2}\sqrt[4]{\frac{K}{4\rho^2\nu^3 J_1}}\,, \quad \left(J_1 = \int\limits_0^\infty FF'\,\mathrm{d}\eta\right)$
	IIa	$\Gamma(\mathrm{Pr}) = \left[\int\limits_0^\infty \theta^{3/2}\,\mathrm{d}\eta (K_\mathrm{T} B)^{-1}\right]^{4/3}$
	IIb	$\Gamma = \frac{Q}{c_\mathrm{p}}\sqrt[4]{\frac{J_1}{4\rho^2\nu K}}\left(\int\limits_0^\infty F'\theta\,\mathrm{d}\eta\right)^{-1}$
	IIc	$(\Gamma = T_\mathrm{w} - T_\infty)$
Integral invariants	I	$K = \int\limits_0^\infty \rho u^2\left(\int\limits_0^y \rho u\,\mathrm{d}y\right)\mathrm{d}y = \int\limits_0^\infty \rho u\left(\int\limits_y^\infty \rho u^2\,\mathrm{d}y\right)\mathrm{d}y = \mathrm{const}$
	IIa	$K_\mathrm{T} = \int\limits_0^\infty (T - T_\infty)^{3/2}\,\mathrm{d}y = \mathrm{const}$
	IIb	$Q = \int\limits_0^\infty \rho c_\mathrm{p} u(T - T_\infty)\,\mathrm{d}y = \mathrm{const}$
	IIc	–
Self-similar equations	I	$F''' + FF'' + 2F'^2 = 0$
	IIa	$\frac{1}{\mathrm{Pr}}\theta'' + F\theta' + 2F'\theta = 0$
	IIb	$\theta'' + \mathrm{Pr}(F\theta)' = 0$
	IIc	$\theta'' + \mathrm{Pr}\,F\theta' = 0$
Self-similar boundary conditions	I	$F(0) = F'(0) = 0\,; \quad F'(\infty) = 0$
	IIa	$\theta(0) = 0\,, \quad \theta(\infty) = 0$
	IIb	$\theta'(0) = 0\,, \quad \theta(\infty) = 0$
	IIc	$\theta(0) = 1\,, \quad \theta(\infty) = 0$
Self-similar solutions	I	$\eta = \frac{1}{2F_\infty}\ln\frac{F+\sqrt{FF_\infty}+F_\infty}{(\sqrt{F_\infty}-\sqrt{F})^2} + \frac{\sqrt{3}}{F_\infty}\left(\arctan\frac{2\sqrt{F}+\sqrt{F_\infty}}{\sqrt{3F_\infty}} - \arctan\frac{1}{\sqrt{3}}\right)\,, \quad F' = \frac{2}{3}(F_\infty^{2/3}F^{1/2} - F^2)\,,$ $F_\infty = F(\infty) = 1.7818$
	IIa	$\theta(\eta)_{\mathrm{Pr}=1} = F'(\eta)$
	IIb	$\theta(\eta) = \exp\left[-\mathrm{Pr}\int\limits_0^\eta F(\xi)\,\mathrm{d}\xi\right]$
	IIc	$\theta(\eta) = 1 - \left[\int\limits_0^\eta \exp\left(-\mathrm{Pr}\int\limits_0^\zeta F\,\mathrm{d}\xi\right)\mathrm{d}\zeta\right]\left[\int\limits_0^\infty \exp\left(-\mathrm{Pr}\int\limits_0^\zeta F\,\mathrm{d}\xi\right)\mathrm{d}\zeta\right]^{-1}$
Integral characteristics	I	$G = \int\limits_0^\infty \rho u\,\mathrm{d}y = F_\infty\sqrt[4]{\frac{4\rho^2\nu K x}{J_1}}\,; \quad J_x = \sqrt[4]{\frac{K^3}{4\rho^2\nu J_1^3 x}}\left(\int\limits_0^\infty F'^2\,\mathrm{d}\eta\right)\,; \quad E = \frac{K}{4\rho J_1}\sqrt[4]{\frac{K}{4\rho^2\nu^3 J_1 x^3}}$
	IIa	$Q = \rho c_\mathrm{p}\frac{A\Gamma}{B}x^{-1/4}\int\limits_0^\infty F'\theta\,\mathrm{d}\varphi$
	IIb	–
	IIc	$Q = \sqrt[4]{\frac{4\rho^2\nu K x}{J_1}}c_\mathrm{p}(T_\mathrm{w} - T_\infty)\int\limits_0^\infty F'\theta\,\mathrm{d}\eta$

Table 2.7 (continued)

Flow type: slightly swirling jet propagating along a cone		
Differential equations	I	$u\partial u/\partial x + v\partial u/\partial y = \nu\partial^2 u/\partial y^2\,;\quad \rho\frac{w^2}{x}\operatorname{cotan}\omega = \partial p/\partial y\,;\quad u\partial w/\partial x + v\partial w/\partial y + \frac{uw}{x} = \nu\partial^2 w/\partial y^2\,;$ $\partial/\partial x(xu) + \partial/\partial y(xv) = 0$
	II	$u\partial T/\partial x + v\partial T/\partial y = \alpha\partial^2 T/\partial y^2$
Boundary conditions	I	$u(x,0) = v(x,0) = w(x,0) = 0\,;\quad u(x,\infty) = w(x,\infty) = 0\,;\quad p(x,\infty) = p_\infty$
	IIa	$T(x,0) = T_\infty\,,\ T(x,\infty) = T_\infty$
	IIb	$\partial T/\partial y\vert_{y=0} = 0\,,\ T(x,\infty) = T_\infty$
	IIc	$T(x,0) = T_\mathrm{w}\,,\ T(x,\infty) = T_\infty$
General structure of the self-similar solutions	I	$\frac{u}{u_\mathrm{m}} = F'(\eta)\,,\quad \frac{w}{w_\mathrm{m}} = \Phi(\eta)\,,\quad \frac{p_\infty - p}{p_\infty - p_\mathrm{m}} = P(\eta)\,;\quad u_\mathrm{m} = Ax^\alpha\,,\quad w_\mathrm{m} = Cx^\varepsilon\,,\quad p_\infty - p_\mathrm{m} = Dx^\delta\,,\quad \eta = Byx^\beta$
	IIa	$\frac{T-T_\infty}{T_\mathrm{m}-T_\infty} = \theta(\eta)\,,\ T_\mathrm{m} - T_\infty = \Gamma x^\gamma$
	IIb	$\frac{T-T_\infty}{T_\mathrm{m}-T_\infty} = \theta(\eta)\,,\ T_\mathrm{m} - T_\infty = \Gamma x^\gamma$
	IIc	$\frac{T-T_\infty}{T_\mathrm{w}-T_\infty} = \theta(\eta)\quad (\Gamma = T_\mathrm{w} - T_\infty)$
Exponents in the self-similar solutions	I	$\alpha = -\frac{3}{2}\,,\quad \beta = -\frac{5}{4}\,,\quad \varepsilon = -\frac{5}{2}\,,\quad \delta = -\frac{19}{4}$
	IIa	$\gamma = -\frac{3}{2}$
	IIb	$\gamma = -\frac{3}{4}$
	IIc	$(\gamma = 0)$
Constants in the self-similar solutions	I	$A = \sqrt{\frac{3K}{4\rho^2\nu J_1}}\,,\quad B = \sqrt[4]{\frac{27K}{64\rho^2\nu^3 J_1}}\,,\quad C = \frac{N}{\rho}\sqrt{\frac{3}{4\nu K J_1}}\,,\quad D = \operatorname{cotan}\omega\left(\frac{N}{K}\right)^2\sqrt[4]{\frac{3}{4\rho^2\nu}\left(\frac{K}{J_1}\right)^3}\,,\quad \left(J_1 = \int_0^\infty F F'^2\,\mathrm{d}\eta\right)$
	IIa	$\Gamma(\mathrm{Pr}) = \left[\int_0^\infty \theta^{3/2}\,\mathrm{d}\eta (BK_\mathrm{T})^{-1}\right]^{-2/3}$
	IIb	$\Gamma = \frac{Q}{2\pi\rho c_\mathrm{p}\sin\omega}\sqrt[4]{\frac{3J_1}{4\rho^2\nu K}}\left(\int_0^\infty F'\theta\,\mathrm{d}\eta\right)^{-1}$
	IIc	$\Gamma = T_\mathrm{w} - T_\infty$
Integral invariants	I	$K = \int_0^\infty \rho x u^2\left(\int_0^y \rho x u\,\mathrm{d}y\right)\mathrm{d}y = \mathrm{const}\,,\quad N = \int_0^\infty \rho x^2 u w\left(\int_0^y \rho x u\,\mathrm{d}y\right)\mathrm{d}y = \mathrm{const}$
	IIa	$K_\mathrm{T} = \int_0^\infty (T - T_\infty)^{3/2} x\,\mathrm{d}y = \mathrm{const}$
	IIb	$Q = 2\pi\sin\omega\int_0^\infty \rho x u c_\mathrm{p}(T - T_\infty)\mathrm{d}y = \mathrm{const}$
	IIc	–
Self-similar equations	I	$F''' + FF'' + 2F'^2 = 0\,;\quad P' = -\Phi^2\,;\quad \Phi'' + F\Phi' + 2F'\Phi = 0$
	IIa	$\frac{1}{\mathrm{Pr}}\theta'' + F\theta' + 2F'\theta = 0$
	IIb	$\theta'' + \mathrm{Pr}(F\theta)' = 0$
	IIc	$\theta'' + \mathrm{Pr}\,F\theta' = 0$
Self-similar boundary conditions	I	$F(0) = F'(0) = \Phi(0) = 0\,;\quad F'(\infty) = \Phi(\infty) = P(\infty) = 0$
	IIa	$\theta(0) = 0\,,\quad \theta(\infty) = 0$
	IIb	$\theta'(0) = 0\,,\quad \theta(\infty) = 0$
	IIc	$\theta(0) = 1\,,\quad \theta(\infty) = 0$

Table 2.7 (continued)

Self-similar solutions	I	$\eta = \frac{1}{2F_\infty}\left[\ln\frac{F+\sqrt{FF_\infty}+F_\infty}{(\sqrt{F}-\sqrt{F_\infty})^2}+2\sqrt{3}\left(\arctan\frac{2\sqrt{F}+\sqrt{F_\infty}}{\sqrt{3F_\infty}}-\arctan\frac{1}{\sqrt{3}}\right)\right]$; $F' = \Phi = \frac{2}{3}(F_\infty{}^{3/2}F^{1/2}-F^2)$, $P = -\int_\eta^\infty F'^2\,\mathrm{d}\eta$; $F_\infty = F(\infty) = 1.7818$
	IIa	$\theta(\eta)_{\mathrm{Pr}=1} = F'(\eta)$
	IIb	$\theta(\eta) = \exp\left[-\mathrm{Pr}\int_0^\eta F(\xi)\,\mathrm{d}\xi\right]$
	IIc	$\theta(\eta) = 1-\left[\int_0^\eta \exp\left(-\mathrm{Pr}\int_0^\zeta F\,\mathrm{d}\xi\right)\mathrm{d}\zeta\right]\left[\int_0^\infty \exp\left(-\mathrm{Pr}\int_0^\zeta F\,\mathrm{d}\xi\right)\mathrm{d}\zeta\right]^{-1}$
Integral characteristics	I	$G = 2\pi\rho F_\infty \sin\omega\frac{A}{B}x^{3/4}$; $J_x = 2\pi\rho\sin\omega\frac{A^2}{B}x^{-3/4}\int_0^\infty F'^2\,\mathrm{d}\eta$; $M = 2\pi\rho\frac{AC}{B}\sin^2\omega x^{-3/4}\int_0^\infty F'^2\,\mathrm{d}\eta$; $E = \pi\rho\sin\omega\frac{A^3}{B}x^{-9/4}\int_0^\infty F'^3\,\mathrm{d}\eta$
	IIa	$Q = 2\pi\rho c_\mathrm{p}\frac{A\Gamma}{B}x^{-3/4}\sin\omega\int_0^\infty F'\theta\,\mathrm{d}\eta$
	IIb	–
	IIc	$Q = 2\pi\rho c_\mathrm{p}\sin\omega\frac{A}{B}(T_\mathrm{w}-T_\infty)x^{3/4}\int_0^\infty F'\theta\,\mathrm{d}\eta$

Since L is not given, only functions of a special, self-similar type, $f(\overline{x},\overline{y}) = \overline{x}f_1(\overline{y}/\overline{x})$ can be admitted. The latter automatically reduces (2.162) to the following form

$$\psi = \nu x f_1\left[\frac{y}{x}\left(\frac{J_x}{2\pi\rho\nu^2}\right)^{1/2}\right], \tag{2.163}$$

where L is absent. Obviously, any dimensionless factor could be introduced in the self-similar variable following from (2.163). For consistency with literature, we take it as $(3/4)^{1/2}$. Then the self-similar solution corresponding to (2.163) has the form

$$\psi = \nu x F(\eta)\,, \quad \eta = \frac{y}{x}\left(\frac{3J_x}{8\pi\rho\nu^2}\right)^{1/2}. \tag{2.164}$$

Substitution of the self-similar solution (2.164) into (2.158), the boundary and integral conditions (2.156) and (2.157) yields the following boundary-value problem

$$\left(F''-\frac{F'}{\eta}+\frac{FF'}{\eta}\right)' = 0\,,$$
$$\eta = 0\,, \quad F = \frac{F''\eta-F'}{\eta^2} = 0\,,$$
$$\eta = \infty\,, \quad \frac{F'}{\eta} = 0\,,$$
$$\int_0^\infty\left(\frac{F'}{\eta}\right)^2\eta\,\mathrm{d}\eta = \frac{4}{3}\,, \tag{2.165}$$

which has a solution

$$F = \frac{\eta^2/2}{1+\eta^2/8}\,, \tag{2.166}$$

The velocity profile rendered dimensionless by the maximal (axial) velocity $u_\mathrm{m}(x)$ reads

$$\frac{u}{u_\mathrm{m}} = \frac{F'}{\eta} = \frac{1}{(1+\eta^2/8)^2}\,, \tag{2.167}$$

where $u_\mathrm{m}(x) = 3J_x/(8\pi\rho\nu x)$.

It is emphasized that the fact that the flow in the far-field zone of the jet should be self-similar, can be (and has been) established without solution of the governing equations, just by consideration of the problem as posed.

The thermal field in the jet also possesses an invariant, an excess heat flux along the jet $Q = \mathrm{const}$, namely

$$2\pi\rho c_\mathrm{p}\int_0^\infty u(T-T_\infty)y\,\mathrm{d}y = Q\,, \tag{2.168}$$

where c_p is the specific heat at constant pressure. The corresponding self-similar solution for the temperature field has the form

$$\theta(\eta) = \frac{T-T_\infty}{T_\mathrm{m}-T_\infty} = \frac{1}{(1+\eta^2/8)^{2\,\mathrm{Pr}}}\,, \tag{2.169}$$

where the maximal (axial) excess temperature $T_\mathrm{m}-T_\infty$ is given by

$$T_\mathrm{m}-T_\infty = \frac{(2\,\mathrm{Pr}+1)Q}{8\pi\rho\nu c_\mathrm{p}x}\,. \tag{2.170}$$

Table 2.8 Self-similar turbulent jets

Flow type: planar submerged jet		
Differential equations	I	$u\partial u/\partial x + v\partial u/\partial y = \partial/\partial y\,(\nu_\mathrm{T}\partial u/\partial y)\;;\quad \partial u/\partial x + \partial v/\partial y = 0\,,\quad (\nu_\mathrm{T} = KAx^{\alpha-\beta})$
	II	$u\partial T/\partial x + v\partial T/\partial y = \partial/\partial y\,(\alpha_\mathrm{T}\partial T/\partial y)\;,\quad \left(\alpha_\mathrm{T} = K_q Ax^{\alpha-\beta}\right)$
Boundary conditions	I	$v(x,0) = 0\,,\quad \partial u/\partial y|_{y=0} = 0\,;\quad u(x,\pm\infty) = 0$
	IIa	$\partial T/\partial y|_{y=0} = 0\,,\quad T(x,\pm\infty) = T_\infty$
	IIb	$T(x,+\infty) = T_1\,,\quad T(x,-\infty) = T_2$
General structure of the self-similar solutions	I	$\frac{u}{u_\mathrm{m}} = F'(\eta)\,,\quad u_\mathrm{m} = Ax^\alpha\,,\quad \eta = Byx^\beta\quad \left(B \equiv \frac{1}{a}\right)$
	IIa	$\frac{T-T_\infty}{T_\mathrm{m}-T_\infty} = \theta(\eta)\,,\quad T_\mathrm{m} - T_\infty = \Gamma x^\gamma$
	IIb	$\frac{T-T_2}{T_1-T_2} = \theta(\eta)\quad (\Gamma = T_1 - T_2)$
Exponents in the self-similar solutions	I	$\alpha = -\frac{1}{2}\,,\quad \beta = -1$
	IIa	$\gamma = -\frac{1}{2}$
	IIb	$(\gamma = 0)$
Constants in the self-similar solutions	I	$A = \sqrt{\frac{3J_x}{8\rho\sqrt{K}}}\,,\quad B = \frac{1}{2\sqrt{K}}$
	IIa	$\Gamma = \frac{Q}{c_\mathrm{p}}\sqrt{\frac{2}{3\rho J_x\sqrt{K}}}\left(\int_{-\infty}^{+\infty} F'\theta\,\mathrm{d}\eta\right)^{-1}$
	IIb	$\Gamma = T_1 - T_2$
Integral invariants	I	$J_x = \int_{-\infty}^{+\infty} \rho u^2\,\mathrm{d}y = \mathrm{const}$
	IIa	$Q = \int_{-\infty}^{+\infty} \rho c_\mathrm{p} u(T - T_\infty)\,\mathrm{d}y = \mathrm{const}$
	IIb	–
Self-similar equations	I	$F''' + 2(FF')' = 0$
	IIa	$\theta'' + 2\mathrm{Pr}_\mathrm{T}(F\theta)' = 0$
	IIb	$\theta'' + 2\mathrm{Pr}_\mathrm{T} F\theta' = 0$
Self-similar coordinate $\eta_{1/2}$ corresponding to $u/u_\mathrm{m} = 1/2$	I	$\eta_{1/2} = 0.88$
Self-similar boundary conditions	I	$F(0) = 0\,,\quad F'(0) = 1\,,\quad F'(\pm\infty) = 0$
	IIa	$\theta(0) = 1\,,\quad \theta(\pm\infty) = 0$
	IIb	$\theta(+\infty) = 1\,,\quad \theta(-\infty) = 0$
Self-similar solutions	I	$F = \tanh\eta\,,\quad F' = 1/\cosh^2\eta$
	IIa	$\theta(\eta) = (F')^{\mathrm{Pr}_\mathrm{T}} = 1/\cosh^{2\mathrm{Pr}_\mathrm{T}}\eta$
	IIb	$\theta(\eta) = \left[\int_{-\infty}^{\eta} (\cosh\xi)^{-2\mathrm{Pr}_\mathrm{T}}\,\mathrm{d}\xi\right]\left[\int_{-\infty}^{+\infty} (\cosh\xi)^{-2\mathrm{Pr}_\mathrm{T}}\,\mathrm{d}\xi\right]^{-1}$
Mass flow rate (G), kinetic energy flux (E), etc., as well as turbulent kinematic viscosity (ν_T) and thermal diffusivity (α_T)	I	$G \sim x^{1/2}\,,\quad E \sim x^{1/2}\,;\quad \nu_\mathrm{T} \sim x^{1/2}$
	IIa	$\alpha_\mathrm{T} \sim x^{1/2}$
	IIb	$Q \sim x^{1/2}\,,\quad \alpha_\mathrm{T} \sim x^{1/2}$
Flow type: free mixing layers		
Differential equations	I	$u\partial u/\partial x + v\partial u/\partial y = \partial/\partial y\,(\nu_\mathrm{T}\partial u/\partial y)\;;\quad \partial u/\partial x + \partial v/\partial y = 0\,,\quad \left[\nu_\mathrm{T} = K(u_1 - u_2)x^{\alpha-\beta}\right]$
	II	$u\partial T/\partial x + v\partial T/\partial y = \partial/\partial y\,(\alpha_\mathrm{T}\partial T/\partial y)\;,\quad \left[\alpha_\mathrm{T} = K_q(u_1 - u_2)x^{\alpha-\beta}\right]$

Table 2.8 (continued)

Boundary conditions	I	$u(x,+\infty)=u_1\,,\quad \partial u/\partial y|_{y=\pm\infty}=0\,;\quad u(x,-\infty)=u_2$
	IIa	–
	IIb	$T(x,+\infty)=T_1\,,\quad T(x,-\infty)=T_2$
General structure of the self-similar solutions	I	$\frac{u}{u_\mathrm{m}}=F'(\eta)\,,\quad u_\mathrm{m}=u_1=\mathrm{const}\,,\quad \eta=Byx^\beta\quad \left(B\equiv\frac{1}{a}\right)$
	IIa	–
	IIb	$\frac{T-T_2}{T_1-T_2}=\theta(\eta)$
Exponents in the self-similar solutions	I	$\alpha=0\,,\quad \beta=-1$
	IIa	–
	IIb	$\gamma=0$
Constants in the self-similar solutions	I	$A=u_1\,,\quad B=\frac{1}{a}=\frac{1}{\sqrt{2K(1-m)}}\,,\quad \left(m=\frac{u_2}{u_1}\right)$
	IIa	–
	IIb	$\Gamma=T_1-T_2$
Integral invariants	I	–
	IIa	–
	IIb	–
Self-similar equations	I	$F'''+2FF''=0$
	IIa	–
	IIb	$\theta''+2\mathrm{Pr_T}F\theta'=0$
Self-similar coordinate $\eta_{1/2}$ corresponding to $u/u_\mathrm{m}=1/2$	I	$\eta_{1/2}\approx-0.33\quad(\text{for } m=0)$
Self-similar boundary conditions	I	$F'(+\infty)=1\,,\quad F''(\pm\infty)=0\,;\quad F'(-\infty)=m$
	IIa	–
	IIb	$\theta(+\infty)=1\,,\quad \theta(-\infty)=0$
Self-similar solutions	I	$F'(\eta)=\frac{u}{u_1}=1+\frac{1}{2}(m-1)\left[1-\mathrm{erf}(\eta+\eta_0)\right]\,.\quad(\eta_0\approx0.33)$
	IIa	–
	IIb	$\theta=\frac{1}{2}\left[1+\mathrm{erf}(\eta+\eta_0)\sqrt{\mathrm{Pr}_T}\right]$
Mass flow rate (G), kinetic energy flux (E), etc., as well as turbulent kinematic viscosity (ν_T) and thermal diffusivity (α_T)	I	$\nu_\mathrm{T}\sim x$
	IIa	–
	IIb	$\alpha_\mathrm{T}\sim x$
Flow type: axisymmetric submerged jet: swirling if $w\neq0$; no swirling if $w=0$		
Differential equations	I	$u\partial u/\partial x+v\partial u/\partial y=\frac{\nu_\mathrm{T}}{y}\partial/\partial y\,(y\partial u/\partial y)\,;\quad \frac{\rho w^2}{y}=\partial p/\partial y\,;$ $u\partial w/\partial x+v\partial w/\partial y+\frac{vw}{y}=\nu_\mathrm{T}\left[\frac{1}{y}\partial/\partial y\,(y\partial w/\partial y)-\frac{w}{y^2}\right]\,;\quad \partial/\partial x(yu)+\partial/\partial y(yv)=0$
	II	$u\partial T/\partial x+v\partial T/\partial y=\alpha_\mathrm{T}\frac{1}{y}\partial/\partial y\,(y\partial T/\partial y)$
Boundary conditions	I	$v(x,0)=w(x,0)=\partial u/\partial y|_{y=0}=0\,,\quad u(x,\infty)=w(x,\infty)=0\,,\quad p(x,\infty)=p_\infty$
	IIa	$\partial T/\partial y|_{y=0}=0\,;\quad T(x,\infty)=T_\infty$
	IIb	–
General structure of the self-similar solutions	I	$\frac{u}{u_\mathrm{m}}=\frac{F'(\eta)}{\eta}\,,\quad \frac{w}{w_\mathrm{m}}=\Phi(\eta)\,,\quad \frac{p-p_\infty}{p_\mathrm{m}-p_\infty}=P(\eta)\,;$ $u_\mathrm{m}=Ax^\alpha\,,\quad w_\mathrm{m}=Cx^\varepsilon\,,\quad p_\mathrm{m}-p_\infty=\rho Dx^\delta\,,\quad \eta=Byx^\beta$
	IIa	$\frac{T-T_\infty}{T_\mathrm{m}-T_\infty}=\theta(\eta)\,,\quad T_\mathrm{m}-T_\infty=\Gamma x^\gamma$
	IIb	–

Table 2.8 (continued)

Exponents in the self-similar solutions	I	$\alpha=-1\,,\quad \beta=-1\,,\quad \varepsilon=-2\,,\quad \delta=-4$
	IIa	$\gamma=-1$
	IIb	–
Constants in the self-similar solutions	I	$A=\sqrt{\frac{3J_x}{8\pi\rho K}}\,,\quad B=\frac{1}{a}=\frac{1}{\sqrt{K}}\,,\quad C=\frac{3M_x}{32\pi\rho K}\sqrt{\frac{8\pi\rho}{3J_x}}\,,\quad D=\frac{M_x^2}{32\pi\rho K^2 J_x}\quad (K=a^2)$
	IIa	$\Gamma=\left(\mathrm{Pr_T}+\frac{1}{2}\right)\frac{Q}{c_\mathrm{p}}\frac{1}{\sqrt{6\pi\rho K J_x}}$
	IIb	–
Integral invariants	I	$J_x=2\pi\int\limits_0^\infty \rho u^2 y\,\mathrm{d}y=\mathrm{const}\,,\quad M_x=2\pi\int\limits_0^\infty \rho u w y^2\,\mathrm{d}y=\mathrm{const}$
	IIa	$Q=2\pi\int\limits_0^\infty \rho c_\mathrm{p} u(T-T_\infty)y\,\mathrm{d}y=\mathrm{const}$
	IIb	–
Self-similar equations	I	$\left(F''-\frac{F'}{\eta}\right)+\left(\frac{FF'}{\eta}\right)'=0\,;\quad P'=\frac{\Phi^2}{\eta}\,;\quad \Phi''+\frac{1+F}{\eta}\Phi'+\frac{\eta F'+F-1}{\eta^2}\Phi=0$
	IIa	$(\eta\theta')'+\mathrm{Pr_T}(F\theta)'=0$
	IIb	–
Self-similar coordinate $\eta_{1/2}$ corresponding to $u/u_\mathrm{m}=1/2$	I	$\eta_{1/2}=1.82$
Self-similar boundary conditions	I	$\left.\frac{F'}{\eta}\right\|_{\eta=0}=1\,,\quad \left.\frac{F}{\eta}\right\|_{\eta=0}=0\,,\quad \Phi(0)=0\,;\quad \left.\frac{F'}{\eta}\right\|_{\eta=\infty}=0\,,\quad \Phi(\infty)=P(\infty)=0$
	IIa	$\theta'(0)=0\,,\quad \theta(\infty)=0$
	IIb	–
Self-similar solutions	I	$F(\eta)=\frac{\frac{1}{2}\eta^2}{1+\frac{1}{8}\eta^2}\,;\quad F'(\eta)=\frac{\eta}{\left(1+\frac{1}{8}\eta^2\right)^2}\,;\quad \Phi=\frac{\eta}{\left(1+\frac{1}{8}\eta^2\right)^2}\,,\quad P(\eta)=\frac{1}{\left(1+\frac{1}{8}\eta^2\right)^3}$
	IIa	$\theta(\eta)=\left(\frac{F'}{\eta}\right)^{\mathrm{Pr_T}}=\left(1+\frac{1}{8}\eta^2\right)^{-2\mathrm{Pr_T}}$
	IIb	–
Mass flow rate (G), kinetic energy flux (E), etc., as well as turbulent kinematic viscosity (ν_T) and thermal diffusivity (α_T)	I	$G\sim x\,,\quad E\sim x^{-1}\,,\quad \nu_\mathrm{T}=KA=\mathrm{const}$
	IIa	$\alpha_\mathrm{T}=K_q A=\mathrm{const}\,;\quad \mathrm{Pr_T}=\frac{K}{Kq}$
	IIb	–
Flow type: submerged radial swirling jet		
Differential equations	I	$u\partial u/\partial x+v\partial u/\partial y=\partial/\partial y\,(\nu_\mathrm{T}\partial u/\partial y)\,;\quad u\partial w/\partial x+v\partial w/\partial y+\frac{uw}{x}=\partial/\partial y\,(\nu_\mathrm{T}\partial w/\partial y)\,;$ $\partial/\partial x(xu)+\partial/\partial y(xv)=0$
	II	$u\partial T/\partial x+v\partial T/\partial y=\partial/\partial y\,(\alpha_\mathrm{T}\partial T/\partial y)$
Boundary conditions	I	$v(x,0)=0\,,\quad \partial u/\partial y\|_{y=0}=\partial w/\partial y\|_{y=0}=0\,,\quad u(x,\pm\infty)=w(x,\pm\infty)=0$
	IIa	$\partial T/\partial y\|_{y=0}=0\,,\quad T(x,\pm\infty)=T_\infty$
	IIb	$T(x,+\infty)=T_1\,,\quad T(x,-\infty)=T_2$
General structure of the self-similar solutions	I	$\frac{u}{u_\mathrm{m}}=F'(\eta)\,,\quad \frac{w}{w_\mathrm{m}}=\Phi(\eta)\,,\quad u_\mathrm{m}=Ax^\alpha\,,\quad w_\mathrm{m}=Cx^\varepsilon\,,\quad \eta=Byx^\beta\,,\quad \left(B\equiv\frac{1}{a}\right)$
	IIa	$\frac{T-T_\infty}{T_\mathrm{m}-T_\infty}=\theta(\eta)\,,\quad T_\mathrm{m}-T_\infty=\Gamma x^\gamma$
	IIb	$\frac{T-T_2}{T_1-T_2}=\theta(\eta)$
Exponents in the self-similar solutions	I	$\alpha=-1\,,\quad \beta=-1\,,\quad \varepsilon=-2$
	IIa	$\gamma=-1$
	IIb	$\gamma=0$

Table 2.8 (continued)

Constants in the self-similar solutions	I	$A=\sqrt{\frac{3J_x}{8\pi\rho\sqrt{2K}}}\,,\quad B=\frac{1}{\sqrt{2K}}\,,\quad C=M_y\sqrt{\frac{3}{8\pi\rho J_x\sqrt{2K}}}$
	IIa	$\Gamma=\frac{Q\sqrt[4]{2}}{c_p}\frac{1}{\sqrt{3\pi\rho J_x\sqrt{K}}}\left(\int\limits_{-\infty}^{+\infty}F'\theta\,\mathrm{d}\eta\right)^{-1}$
	IIb	$(\Gamma=T_1-T_2)$
Integral invariants	I	$J_x=2\pi x\int\limits_{-\infty}^{+\infty}\rho u^2\,\mathrm{d}y=\text{const}\,,\quad M_y=2\pi x^2\int\limits_{-\infty}^{+\infty}\rho uw\,\mathrm{d}y=\text{const}$
	IIa	$Q=2\pi x\int\limits_{-\infty}^{+\infty}\rho c_p u(T-T_\infty)\,\mathrm{d}y=\text{const}$
	IIb	–
Self-similar equations	I	$F'''+2(FF')'=0\,,\quad \Phi''+2(F\Phi)'=0$
	IIa	$\theta''+2\mathrm{Pr_T}(F\theta)'=0$
	IIb	$\theta''+2\mathrm{Pr_T}F\theta'=0$
Self-similar coordinate $\eta_{1/2}$ corresponding to $u/u_m=1/2$	I	$\eta_{1/2}=0.88$
Self-similar boundary conditions	I	$F(0)=0\,,\quad F'(0)=\Phi(0)=1\,,\quad F''(\pm\infty)=\Phi(\pm\infty)=0$
	IIa	$\theta'(0)=0\,,\quad \theta(\pm\infty)=0$
	IIb	$\theta(+\infty)=1\,,\quad \theta(-\infty)=0$
Self-similar solutions	I	$F=\tanh\eta\,,\quad F'=1/\cosh^2\eta\,;\quad \Phi=F'=1/\cosh^2\eta$
	IIa	$\theta(\eta)=(F')^{\mathrm{Pr_T}}=(\cosh\eta)^{-2\mathrm{Pr_T}}$
	IIb	$\theta(\eta)=\left[\int\limits_{-\infty}^{\eta}(\cosh\xi)^{-2\mathrm{Pr_T}}\,\mathrm{d}\xi\right]\left[\int\limits_{-\infty}^{+\infty}(\cosh\xi)^{-2\mathrm{Pr_T}}\,\mathrm{d}\xi\right]^{-1}$
Mass flow rate (G), kinetic energy flux (E), etc., as well as turbulent kinematic viscosity (ν_T) and thermal diffusivity (α_T)	I	$G\sim x\,,\quad E\sim x^{-1}\,,\quad \nu_T=KA=\text{const}\quad\left(K=\frac{a^2}{2}\right)$
	IIa	$\alpha_T=K_qA=\text{const}$
	IIb	$\alpha_T=K_qA=\text{const}\quad\left(\mathrm{Pr_T}=\frac{K}{K_q}\right)$

Comments:
In items *Differential equations*, *Boundary conditions*, etc.: I represents the dynamic problem; II the thermal one.
In items *Boundary conditions*, *General structure of the self-similar solutions*, etc.: IIa represents the thermal problem with symmetric boundary conditions for temperature; IIb that with asymmetric ones.

Comparison of (2.167) and (2.169) shows that

$$\frac{T-T_\infty}{T_m-T_\infty}=\left(\frac{u}{u_m}\right)^{\mathrm{Pr}}\,. \tag{2.171}$$

The effective dynamic radius of the jet is

$$\delta=\frac{8.49x}{\left(3J_x/8\pi\rho\nu^2\right)^{1/2}} \tag{2.172}$$

while the effective thermal radius δ_T depends on the Prandtl number, i. e.,

$$\begin{aligned}
\delta_T&=\frac{28.14x}{\left(3J_x/8\pi\rho\nu^2\right)^{1/2}} && \text{for}\quad \mathrm{Pr}=0.5\,,\\
\delta_T&=\delta && \text{for}\quad \mathrm{Pr}=1\,,\\
\delta_T&=\frac{4.16x}{\left(3J_x/8\pi\rho\nu^2\right)^{1/2}} && \text{for}\quad \mathrm{Pr}=2\,.
\end{aligned} \tag{2.173}$$

There are many other types of laminar jet flows with self-similar behavior in the far-field zone. Several such cases are shown schematically in Fig. 2.20. Their self-similarity is established in a similar manner to the case of the axisymmetric submerged jet considered above. The results are compiled in Table 2.7 with those for the axisymmetric submerged jet considered above being included as a particular case without swirling, i. e., where the angular velocity component about the jet axis $w=0$. (When swirling is present, $w\neq 0$, a radial pressure (p) distribution forms in the jet.) It is emphasized that boundary-layer theory does not account for the effect of vertical walls shown in Figs. 2.19, 2.20a on laminar jets emerging from them. The corresponding minor corrections were discussed in the literature.

All the self-similar solutions discussed in the present section hold in the far-field zones. Numerical calculations and measurements show that the corresponding non-self-similar flow structures existing in the near-field zones close to real nozzles always tend to the self-similar ones as x increases and becomes much larger than the nozzle size y_0.

The flows considered in the present section are incompressible. Generalizations to compressible cases can be realized with aid of the Dorodnitsyn–Howarth transformation [2.21, 23].

Turbulent jets also tend to a self-similar behavior sufficiently far from the nozzle (at $x \gtrsim 30 y_0$, where y_0 is the nozzle size). The kinematic eddy viscosity ν_T and the turbulent thermal diffusivity α_T in the free boundary layers (in distinction from the near-wall ones) are described rather accurately within the framework of Prandtl's second semi-empirical theory of turbulence. Both ν_T and α_T are given by power laws as per

$$\nu_T = K A x^{\Omega} , \quad \alpha_T = K_q A x^{\Omega} , \tag{2.174}$$

where K and K_q are dimensionless empirical constants, x is the axial coordinate in the jet, A is a dimensional constant (Table 2.8). A and the exponent Ω depend on the specific type of jet. The turbulent Prandtl number $\mathrm{Pr}_T = K/K_q$ has a value close to 0.75 for fluids whose molecular Prandtl numbers span the whole range from liquid metals to oils ($\mathrm{Pr} \approx 10^{-2}$–$10^3$).

The corresponding self-similar solutions for free (not near-wall) turbulent jets and mixing layers resemble those for laminar jets. These solutions are presented in Table 2.8, the notation following that of Table 2.7. The only unknown empirical constant K is related to a (via B), which is thus the only empirical constant to be found by comparing the result of Table 2.8 with experimental. For example, for planar submerged jets $a \approx 0.1$–0.12, for mixing layers $a \approx 0.09$–0.12 (for $m = u_2/u_1 = 0$), and for axisymmetric submerged jets $a \approx 0.045$–0.055.

In practice, self-similar solutions can be used even at distance, $x < 30 y_0$. However, when a finite nozzle is replaced by a pointwise one (which, in fact, is done in such cases) a jet polar distance should be introduced [2.24]. This means that in all the self-similar solutions x should be replaced by $x - x_0$, where an appropriate value of x_0 corresponds to the polar distance.

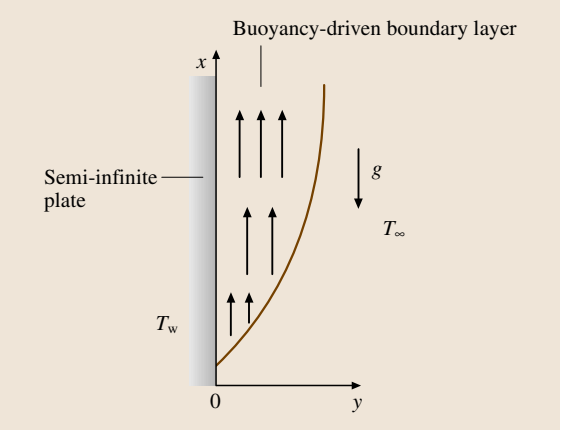

Fig. 2.22 Laminar boundary layer near vertical semi-infinite plate. The plate is kept isothermal at a temperature $T_w > T_\infty$

Boundary Layers in Natural Convection

Consider briefly laminar natural convection in the boundary layer of a hot vertical wall (Fig. 2.21). If the temperature difference between wall and fluid far from it is not too large, say $T_w - T_\infty = \mathcal{O}(10\,^\circ\mathrm{C})$, the flow and heat transfer can be described by the following fully coupled dynamic and thermal boundary layer equations [2.16, 25]

$$\begin{aligned} &\frac{\partial u}{\partial x} + \frac{\partial v}{\partial y} = 0 , \\ &u\frac{\partial u}{\partial x} + v\frac{\partial u}{\partial y} = \beta g (T_w - T_\infty)\theta + \nu \frac{\partial^2 u}{\partial y^2} , \\ &u\frac{\partial \theta}{\partial x} + v\frac{\partial \theta}{\partial y} = \alpha \frac{\partial^2 \theta}{\partial y^2} , \end{aligned} \tag{2.175}$$

where β is the thermal expansion coefficient with dimensionality 1/K, and g is the gravity acceleration; the normalized excess temperature $\theta = (T - T_\infty)/(T_w - T_\infty)$. The solutions of (2.175) are subject to the following boundary conditions

$$\begin{aligned} &y = 0 , \quad u = v = 0 , \quad \theta = 1 , \\ &y = \infty , \quad u = 0 , \quad \theta = 0 . \end{aligned} \tag{2.176}$$

In the case of a semi-infinite plate a length scale for x is not given, and can be taken arbitrarily as some L, since the scale $(\nu^2/g)^{1/3}$ is too small to be taken as a natural scale of the problem ($\approx 10^{-4}$ m). A velocity scale is not given either, but can be expressed via L as $U = [L\beta g(T_w - T_\infty)]^{1/2}$. The length scale in the y-direction, as usual in boundary layers, is

$$\delta = \frac{L}{(LU/\nu)^{1/2}} = \left[\frac{L\nu^2}{\beta g (T_w - T_\infty)}\right]^{1/4} \sim L^{1/4} . \tag{2.177}$$

The fact that an arbitrary L should disappear, similarly to the case considered in the section on *Flow and Heat*

Transfer in Laminar Boundary Layers Near a Flat Wall in Sect. 2.3.4, leads to the self-similar solution of the following form

$$\psi = 4\nu C x^{3/4} F(\eta)\,, \qquad \eta = C\frac{y}{x^{1/4}}\,,$$
$$C = \left[\frac{\beta g(T_\mathrm{w} - T_\infty)}{4\nu^2}\right]^{1/4}\,, \qquad \theta = \theta(\eta)\,, \qquad (2.178)$$

where ψ is the stream function ($u = \partial\psi/\partial y$, $v = -\partial\psi/\partial x$).

As before, the self-similarity can be (and has been) established without recourse to the solutions of the governing equations, just from the given data. However, if a detailed flow and thermal structure is needed, the functions $F(\eta)$ and $\theta(\eta)$ should be found, either using the self-similar equations following from (2.175)

$$\begin{aligned} F''' + 3FF'' - 2F'^2 + \theta &= 0\,,\\ \theta'' + 3\,\mathrm{Pr}\,F\theta' &= 0\,,\\ F(0) = F'(0) &= 0\,, \quad \theta(0) = 1\,,\\ F'(\infty) = \theta(\infty) &= 0 \end{aligned} \qquad (2.179)$$

Table 2.9 The function $H(\mathrm{Pr})$

Pr	H(Pr)
$\mathrm{Pr} \to 0$	$0.600\,\mathrm{Pr}^{1/2}$
0.01	0.0570
0.72	0.357
1.0	0.401
2.0	0.507
5.0	0.675
7.0	0.754
10	0.826
10^2	1.55
10^3	2.80
10^4	5.01
$\mathrm{Pr} \to \infty$	$0.503\,\mathrm{Pr}^{1/4}$

or experimentally. (The fact that the flow is self-similar allows one to make measurements in a single cross section of the boundary layer.) Equation (2.179) were solved numerically; the results are shown in Fig. 2.22 where the vertical velocity distribution across the boundary layer [$\tilde{u}(\eta) = u/(4\nu C^2 x^{1/2}) = F'(\eta)$] and

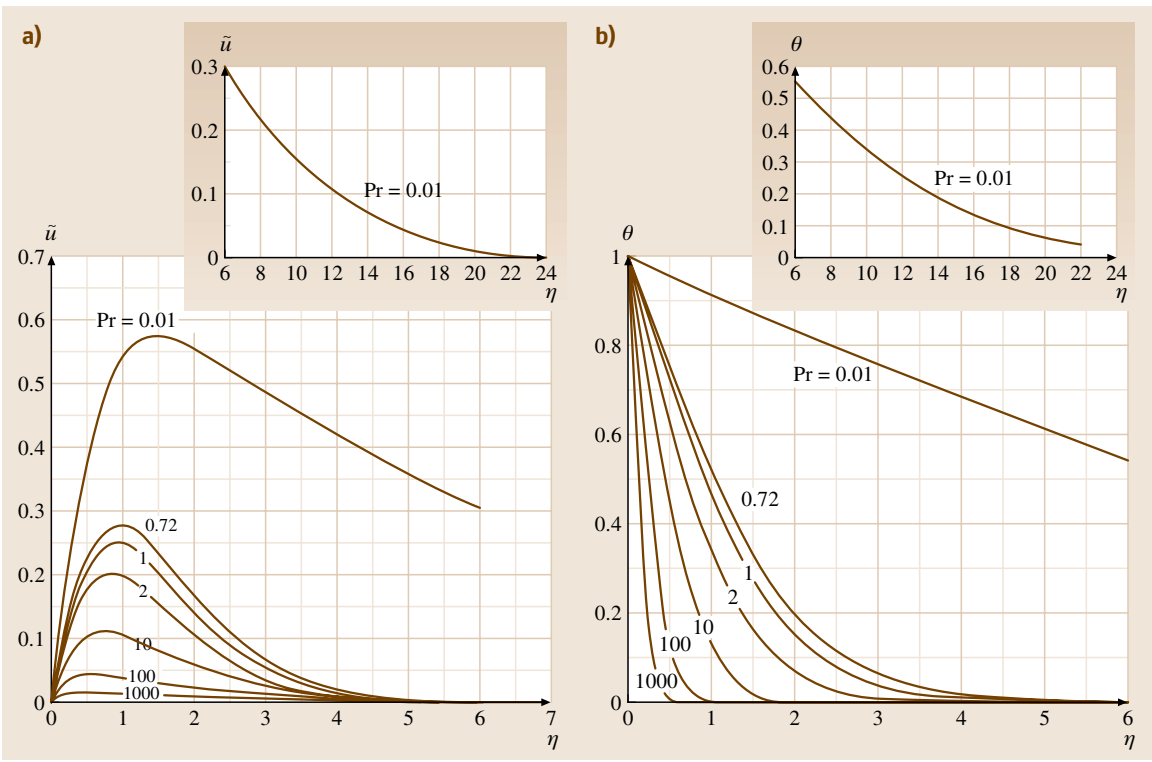

Fig. 2.23a,b Vertical velocity and temperature variation across the boundary layer for flow over an isothermal, vertical wall: **(a)** Vertical velocity, **(b)** temperature

the temperature $\theta(\eta)$ are plotted for a range of the Prandtl number. The local heat transfer coefficient $h(x)$ is calculated accordingly. Its normalized form, the Nusselt number $\mathrm{Nu} = kx/k$ where k is the fluid thermal conductivity, is given by

$$\mathrm{Nu} = H(\mathrm{Pr})\mathrm{Gr}_x^{1/4} . \tag{2.180}$$

The Grashof number is $\mathrm{Gr}_x = \beta g x^3 (T_\mathrm{w} - T_\infty)/\nu^2$, and the function $H(\mathrm{Pr})$ is given in Table 2.9.

Planar and axisymmetric plumes rising vertically above a heated horizontal cylinder or a sphere with a constant heat release also manifest self-similarity of the velocity and temperature distributions in the far-field zone. In a sense, they are kindred to the submerged jets. The corresponding self-similar solutions can be found in [2.25, 26].

2.3.5 Gas Dynamics: Strong Explosion

Gas dynamics also provides us with examples of important self-similar solutions. One such example is a strong explosion of a charge in a gas [2.16, 19, 27–29]. The gas is assumed to be compressible and inviscid and its motion after the explosion spherically symmetric. The corresponding set of gas dynamics equations reads

$$\frac{\partial v}{\partial t} + v\frac{\partial v}{\partial r} + \frac{1}{\rho}\frac{\partial p}{\partial r} = 0 , \tag{2.181}$$

$$\frac{\partial \rho}{\partial t} + \frac{\partial \rho v}{\partial r} + 2\frac{\rho v}{r} = 0 , \tag{2.182}$$

$$\frac{\partial}{\partial t}\left(\frac{p}{\rho^\gamma}\right) + v\frac{\partial}{\partial r}\left(\frac{p}{\rho^\gamma}\right) = 0 . \tag{2.183}$$

Equation (2.181) represents the momentum balance, (2.182) is the continuity equation, and (2.183) the energy equation, r being the radial (spherical) coordinate, t the time, v the radial velocity of gas, ρ the density, p the pressure and γ the ratio of the specific heat at constant pressure to the specific heat at constant volume. At $t = 0$ the explosive instantaneously releases an energy E_0 of dimensionality $[E_0] = \mathrm{J}$ and a spherical shock wave propagates outwards, subdividing the gas into an infinite region ahead of the shock wave with unperturbed constant values of the pressure and density p_1 and ρ_1, and a region behind the shock wave where the flow is described by (2.181–2.183). The standard jump conditions should be satisfied at the shock front.

To make the gas flow self-similar, we have to assume that the explosion is pointwise. In other words, the charge is considered to be negligibly small compared to the relevant distances r. This, however, does not mean that no length scale is involved, since one can be constructed as $\ell = (E/p_1)^{1/3}$. However, in mega-explosions, (e.g., nuclear ones) pressurization by the shock wave is typically so strong that the pressure ahead of the shock wave p_1 can be neglected. The length scale ℓ is then lost and the problem becomes self-similar. An arbitrary length scale L can then be used, while the corresponding time scale becomes $(\rho_1 L^5/E)^{1/2}$. When the radial coordinate r and time are rendered dimensionless by these scales, $\overline{r} = r/L$, $\overline{t} = t/(\rho_1 L^5/E)^{1/2}$, the current position of the shock wave r_2, the pressure, gas velocity and density distributions behind it can be presented in the following form

$$r_2 = L f_1(\overline{t}, \gamma) , \tag{2.184}$$

$$p = \frac{E}{L^3} f_2(\overline{r}, \overline{t}, \gamma) , \tag{2.185}$$

$$v = \left(\frac{E}{L^3\rho_1}\right)^{1/2} f_3(\overline{r}, \overline{t}, \gamma) , \tag{2.186}$$

$$\rho = \rho_1 f_4(\overline{r}, \overline{t}, \gamma) . \tag{2.187}$$

Since the final results should not contain L, the dimensionless functions $f_1 - f_4$ in (2.184–2.187) require the form

$$f_1(\overline{t}) = F_1(\gamma)\overline{t}^{2/5} , \tag{2.188}$$

$$f_2(\overline{r}, \overline{t}, \gamma) = \frac{1}{\overline{t}^{6/5}}\tilde{F}_2\left(\frac{\overline{r}}{\overline{t}^{2/5}}, \gamma\right) , \tag{2.189}$$

$$f_3(\overline{r}, \overline{t}, \gamma) = \frac{1}{\overline{t}^{3/5}}\tilde{F}_3\left(\frac{\overline{r}}{\overline{t}^{2/5}}, \gamma\right) , \tag{2.190}$$

$$f_4(\overline{r}, \overline{t}, \gamma) = \tilde{F}_4\left(\frac{\overline{r}}{\overline{t}^{2/5}}, \gamma\right) . \tag{2.191}$$

From (2.184) and (2.188) we see that

$$\frac{r}{r_2} = \frac{\overline{r}}{F_1(\gamma)\overline{t}^{2/5}} , \tag{2.192}$$

which shows that the ratio r/r_2 defines, in fact, the self-similar variable of the distributions (2.189–2.191). Namely, we take

$$\eta = \frac{\overline{r}}{\overline{t}^{2/5}F_1(\gamma)} = \frac{r\rho_1^{1/5}}{t^{2/5}E^{1/5}}\frac{1}{F_1(\gamma)} \tag{2.193}$$

and present (2.189–2.191) as

$$p = \frac{E^{2/5}\rho_1^{3/5}}{t^{6/5}}F_2^*(\eta, \gamma) , \tag{2.194}$$

$$v = \frac{E^{1/5}}{\rho_1^{1/5}t^{3/5}}F_3^*(\eta, \gamma) , \tag{2.195}$$

$$\rho = \rho_1 F_4^*(\eta, \gamma) . \tag{2.196}$$

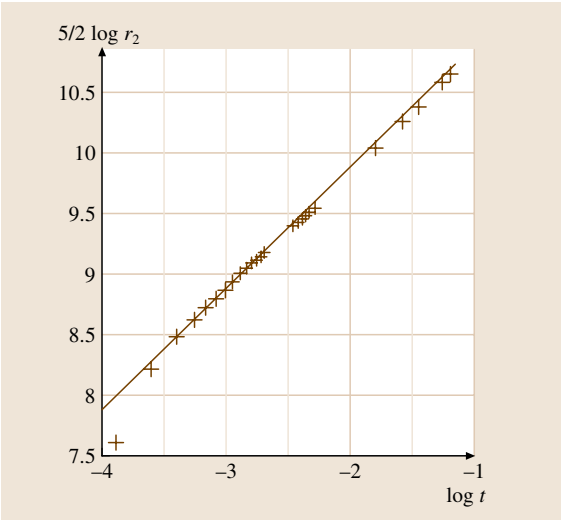

Fig. 2.24 Experimental results, shown by *crosses*, lie on a line inclined at 45° to the coordinate axes which confirms the scaling of (2.203)

It can be shown [2.19] that the pressure, gas velocity and density at the shock wave front are given by

$$p_2 = \frac{8\rho_1}{25(\gamma+1)}\left(\frac{E}{\rho_1}\right)^{2/5}\frac{1}{t^{6/5}}\,, \tag{2.197}$$

$$v_2 = \frac{4}{5}\frac{1}{(\gamma+1)}\left(\frac{E}{\rho_1}\right)^{1/5}\frac{1}{t^{3/5}}\,, \tag{2.198}$$

$$\rho_2 = \frac{\gamma+1}{\gamma-1}\rho_1\,. \tag{2.199}$$

Equations (2.197-2.199) enable us to present (2.194–2.196) in the following self-similar form

$$\frac{p}{p_2} = F_2(\eta,\gamma)\,, \tag{2.200}$$

$$\frac{v}{v_2} = F_3(\eta,\gamma)\,, \tag{2.201}$$

$$\frac{\rho}{\rho_2} = F_4(\eta,\gamma) \tag{2.202}$$

and according to (2.184) and (2.188) the position of shock wave is given by

$$r_2 = F_1(\gamma)\left(\frac{E}{\rho_1}\right)^{1/5} t^{2/5}\,. \tag{2.203}$$

The scaling $r_2 \sim t^{2/5}$ or $(5/2)\log r_2 \sim \log t$ is, indeed, supported by the experimental data (Fig. 2.23). The functions F_2–F_4 from (2.200-2.202) were found analytically [2.19, 27, 29]. The results are shown in Fig. 2.24 and in Table 2.10 for the case of $\gamma = 1.4$ (air). The corresponding temperature distribution, rendered dimensionless by that at the front of the shock wave T_2, can be found as $T/T_2 = (p/\rho)/(p_2/\rho_2)$ (where the gas is assumed to be ideal).

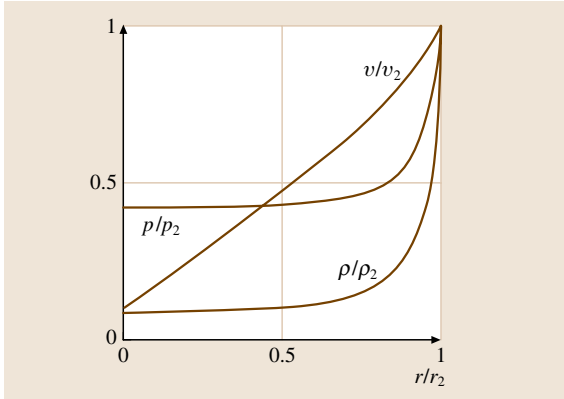

Fig. 2.25 Self-similar distribution of pressure, gas velocity and density behind the shock wave front

2.3.6 Free-Surface Flows

As an example of self-similar behavior arising in free-surface flows, consider patterns of capillary waves propagating over the free surface of a thin liquid film

Table 2.10 Self-similar distributions of pressure, gas velocity and density behind the shock wave front

$\frac{r}{r_2}$	$\frac{p}{p_2}$	$\frac{v}{v_2}$	$\frac{\rho}{\rho_2}$
1	1	1	1
0.9913	0.9109	0.9814	0.8379
0.9773	0.7993	0.9529	0.6457
0.9622	0.7078	0.9237	0.4978
0.9342	0.5923	0.8744	0.3241
0.9080	0.5241	0.8335	0.2279
0.8747	0.4674	0.7872	0.1509
0.8359	0.4272	0.7397	0.0967
0.7950	0.4021	0.6952	0.0621
0.7493	0.3856	0.6496	0.0379
0.6788	0.3732	0.5844	0.0174
0.5794	0.3672	0.4971	0.0052
0.4560	0.3656	0.3909	0.0009
0.3600	0.3655	0.3086	0.0002
0.2960	0.3655	0.2538	0.0000
0.2000	0.3655	0.1714	0.0000
0.1040	0.3655	0.0892	0.0000
0.0000	0.3655	0.0000	0.0000

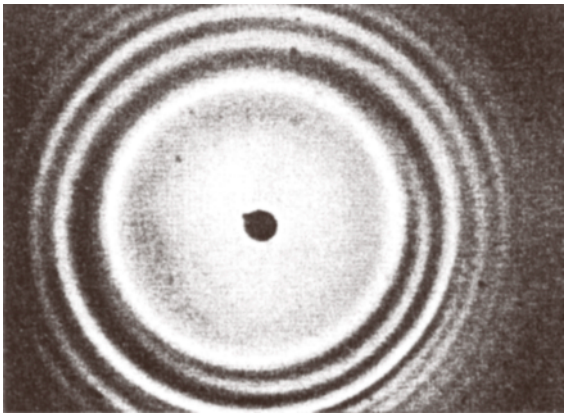

Fig. 2.26 Top view of a pattern of capillary waves taken 5 ms after impact of a copper stick onto an ethanol film of 1.4 mm thickness. The whole picture covers an area of about 25 mm × 35 mm (courtesy of Cambridge University Press)

from the point where it was impacted normally by a tiny droplet or a stick (Fig. 2.25) [2.30]. For scales of the order of several mm the gravity effect on the waves is negligibly small, and for time scales of the order of several ms viscosity effects can also be neglected. The dynamics of the wave propagation is then governed by the following set of quasi-one-dimensional equations [2.30]

$$\frac{\partial rh}{\partial t} + \frac{\partial rhV}{\partial r} = 0\,, \tag{2.204}$$

$$\rho h\left(\frac{\partial V}{\partial t} + V\frac{\partial V}{\partial r}\right) = \sigma\frac{\partial}{\partial r}\left(h\frac{\partial^2 h}{\partial r^2}\right)\,. \tag{2.205}$$

Equation (2.204) is the continuity equation and (2.205) represents the momentum balance, which describes the competition of the inertial forces and surface tension. The waves are assumed to be axisymmetric and propagating outwards along the radial coordinate r. The fluid velocity is denoted by V, the film thickness by h, the density by ρ, the surface tension coefficient by σ, and time by t. If we consider the waves as small perturbations propagating over a liquid layer initially at rest, and of unperturbed thickness h_0, then, linearizing (2.204) and (2.205) for small perturbations of the film thickness $\chi(r,t)$, such that

$$h = h_0[1+\chi(r,t)]\,, \tag{2.206}$$

we obtain the following equation for χ

$$\frac{\partial^2\chi}{\partial t^2} + \frac{a^2}{r}\frac{\partial}{\partial r}\left(r\frac{\partial^3\chi}{\partial r^3}\right) = 0\,. \tag{2.207}$$

The parameter a combines all the given physical parameters as per

$$a = \left(\frac{\sigma h_0}{\rho}\right)^{1/2} \tag{2.208}$$

and fully determines the wave propagation: $[a] = \mathrm{m}^2/\mathrm{s}$.

The initial impactor is assumed to be pointwise, which means that we are considering the wave pattern at distances r much larger than its diameter. Since no length scale is given, an arbitrary one, L can be used. The dimensionless wave pattern should be of the form

$$\chi = f\left(\frac{r}{L}, \frac{t}{L^2/a}\right)\,. \tag{2.209}$$

However, in the final result an arbitrary length scale L should automatically disappear, which means that the function f in (2.209) should depend not on its two variables separately but on their specific combination, namely,

$$\eta = \frac{r/L}{\left[t/(L^2/a)\right]^{1/2}} = \frac{r}{(at)^{1/2}}\,. \tag{2.210}$$

The corresponding self-similar wave pattern $\chi = F(\eta)$ should satisfy (2.207), which yields

$$F'''' + \frac{1}{\eta}F''' + \frac{\eta^2}{4}F'' + \frac{3}{4}\eta F' = 0\,. \tag{2.211}$$

The solution should correspond to the following initial perturbation

$$t = 0\,, \quad \chi = 4\pi S\frac{\delta(\eta)}{2\pi\eta}\,, \tag{2.212}$$

where S (dimensionless) corresponds to the impact intensity, and $\delta(\eta)$ is the delta function.

Using the solution of (2.211), we find that for large η the axisymmetric waves are described by the following expression

$$\chi = \frac{2S}{\Gamma\left(\frac{1}{4}\right)}\frac{1}{\eta^{3/2}} \times\left[\cos\left(\frac{1}{4}\eta^2 + \frac{1}{8}\pi\right) + \sin\left(\frac{1}{4}\eta^2 + \frac{1}{8}\pi\right)\right]\,, \tag{2.213}$$

where the gamma function of the argument 1/4 equals to 3.6256. The corresponding fluid velocity is given by

$$V = \left(\frac{a}{t}\right)^{1/2} \frac{S}{\Gamma\left(\frac{1}{4}\right)} \frac{1}{\eta^{1/2}} \times \left[\cos\left(\frac{1}{4}\eta^2 + \frac{1}{8}\pi\right) + \sin\left(\frac{1}{4}\eta^2 + \frac{1}{8}\pi\right)\right] . \tag{2.214}$$

Equation (2.213) with $\eta = r/(at)^{1/2}$ agrees pretty well with experimental data. Moreover, it shows that wave patterns similar to those of Fig. 2.25 shot at different time moments can be collapsed onto a single self-similar pattern given by (2.213), which indeed happens [2.30].

It is emphasized that self-similarity of the wave pattern in the far-field zone has been established without solution of the governing equation. The detailed wave structure has been found afterwards, theoretically and experimentally.

References

2.1 S. Moreau, D. Neal, Y.Khalighi, M. Wang, G. Iaccarino: Validation of unstructured-mesh LES of the trailing edge flow and noise of a Controlled-Diffusion airfoil, *Studying Turbulence Using Numerical Simulation Databases–XI: Proceedings of the Summer Programm 2006*, Center for Turbulence Research, Stanford University

2.2 M.C. Potter, J.F. Foss: *Fluid Mechanics* (Great Lakes, Wildwood 1982) p. 448

2.3 P.A. Thompson: *Compressible-Fluid Dynamics* (McGraw-Hill, New York 1972)

2.4 S.C. Morris, J.F. Foss: Turbulent boundary layer to single-stream shear layer: the transition region, J. Fluid Mech. **494**, 187–221 (2003)

2.5 T. von Kármán: Über laminare und turbulente Reibung, Z. Angew. Math. Mech. **1**, 233–252 (1921)

2.6 F.M. White: *Viscous Fluid Flow*, 2nd edn. (McGraw-Hill, New York 1991)

2.7 R. Kobayashi, Y. Kohama, C. Takamadate: Spiral vortices in boundary layer transition regime on a rotating disk, Acta Mech. **25**, 71–82 (1980)

2.8 P.W. Bridgman: *Dimensional Analysis* (Yale Univ. Press, New Haven 1922)

2.9 R.L. Panton: *Incompressible Flow*, 3rd edn. (Wiley, New York 2005)

2.10 F.M. White: *Fluid Mechanics*, 5th edn. (McGraw-Hill, New York 2003)

2.11 Y.A. Çengel, J.M. Cimbala: *Fluid Mechanics* (McGraw-Hill, New York 2006)

2.12 R.M. Schmidt, K.R. Housen: Problem solving with dimensional analysis, The Industrial Physicist **1**, 21 (1995)

2.13 J.C. Klewicki, H. Miner: *Wall pressure structure at high Reynolds number*, Division Fluid Dynamics Meeting, Bull. Am. Phys. Soc. (APS, College Park 2002), FH 001

2.14 R.L. Panton: Review of wall turbulence described by composite expansions, Appl. Mech. Rev. **58**, 1–36 (2005)

2.15 J.M.J. den Toonder, F.T.M. Nieuwstadt: Reynolds number effects in a turbulent pipe flow for low to moderate Re, Phys. Fluids **9**(11), 3398 (1997)

2.16 L.D. Landau, E.M. Lifshitz: *Fluid Mechanics*, 2nd edn. (Pergamon, Oxford 1987)

2.17 G.I. Barenblatt: *Similarity, Self-Similarity and Intermediate Asymptotics* (Cambridge Univ. Press, Cambridge 1996)

2.18 H. Schlichting: *Boundary Layer Theory*, 8th edn. (Springer, Berlin, Heidelberg 2000)

2.19 L.I. Sedov: *Similarity and Dimensional Methods in Mechanics*, 10th edn. (CRC, Boca Raton 1993)

2.20 L. Rosenhead: *Laminar Boundary Layers* (Clarendon, Oxford 1963)

2.21 K. Stewartson: *The Theory of Laminar Boundary Layers in Compressible Fluids* (Clarendon, Oxford 1965)

2.22 S.I. Pai: *Fluid Dynamics of Jets* (van Nostrand, Toronto, New York 1954)

2.23 L.A. Vulis, V.P. Kashkarov: *Theory of Viscous Liquid Jets* (Nauka, Moscow 1965)

2.24 G.N. Abramovich: *The Theory of Turbulent Jets* (MIT, Cambridge 1963)

2.25 Y. Jaluria: *Natural Convection Heat and Mass Transfer* (Pergamon, Oxford 1980)

2.26 Y.B. Zel'dovich: Limiting laws of freely rising convective currents. In: *Selected Works of Ya.B. Zel'dovich, Chemical Physics and Hydrodynamics*, Vol. 1, ed. by J.P. Ostriker (Princeton Univ. Press, Princeton 1992)

2.27 L.I. Sedov: Propagation of strong blast waves, Prikl. Mat. Mekh. **10**(2), 241–250 (1946)

2.28 G.I. Taylor: The formation of a blast wave by a very intense explosion, Proc. Roy. Soc. London A **201**, 159–186 (1950)

2.29 J. von Neumann: The point source solution. In: *Collected Works*, Vol. VI, ed. by A.J. Taub (Pergamon, Oxford 1963)

2.30 A.L. Yarin, D.A. Weiss: Impact of drops on solid surfaces: self-similar capillary waves, and splashing as a new type of kinematic discontinuity, J. Fluid Mech. **283**, 141–173 (1995